

Pohue Bay flow, Mauna Loa, Hawaii: high
AC .H3 no. JU93 15367



Jurado-Chichay, Zinzuni
SOEST Library

**THE POHUE BAY FLOW, MAUNA LOA, HAWAII:
HIGH VOLUMETRIC FLOW-RATE TUBE-FED
PAHOEHOE AND ASSOCIATED FEATURES**

A THESIS SUBMITTED TO THE GRADUATE DIVISION OF THE UNIVERSITY
OF HAWAII IN PARTIAL FULFILLMENT OF THE REQUIREMENTS FOR THE
DEGREE OF

MASTER OF SCIENCE
IN
GEOLOGY & GEOPHYSICS

MAY 1993

BY

Zinzuni Jurado-Chichay

Thesis Committee:

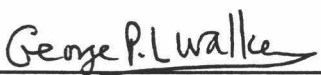
Stephen Self, Chairman
George P.L. Walker
John P. Lockwood

We certify that we have read this thesis and that, in our opinion, it is satisfactory in scope and quality as a thesis for the degree of Master of Science in Geology and Geophysics

THESIS COMMITTEE



Chairperson





ACKNOWLEDGMENTS

I thank the University of Mexico (UNAM) for supporting me while doing graduate work, for letting me use UNAM equipment at the laboratory of paleomagnetism, for funding the ^{14}C analyses (DGAPA project no. IN-103589) and for giving me the freedom to study anything I wanted. My field work was partially supported by the Harold T. Stearns Fellowship and a University of Hawaii ORA seed money grant to Stephen Self.

I also would like to thank Jr. Molcilio and Kahuku Ranch for permission to visit the Pu'u Ki area, as well as Mr. and Mrs. Richard Schultz for access to Pu'u Hou.

I sincerely thank George Walker the best teacher I ever had, for without taking his class by chance, I never would have been exposed to his enthusiasm for volcanology, and might have suffered in paleomagnetism. George, thank you for the idea of studying the Pu'u Ki cones.

Scott Rowland was an unofficial adviser. He advised and helped me in the completion of this work, from the fun of the field work to the tedious hours at the office. Thank you Scott for your patience and for standing me all this time without having the official recognition!

Thorvaldur Thordarsson made critical comments on this work. Without his help a good percentage of this study would have been just imagination.

The section on paleomagnetism would not have been possible without the help of several people including: Jaime Urrutia, who helped me to use the equipment and interpret the results, and Duane Champion, who calculated the solar azimuths after giving up trying to teach me how to do it myself.

Last, but not least, I thank Jack Lockwood, who helped choose the sites, collect the samples, and loaned his precious diamond bit that after drilling all the sites was completely worn out.

John Sinton assisted with the chemical and petrographic interpretations, and Mark Robinson read the final manuscript and helped translate it into a readable version.

I also thank all the members of my committee: George Walker, Stephen Self, and Jack Lockwood for reading several versions of this work.

Finally I thank my parents for more than once not letting me stay home for good, and making sure I finished studying in Hawaii.

ABSTRACT

The Pohue Bay lava flow on the SW rift zone of Mauna Loa has features inherited during emplacement that are unlike any that have been witnessed forming in historic times on Hawaiian volcanoes. Extremely large lava tubes and channels developed in this flow and volumetric flow rates are calculated by the Jeffreys formula to have a range between 1000 and 5600 m³/sec. These calculated flow rates are high in comparison to historical eruptions of pahoehoe ($\leq 10\text{m}^3/\text{sec}$) and a'a lava flows (10-1000 m³/sec) in Hawaii. Large channel and tube overflows and circular littoral cones are associated with these lava flow, and are the two main topics of this thesis.

Pahoehoe textured overflows from the channel/tube system are inferred to have had low viscosities and to have rapidly flowed tens to hundreds of meters (calculated velocities are between 4 and 20 m/sec). The lava in these overflows commonly made a transition to a'a, after which the interior sometimes extruded as pahoehoe, giving an apparent reversal of the usual trend of textural development.

When the Pohue Bay flow reached the ocean strong magma-water interactions took place producing circular littoral cones up to 500 meters in diameter. It is proposed that the explosions occurred when the active tube collapsed into underlying wet hyaloclastites at a point inland from the coast. Later, low intensity explosions filled the rings of lapilli and spatter with spatter and ponded lava. These cones could easily be misinterpreted as primary volcanic vents, having similar attributes.

Table of Contents

Acknowledgements	iii
Abstract.....	v
List of Tables	viii
List of Figures	ix
Chapter I: Introduction	1
Chapter II: Aspects of High Volumetric Flow-Rate Channel Overflows and Apparent Pahoehoe to A'a to Pahoehoe Transitions.....	3
Summary.....	3
Introduction	4
Observations.....	5
Channel and tube system.....	7
The overflows	11
Layered lava balls	17
Transitions to a'a and pahoehoe	21
Toothpaste Lava and Cleft Structures	27
Importance of Channel Overflows	30
Conclusions	31
Chapter III: The Formation of Circular Littoral Cones	32
Summary.....	32
Introduction	33
The Field Area.....	36
Descriptions of the Cones	38
Three-rim cone	38
Puu Ki.....	42
Auau cone	53
Summary of cone structures.....	59
Pohue Bay Cones: Littoral or Primary	59
Proximity to coastline	59
Location with respect to rift zones	60
Presence of dense angular fragments.....	61
Pyroclastic considerations	62
Grain size parameters	63
Density.....	63
Cone morphology	68
Shape	68
Rim diameter/base diameter ratios	68

Relationships between cones and adjacent flows.....	71
Field relationships	71
Chemistry	73
Petrography	76
Paleomagnetism.....	76
Paleomagnetic data summary.....	87
Summary of littoral vs. primary evidence	89
Discussion: The Flow of Lava Into the Ocean.....	91
Scenario for Formation of Circular Littoral Cones	97
Discussion and Conclusions	109
Chapter IV: Conclusions	111
References	112

List of Tables

3.1 Chemical data	67
3.2 Paleomagnetic site locations	77
3.3 Paleomagnetic results	82
3.4 Fisher statistics and paleosecular variation calculations	86
3.5 Compilation of primary and littoral evidence	90

List of Figures

1.1	Location map of field area	2
2.1	Location map of Pohue Bay flow	6
2.2	Detailed map of middle Pohue Bay flow.....	8
2.3	Photograph of large skylight	9
2.4	Diagram for calculating velocities and volumetric flow rates	10
2.5	Photo of sheet-like overflows.....	12
2.6	Photo of small cooling joints	14
2.7	Cross sections of pahoehoe flow units	16
2.8	Photo of layered lava balls	18
2.9	Diagram of formation of layered lava balls	19
2.10	Photo of a'a and flow unit of pahoehoe.....	22
2.11a	Photo of pahoehoe that issued from a'a.....	22
2.11b	Photo of pahoehoe that issued from a'a.....	23
2.11c	Photo of pahoehoe that issued from slabby pahoehoe.....	23
2.12	Diagrams of pahoehoe to a'a to pahoehoe transition	25
2.13	Qualitative graphs of flow type transitions	26
2.14	Photo of toothpaste lava cleft.....	29
3.1	Diagram of standard littoral cone.....	35
3.2	Location map of Pohue Bay and Kolo flows	37
3.3	Geologic map of cones in the Pohue Bay flow.....	39
3.4	Photo of three-rim cone	41
3.5	Photo of S-most cone.....	43
3.6	Cross-section of main Puu Ki cluster.....	45
3.7	Stratigraphic column at N end of Puu Ki cluster.....	46
3.8	Photo of main Puu Ki cluster	48
3.9	Contact between ponded lavas and pyroclastic rim	48
3.10	Photo of ponded lava surface	50
3.11	Photo of N Keliuli cone remnant	50
3.12	Photo of large inland depression.....	52
3.13	Geologic map of Auau cone.....	54
3.14	Photo of Auau cone	56
3.15	Photo of SE-most cone	58
3.16	Plot of $\sigma\phi$ vs. $Md\phi$ vs. $\sigma\phi$	64
3.17	Class densities of sieved samples	65
3.18	Photo of Kamoamoalittoral cone.....	69
3.19	Graph of cone aspect ratios.....	70
3.20	Photo of spatter bomb on Pohue Bay flow	72
3.21	Location map of paleomagnetic and chemical samples.....	74
3.22	Chemical data for Pohue Bay flow and Puu Ki cones	75

3.23	Vector diagrams of demagnetization	79
3.24	Angular dispersion between solar and magnetic azimuths	81
3.25	Hysteresis diagrams	83
3.26	Stereograms of paleomagnetic data	85
3.27	Secular variation curve for Hawaii	88
3.28a	Lava approaches coastline	100
3.28b	Formation of lava bench and hyaloclastite	101
3.28c	Bench collapses	102
3.28d	Strong littoral explosions	103
3.28e	Explosions weaken	104
3.28f	Collapse of seaward edge of cone	105
3.28g	Collapse at Auau cone with molten lava	106
3.28h	Late-stage a'a flowing through Auau cone tube	107
3.28i	Latest a'a at Auau cone	108

CHAPTER I INTRODUCTION

This thesis is concerned with two aspects of the volcanology of the prehistoric Pohue Bay flow on the Southwest rift zone of Mauna Loa. This flow can be followed from the coastline up to an elevation of 920 meters, but its vent area (higher still) has been buried by younger flows (Figure 1.1).

The first part (Chapter II) deals with the overflows from a large channel/tube system in the middle part of the flow (Figure 1.1). Occurrences and mechanisms for formation of isolated patches of pahoehoe lava within a'a flows are discussed in detail.

The second part (Chapter III) describes and examines the origin of the cluster of cones occurring along the coast of the Pohue Bay flow. Several lines of evidence are used to constrain and explain their origin. Also the Auau cone within the prehistoric Kolo flow (Figure 1.1) which is very similar to those within the Pohue Bay flow, has also been studied to gain a better understanding of the formation of these littoral cones.

Chapter III includes a detailed paleomagnetic study of the Pohue Bay flow and cones. It is presented as one line of evidence of their coeval relationship. Additionally this paleomagnetic study provides an age for the flow.

Chapters II and III are completely independent even though they both deal with the same flow. Slightly modified versions of each thesis chapter have been submitted for publication to the Bulletin of Volcanology. Chapter IV presents brief conclusions.

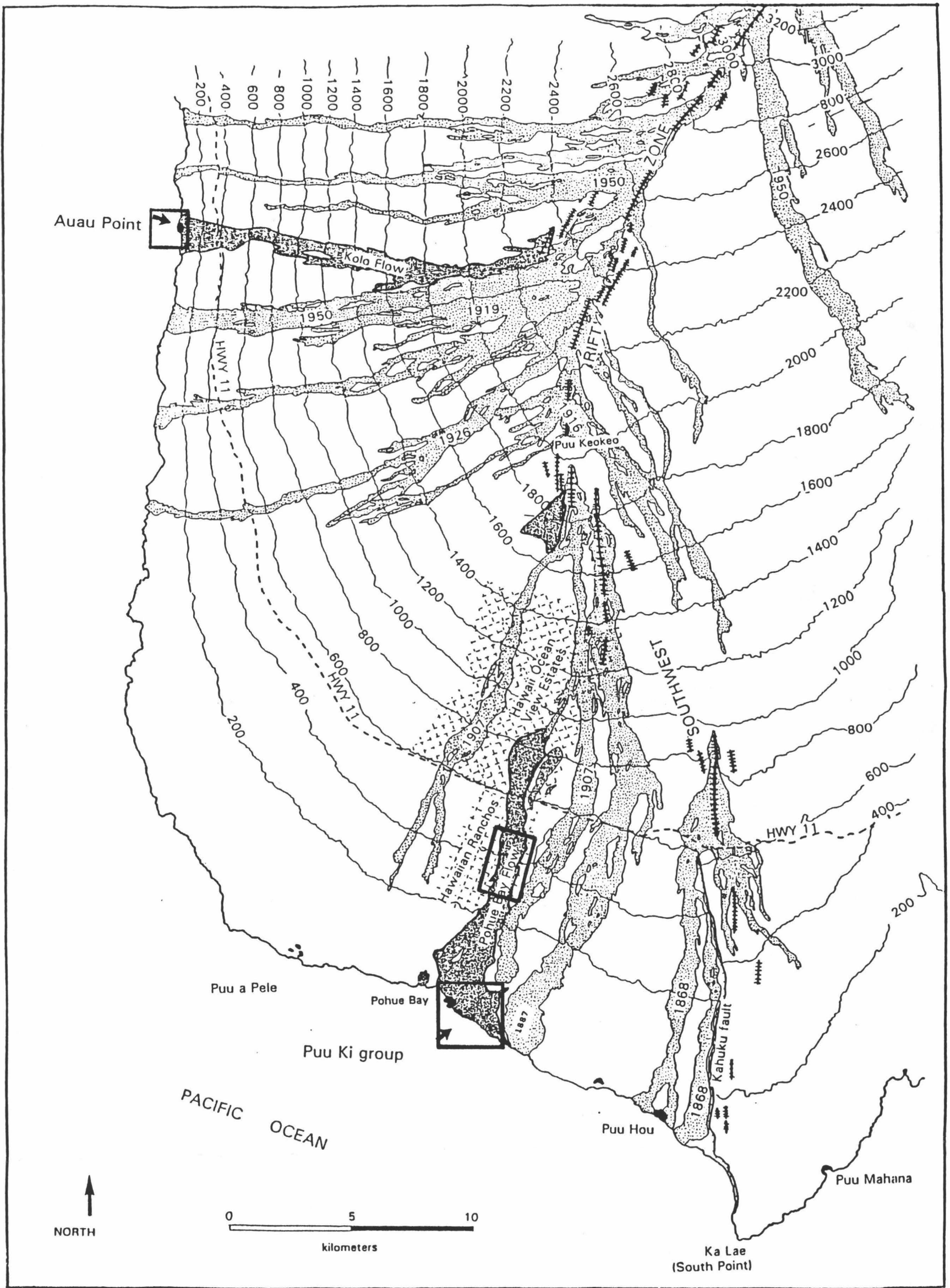


Figure 1.1. Location map of field area. Boxes indicate detailed study areas.

CHAPTER II
ASPECTS OF HIGH VOLUMETRIC FLOW-RATE CHANNEL OVERFLOWS
AND APPARENT PAHOEHOE TO A'A TO PAHOEHOE TRANSITIONS

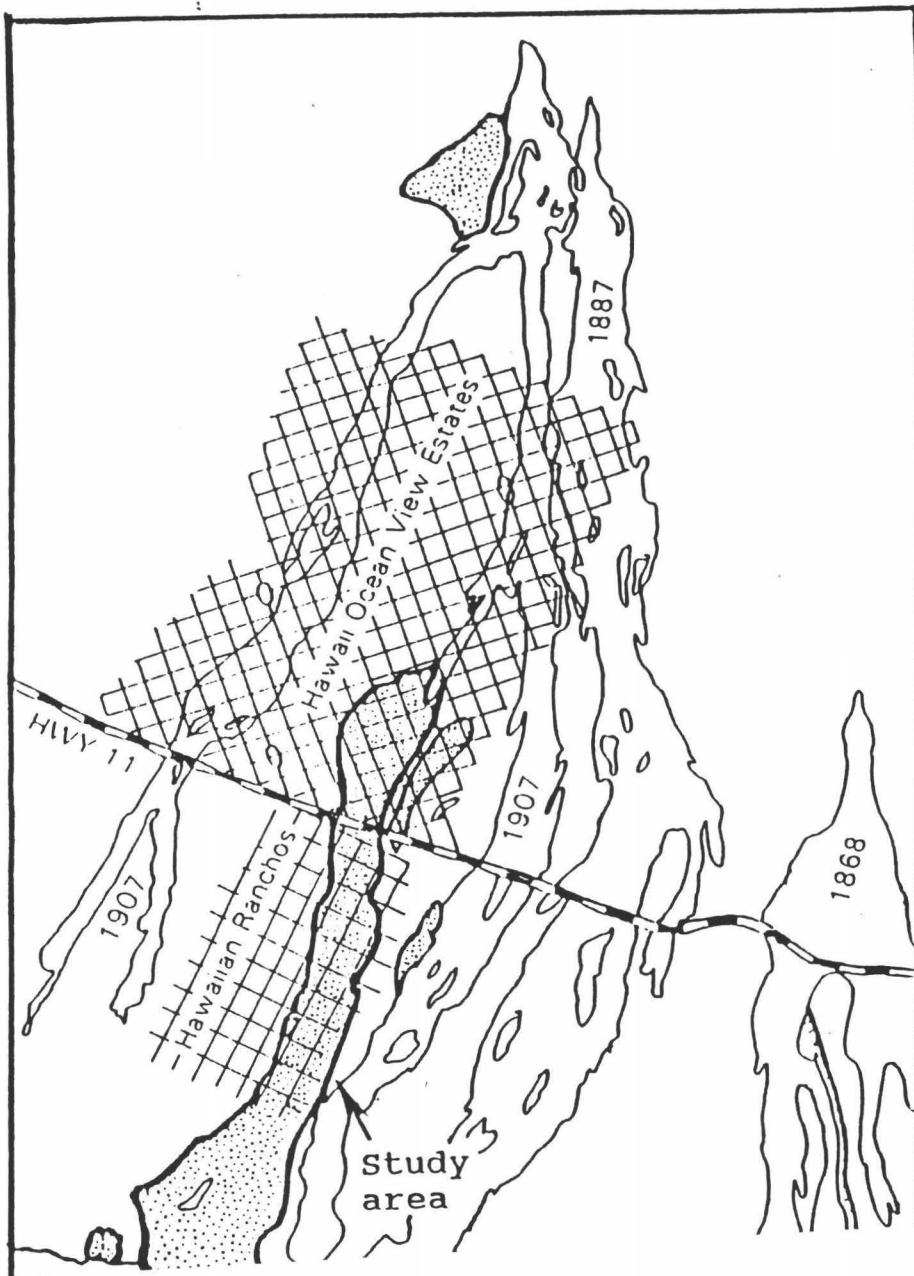
SUMMARY

The surface structure of a lava flow records the interaction between volumetric flow rate and viscosity-induced resistance to flow. Dramatically varying volumetric flow rates can produce different surface morphologies within the same flow; low-viscosity lava flowing at a high volumetric flow rate possesses the greatest range of possible surface textural options. In this chapter a number of high volumetric flow-rate overflows (calculated to have been from 90 to 2800 m³/sec) from a large lava tube and channel system on the SW rift zone of Mauna Loa have been studied. Calculated volumetric flow rates in the channel itself are between 1000 and 5600 m³/sec. Overflows were initially very low viscosity gas-rich pahoehoe (evidenced by flow-unit surfaces and aspect ratios, and vesicle sizes and contents). After traveling tens to hundreds of meters, the semi-solid/solid flow tops of these sheet-like overflows broke up to form a'a-like surfaces composed of clinker and pahoehoe fragments. The molten interiors of these overflows broke out on to the surface forming small pahoehoe flow units once the initial rapid overflow slowed or stopped. Although possessing fewer options, the molten interior of proximal-type a'a flows can also record different volumetric flow rates as is evident by toes of pahoehoe or clefts of

toothpaste lava (low volumetric flow rate) occurring within fields of clinker (high volumetric flow rate). These observations support the idea that the interplay between viscosity and volumetric flow rate determines the final morphological lava type, and although no specific portion of lava ever makes the transition from a'a back to pahoehoe, the flow as a whole may appear to do so.

INTRODUCTION

It is generally assumed that the pahoehoe-to-a'a transition is non-reversible because increase of viscosity and loss of gas and heat are (in nature) unidirectional processes (e.g. Wentworth & Macdonald 1953; Peterson & Tilling 1980; Kilburn 1981). Occurrences of isolated patches of pahoehoe surfaced lava within a'a flows were noted by Macdonald (1953) but were not discussed in detail. In Hawaii, historic tube-fed pahoehoe flows have formed at volumetric flow rates $\leq 10 \text{ m}^3/\text{sec.}$, whereas a'a flows have been erupted at volumetric flow rates ranging from 10-1000 m^3/sec (Rowland & Walker 1990). Around the lower western slopes of Mauna Loa's SW rift zone there are numerous examples of relatively smooth-surfaced lava (pahoehoe or toothpaste lava) that has issued from a'a flows. Fine examples of toothpaste lava at Kapoho (Rowland & Walker 1987) and elsewhere (similar to the "crease structures" in silicic lavas; Anderson & Fink 1992) are additional examples that illustrate the rheological differences between the surfaces and interiors of flows and their emplacement at



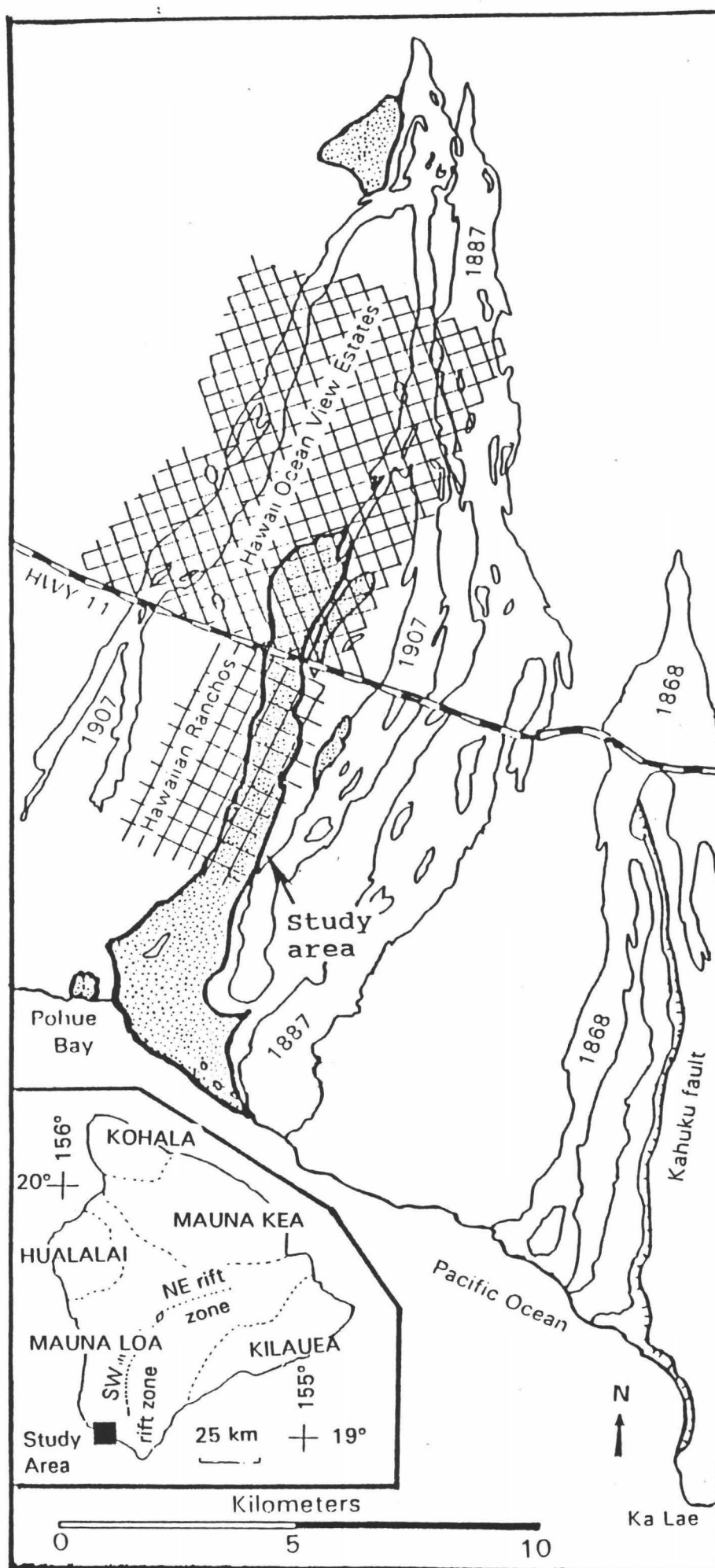


Figure 2.1. Location map showing the Pohue Bay flow (stippled) and its relationship to the lower SW rift zone of Mauna Loa (traced from Lipman & Swenson 1984). Arrow (S) shows study area illustrated in Figure 2.2. Mauna Loa rift zones are dotted on the inset map, and volcano boundaries dashed.

different combinations of viscosity and volumetric flow rate. This chapter documents the eruption of pahoehoe from flows that are otherwise a'a, and attempts to explain the apparent inconsistency with previous ideas. It first describes a number of channel overflows and evidence for their having erupted at high volumetric flow-rates. These channel overflows were a source of lava that could undergo and record numerous flow processes, and they demonstrate a complex interplay between viscosity and flow rates. Also described are occurrences of toothpaste lava that record low volumetric flow rates in otherwise high volumetric flow-rate a'a. Finally, the histories of some hypothetical lava elements are followed as they are emplaced to form a complex flow of both a'a and pahoehoe.

OBSERVATIONS

The age of the Pohue Bay Flow, on the western flank of Mauna Loa's south west rift zone (Figure 2.1) was earlier estimated at 740-910 years (Lipman & Swenson 1984). Recent paleomagnetic work (Chapter III) indicates an age closer to 2700 years. This flow can be traced from the coastline to an elevation of 920 m; its vent area (located farther upslope) has been buried by younger lava flows. The Pohue Bay flow, unlike most Hawaiian lavas, cannot be classified simply as either mainly a'a or pahoehoe. Instead it consists of overflows of a'a and pahoehoe from a very large channel/tube system. Most of this study is focused on some of the

overflows from this system. However, additional examples that illustrate some of the complex flow regimes possible in a'a can also be found nearby; the distal end of the Halepohana flow (Lipman & Swenson 1984) consists of pahoehoe flow units issuing from an a'a front.

Channel and tube system

The channel/tube system of the Pohue Bay flow can be traced 100-400 m above sea level (Figure 2.2). The skylights into the tube range from 30 by 30 to 75 by 600 m, with the long dimension always parallel to the along-flow direction. The larger skylights (Figure 2.3) are 10-25 m deep and more resemble large channels than skylights, but in the upper part of the study area the structure is a true channel. The inner walls of the channel/tube system consist of numerous flows, most of which are vesicular pahoehoe less than a meter thick. In many locations, the walls have a veneer of lava deposited during drainback events following overflows. Much of the floor of this channel/tube system is occupied by an olivine-rich a'a flow that may represent the last event of the Pohue Bay eruption. However, paleomagnetic data (Chapter III) suggest that this a'a flow is probably from a younger eruption that utilized the pre-existing pathway provided by the large Pohue Bay tube/channel system.

I have used Jeffreys' formula (e.g. Johnson 1970; Fink & Zimbelman 1990) to calculate flow velocities and get a rough estimate of flow conditions during the eruption (Figure 2.4). The values input to the formula

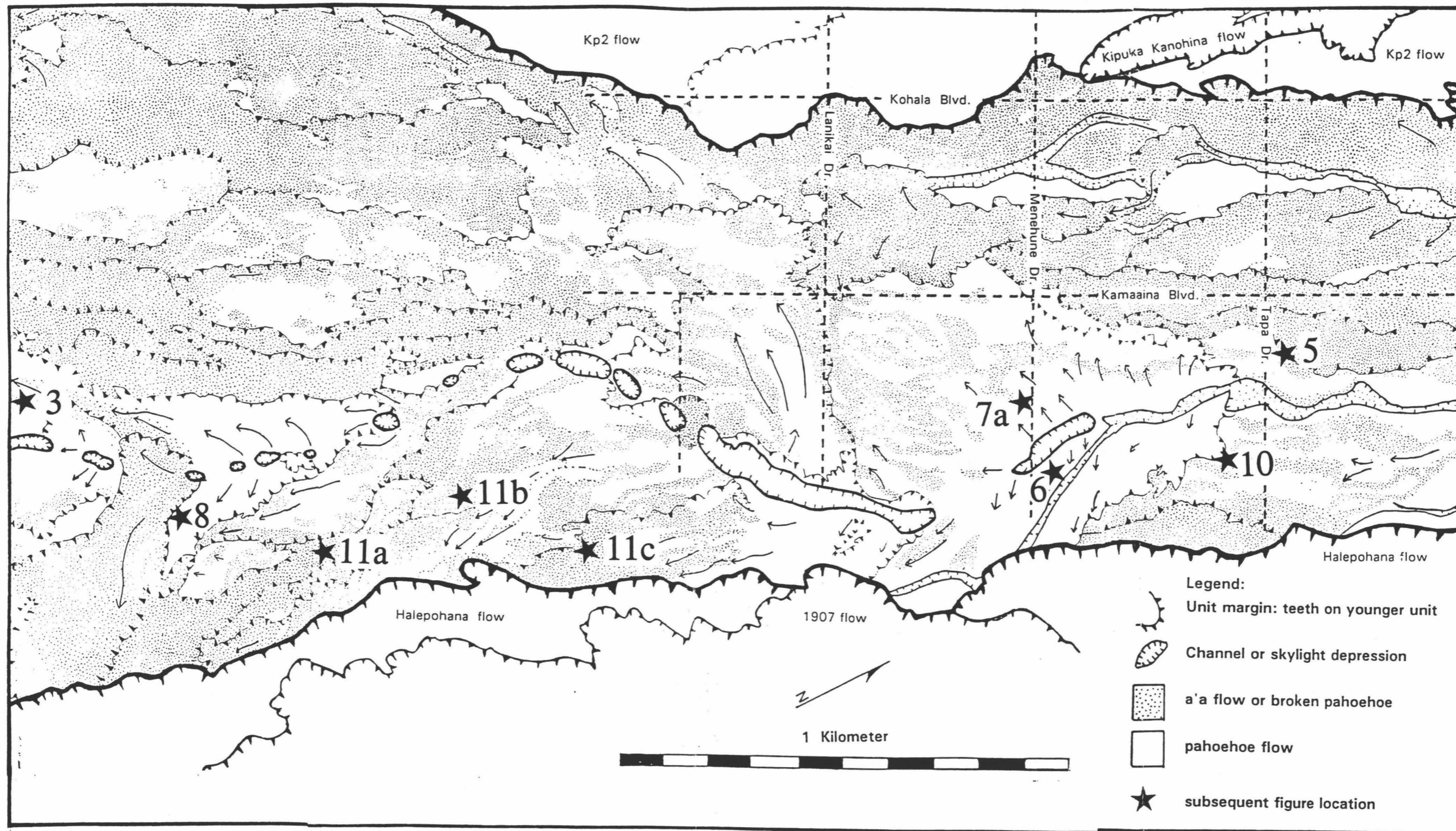


Figure 2.2. Detailed map (drawn from aerial photographs) of the 100-400 m elevation section of the Pohue Bay flow (inside thick lines). Arrows indicate flow directions, and those that lead directly from the channel or skylights (hachured) comprise the overflows discussed in the text. The 1907, Halepohana, and Kipuka Kanohina flows are all a'a. Numbered stars indicate locations of subsequent figures.

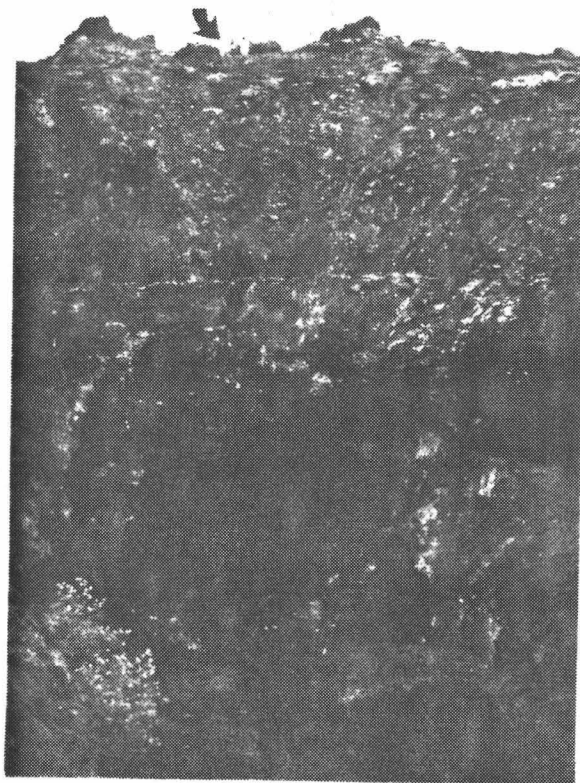


Figure 2.3. Photograph looking across a large skylight (view is upflow) along the channel/tube system. Note people (arrowed) for scale. Photo by GPL Walker.

Channel velocity $V_C = \rho g \sin \theta d^2 / n \eta$

d (m)	n	width (m)	V_C (m/sec)	Q (m ³ /sec)
10	3	20	28	5600
5	2	20	11	1057
5	2	45	11	2380
10	4	10	21	2114

Lobe (overflow) velocity $V_l = \rho g h^2 / 3 \eta$

h (m)	width (m)	v_l (m/sec)	Q (m ³ /sec)
2.5	50	22.5	2800
1.5	50	8.1	606
1.0	25	3.6	90

CONSTANTS:

$$\rho = 1100 \text{ kg/m}^3$$

$$g = 9.8 \text{ m/sec}^2$$

$$\theta = 4.5^\circ$$

$$\eta = 1000 \text{ Pa-sec}$$

$$n = 4 \text{ for near-equant channels, } 2 \text{ for wide channels}$$

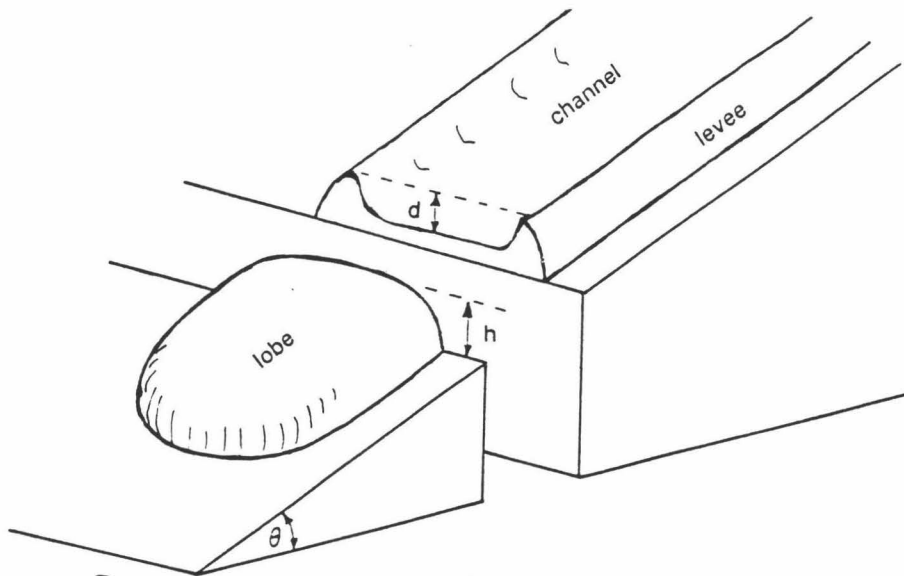


Figure 2.4. Diagram to illustrate variables and dimensions used to calculate velocities and volumetric flow rates. Results presented in boxes above.

are considered conservative and, because channel dimensions vary along the flow, I present calculations for more than one location. These calculations yielded velocities in the channel between 10-30 m/sec, with corresponding volumetric flow rates of 1000-5600 m³/sec. Thus the volumetric flow rate within the Pohue Bay channel, although not tightly constrained, indicate extremely high volumetric flow rates. A different form of the Jeffreys' formula allows for the calculation of flow velocities for non-channelized lavas (i.e. the overflows). These calculations yield flow velocities of 3 to 22 m/sec, with a volumetric flow rate between 90 to 2800 m³/sec.

The overflows

The flow field consists almost entirely of overflows from the main channel/tube system and many can be traced back to specific skylights or sections of the channel (Figure 2.2). These flow units are in places 50 m wide and are up to 750 m long, and formed when surges or blockages downstream caused the level of lava flowing in the channel/tube system to overtop the levees. At their origins (the channel edge) most of these overflows consist of thin (10-20 cm) sheet-like flow units of very smooth-surfaced and highly vesicular pahoehoe (Figure 2.5). These vesicles are generally spherical and of a uniform diameter around 0.5-1 mm in the top and bottom few cm. The average vesicle diameter increases in size toward the middles of the flow units from both the top and bottom; these flows are spongy pahoehoe (Walker 1989). Based on measurements of sawn

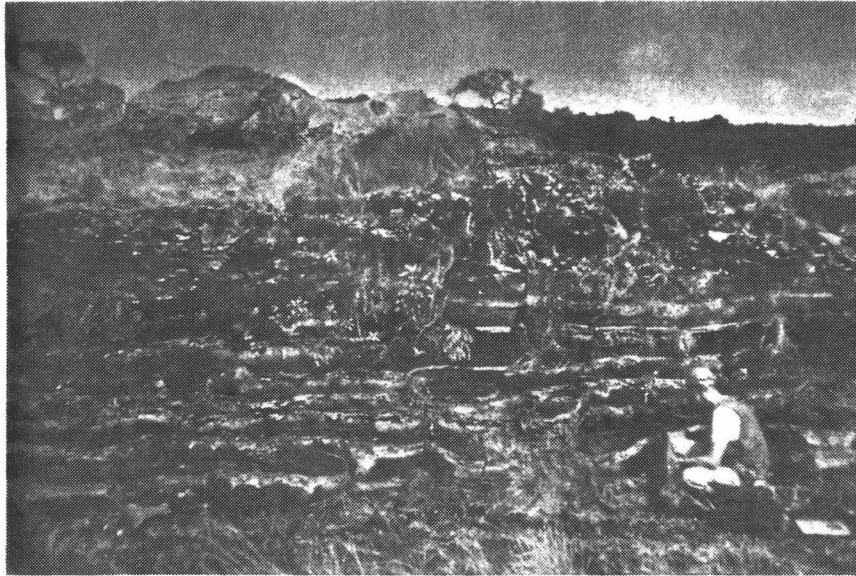


Figure 2.5. Photograph of numerous sheet-like overflows from the channel/tube system exposed in a roadcut cut perpendicular to the direction of flow.

rectilinear blocks, twenty seven samples of the top few cm yield an average density of 1.10 g/cm^3 , which corresponds to a vesicularity of 68% (based on a non-vesicular Pohue Bay sample with a density of 3.4 g/cm^3).

At their source (the channel edge), the surfaces of these pahoehoe flows are very smooth, and rarely have a "ropy" texture (Figure 2.6). This is interpreted to mean that the viscosity of the flowing lava here was extremely low, and that any flow-induced disturbances (ropes or wrinkles) could quickly relax before the skin was able to cool to the point that it would preserve them. Much of the surface is characterized by numerous cooling joints to form "prisms" $5\text{-}10 \text{ cm}^2$ in area, and $5\text{-}10 \text{ cm}$ deep (Figure 2.6). The close spacing of these joints fits an overall trend observed in pahoehoe lavas; extensive field observations have shown that the size and spacing of polygonal cooling joints show a relationship to the vesicularity (the higher the vesicularity, the smaller and more closely-spaced the cooling joints; GPL Walker, pers. comm.).

Overflows very similar to those of the Pohue Bay flow occur in the channel-fed portion of the 1859 Mauna Loa lava flow. One of these is located $\sim 40 \text{ km}$ from the vent (see photograph figure 2b in Walker 1989). Thus, even though the 1859 lava had rapidly traveled 40 km in an open channel, it still contained up to 70% vesicles by volume (Walker 1989). The fact that the channel lava was actually feeding an a'a flow front is instructive because it illustrates the sometimes confusing combination of smooth-surfaced lava (which might be considered as pahoehoe) flowing in

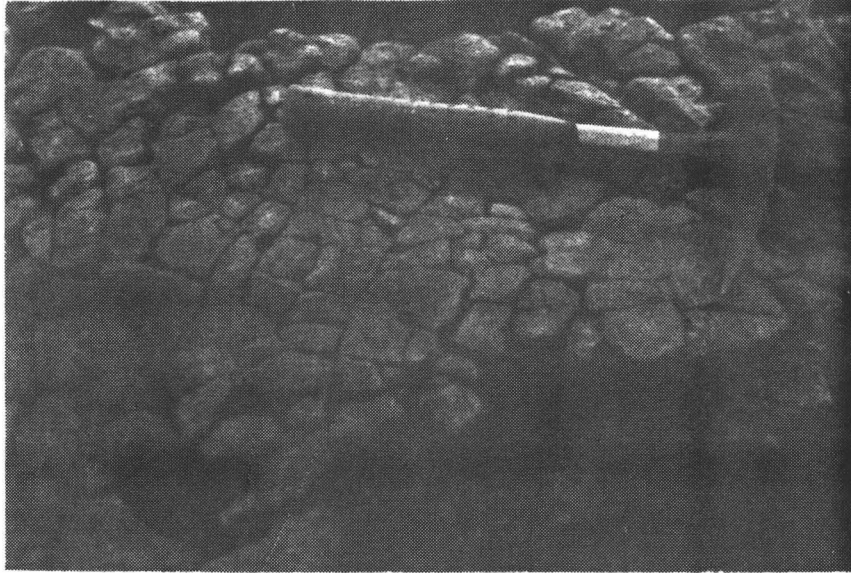


Figure 2.6. Photograph of closely-spaced cooling joints in the surface of a sheet-like overflow. Note the absence of ropy structures. In the dark area at lower left, the top 1-2 cm has spalled off; the light specks are olivines.

and overflowing from a channel that is feeding an a'a flow front. The incandescence and extreme radiant heat means that the apparently smooth flowing surface is actually being continuously torn apart. This is a very efficient mechanism by which to cool the flow, and the result is invariably a'a at the flow front.

At the edge of the Pohue Bay flow channel/tube skylights, these overflows therefore consist of very thin pahoehoe flow units that may be up to 50 m wide. Evidence presented later suggests that these flows were thicker at the time of formation, and that their present thinness is a result mainly of deflation by draining away downslope. In Hawaii, aspect ratios (thickness:width) of pahoehoe flow units typically vary between 1:3 and 1:10, and decrease with overall flow unit size (GPL Walker, pers. comm.). Measured aspect ratios of the Pohue Bay overflows are as small as 1:45 (Figure 2.7). These overflows differ in an additional way from typical tube-fed pahoehoe flow fields in that they generally are not subdivided into numerous toes (Figure 2.7). This sheet-like nature compared to the more common subdivision into small flow units is an indication of a higher volumetric flow rate during emplacement.

One pahoehoe overflow was examined in detail where it is exposed in a roadcut (Figure 2.7). This flow is 22 m wide, and has an average thickness of about 50 cm. The outcrop is approximately perpendicular to the direction of flow and located about 50 m from the edge of the channel from which it issued. It has a flat upper surface and an irregular bottom. These are

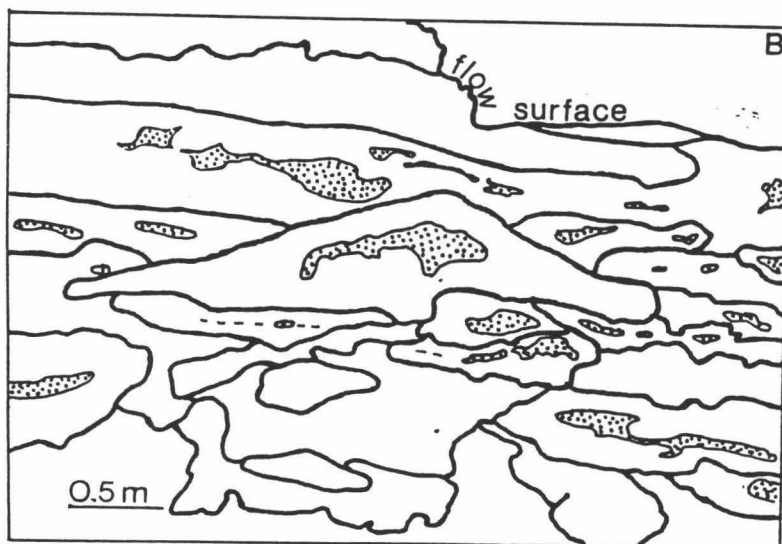
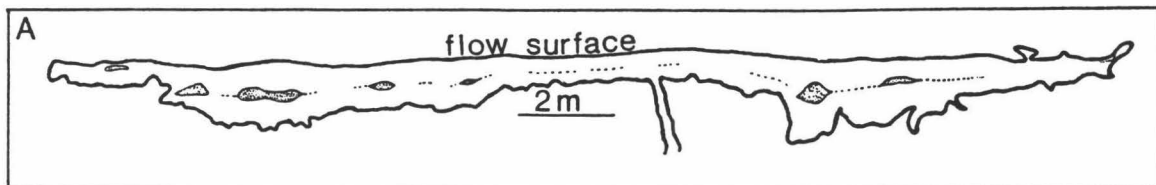


Figure 2.7. Diagrams showing A: a roadcut perpendicular to a pahoehoe overflow (viewed upflow) in the study area 200 m from the E end of Menehune Dr. (see Figure 2.2), and B: roadcut through a typical tube-fed pahoehoe flow (Mauna Ulu, Kilauea). Note the differences in the sizes and number of flow units in these roadcuts. Stipple indicates void space which in A consists of gas blisters, and in B of drained single flow-unit tubes.

indications of its low viscosity when emplaced; upper-surface irregularities could not be maintained or supported, and the lava showed a strong tendency to fill in even small depressions over which it flowed. The morphology of this flow unit contrasts strongly with that of tube-fed pahoehoe (Figure 2.7).

Overflows are very common from tubes and channels in Hawaii, and they characteristically form thin smooth-surfaced sheets. The examples of the Pohue Bay flow are, however, exceptionally extensive and have transported and stranded very large lava balls.

Layered lava balls

The layered lava balls carried by the overflows of the Pohue Bay flow were up to 5 m in diameter (Figure 2.8). Such layered lava balls are commonly found on channel levees in Hawaii, and have been observed floating down active channels (e.g. "lava boats"; Lipman & Banks 1987). They form when pieces of vent structure, channel wall, or tube roof fall into the flowing lava (Figure 2.9). As they are carried along they roll and tumble in the lava stream and accrete layers of lava up to 10 cm in thickness. They float because the internal cavities and spaces between layers provide enough void space to give them a slight positive buoyancy. During large overflows these large lava balls are washed out of the channel/tube. The resulting structures are rounded, concentrically-layered lava balls draped with a layer of the overflow lava. Most are deposited within 100 m of the channel edge. These balls are the pahoehoe equivalent of previously-



Figure 2.8. Photograph of layered lava balls ~50 m from their source channel. In the upper photo, one lava ball (arrow) has cracked open to reveal an interior of numerous thin layered flows (lower photo). It is probably a section of overflow levee which broke off and fell into the active channel.

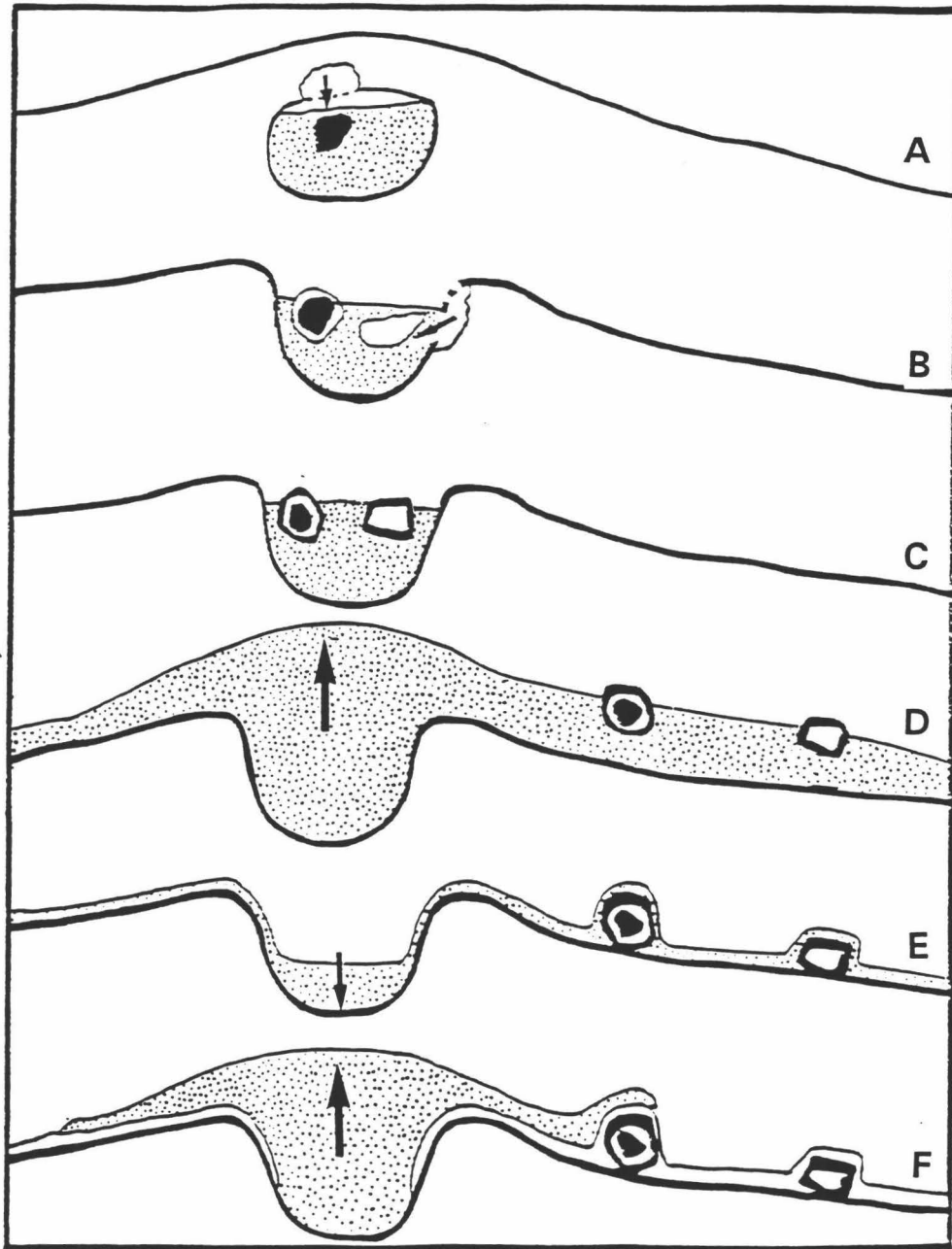


Figure 2.9. Diagrams to show the formation of a layered lava ball. Stipple indicates flowing lava. Pieces of tube ceiling (A) or channel wall (B) fall into the flowing lava and are carried downstream (C) where they accumulate layers of lava. Surges or overflows wash the layered balls out of and away from the channel (D). When the overflow drains away it leaves a thin layer of lava on the lava balls (E). Later overflows slosh over pre-existing lava balls (F).

described accretionary lava balls (e.g. Wentworth & Macdonald 1953; Macdonald *et al.* 1983), which form on a'a flows.

The sizes of the lava balls yield information about the depths of the overflows as they leave the channel/tube. If it is going to lift a lava ball out of a channel, an overflow must be at least as deep as the diameter of the lava ball it is carrying since the balls protrude very little above the surface when floating (Lipman & Banks 1987). Once out of the channel, the lava balls can be pushed along by much thinner flows, especially since the ground surface slopes away from the channel. The balls have diameters of 2-5 m and were brought out of the channel by overflows having final present thicknesses at the channel edge of only 30 cm. This ~10-fold decrease in thickness is due to the ability of these fluid overflows to drain quickly downslope away from the channel, preserving only thin skins at the top and bottom. Some of the layers on the lava balls appear to have been deposited by later overflows after the lava balls reached their final positions, meaning that the lava sheet had a low viscosity and must have been moving very quickly in order to slosh over 2-m high balls and leave only a thin veneer. These later overflows do not completely surround the lava balls, but only occur on their upslope sides. This indicates that they were not emplaced by a thick flow that then drained away, but rather by a fast-moving flow that was thinner than the diameter of the ball.

Transitions to a'a and pahoehoe

At varying distances from their source at the channel, many of the overflows at the Pohue Bay flow became unable to maintain their pahoehoe character. They formed thin a'a flows 1 to 3 m thick, some with surfaces consisting almost entirely of broken and jumbled pahoehoe fragments and others with surfaces of true clinker (Figure 2.10). This was the transition to "slab pahoehoe" or "slab a'a" noted by Peterson & Tilling (1980), and occurred because the pahoehoe flows continued to move after their outer skins could no longer deform plastically. They developed a surface of broken lava fragments. The formation of clinker is also an indication that the lava immediately under the surface cooled to the point that its viscosity did not allow it to well up and heal the ruptures in the surface skin. These unhealed ruptures allowed further heat loss, and the transition to a'a was inevitable. Some of the flows made a further transition to clinkery a'a of the proximal type (Rowland & Walker 1987), wherein not only did an original pahoehoe surface become fragmented but the pasty interior lava just under the rubble layer began to be disrupted into clinkers.

It is important to note that the carapace of broken pahoehoe fragments and clinkers gives an indication only of conditions in the uppermost portions of the overflows. After the overflows came to rest, the lava in the interiors welled up onto the surfaces or out of the flow fronts as pahoehoe (Figures 2.10 & 2.11). This "second generation" pahoehoe was characterized by much larger and less uniform-sized vesicles than the original overflows and tended to subdivide into toes, as is more common for pahoehoe lava.

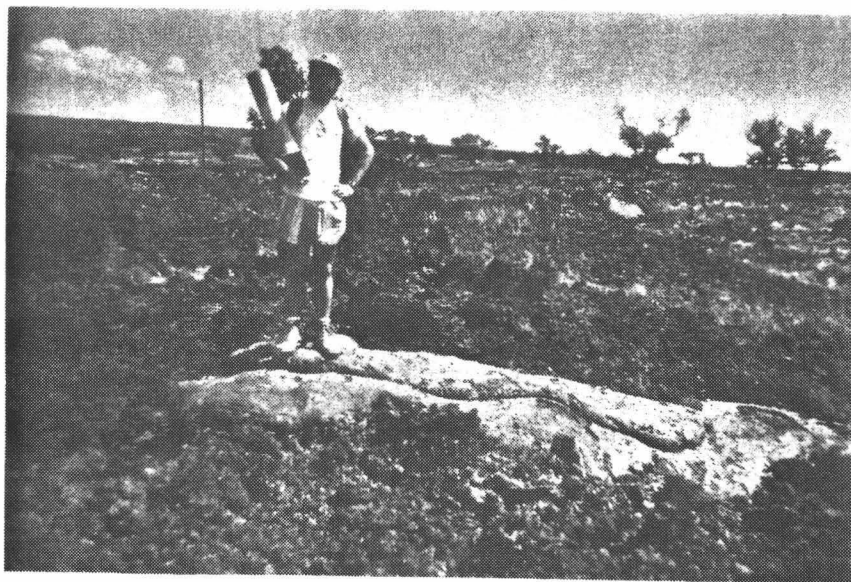


Figure 2.10. Photograph of a'a and a small flow unit of pahoehoe that issued out of it. Note that the a'a flow surface is true clinker and not just broken fragments of pahoehoe.



Figure 2.11 a. Photograph showing pahoehoe that issued out of the top of an a'a flow. This pahoehoe came out from a point under where person is standing and flowed towards the right.

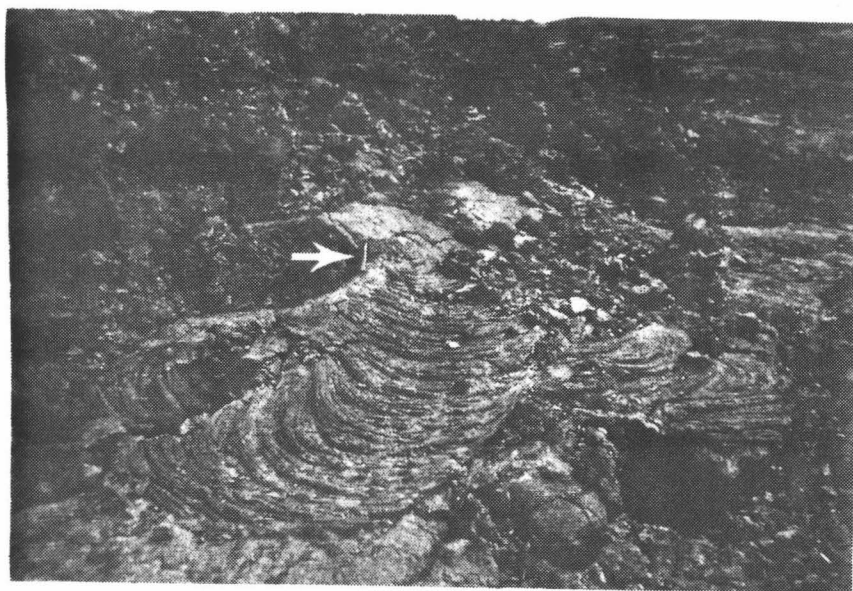


Figure 2.11 b. Lobe of ropy pahoehoe that issued out of an a'a flow (note hammer for scale).

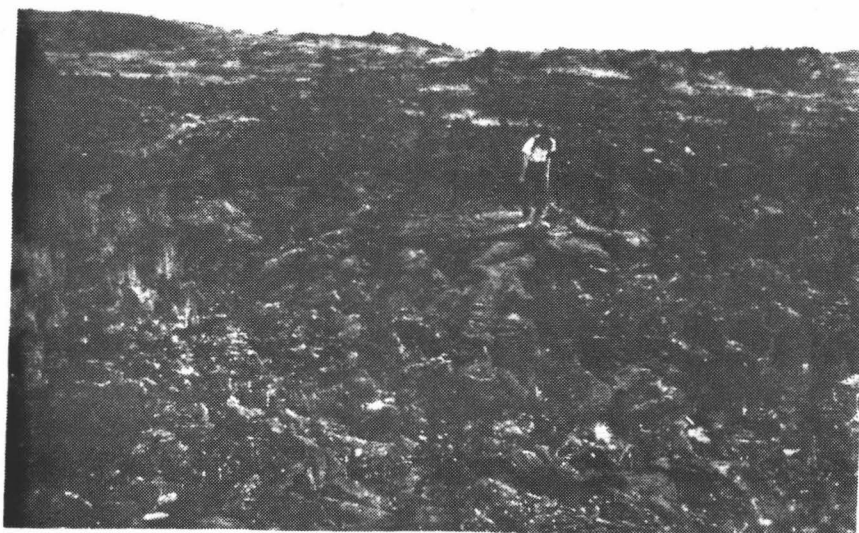


Figure 2.11 c. Photo of pahoehoe lobes that issued from a slabby pahoehoe flow.

Twelve samples of the top few cm yield an average density of 1.44 g/cm^3 , 29% higher than the original overflow samples, and corresponding to 58% vesicularity. These two observations indicate that while flowing away from the channel the lava lost 15% of its gas bubbles, and importantly, that the breaking out of the molten interior lava onto the surface took place at a much lower volumetric flow rate than the initial overflow. This also shows that if lava character is defined by flow surface alone, an initial pahoehoe overflow can make the transition to a'a, and then "back" to pahoehoe (Figure 2.12). It might be argued that if a flow has an interior capable of producing pahoehoe, it is not an a'a flow even though it possesses a clinker surface. In this study flows with clinker surfaces are considered a'a because their surface morphologies (clinker and broken pahoehoe) record rapid and vigorous flow activity that is characteristic of a'a (Rowland & Walker 1990).

In the scenario above, no particular element of lava would go from pahoehoe to a'a back to pahoehoe. To illustrate this the histories of 3 separate elements of lava within an overflow are presented. Diagrams show qualitatively the variation in viscosities and volumetric flow rates of different parts of the flow (Figure 2.13; after Kilburn 1981), and illustrate their separate evolution. The first element represents lava that formed the smooth skinned flow near the edge of the channel. It was initially moving rapidly but soon stopped. It cooled and solidified while stagnant and thus retained its pahoehoe character as it solidified (e.g. Peterson & Tilling 1980).

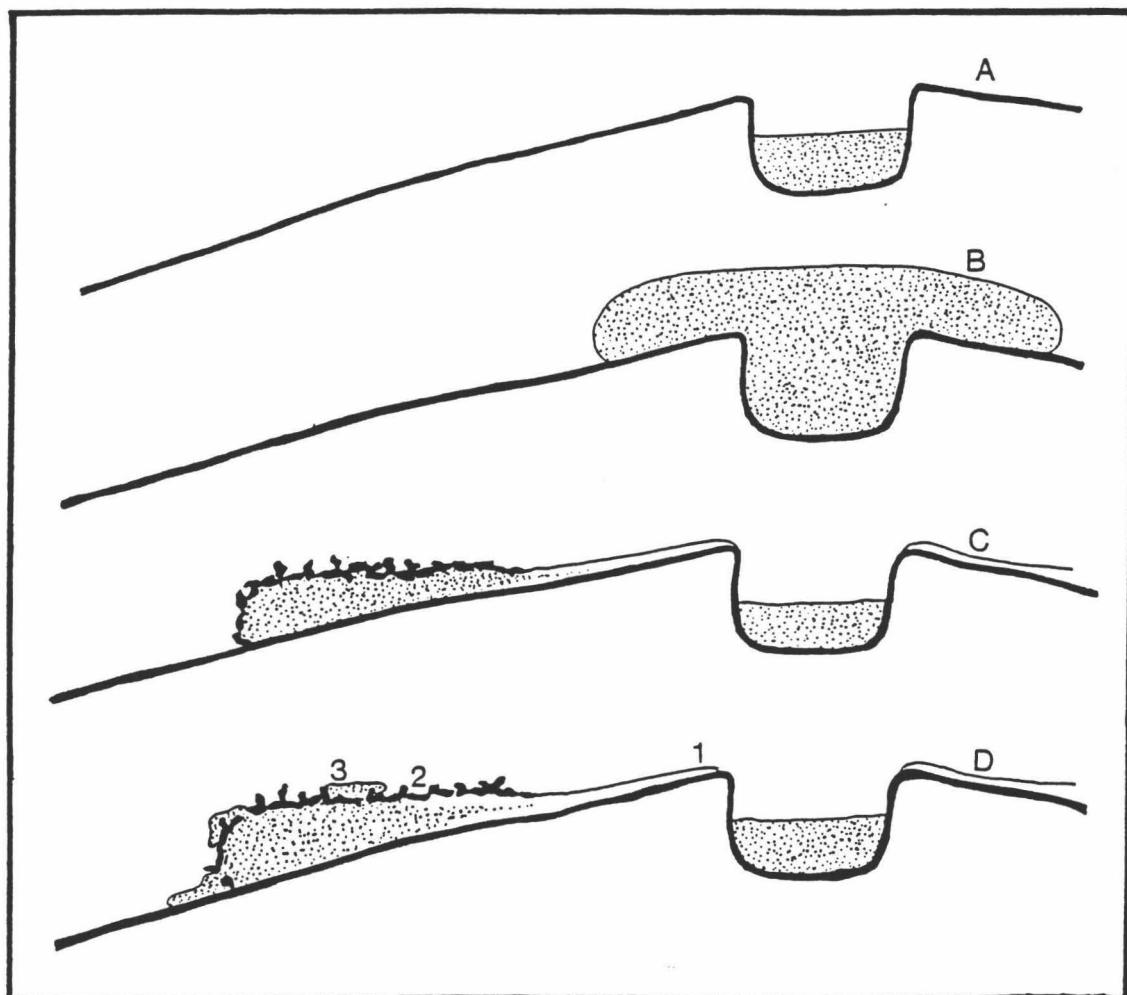


Figure 2.12. Diagrams to show a channel overflow making the transition from pahoehoe to a'a to pahoehoe. Stipple indicates fluid lava, and numbers show the final positions of elements 1, 2, and 3 (see text and Figure 2.13).

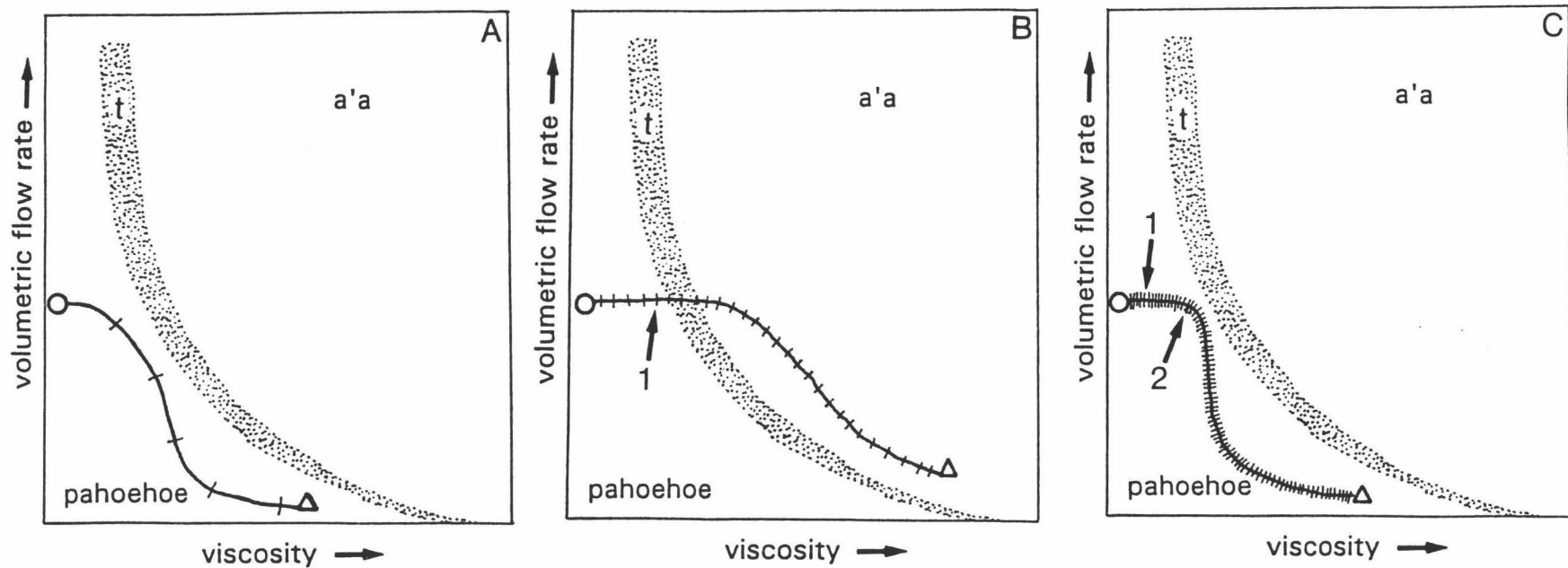


Figure 2.13. Qualitative graphs (after Kilburn 1981) to show the viscosity and volumetric flow-rate paths of different elements of an overflow. Fields of pahoehoe and a'a are shown, as well as the irreversible transitional boundary between them (t). Each lava element is erupted simultaneously at the circle and follows its own path to solidify at a triangle. The hatch marks represent arbitrary units of time and have equal values in A, B, and C. A: element 1 flows for only a short time and comes to rest as pahoehoe long before it gains a high viscosity due to cooling. B: element 2 flows at a high volumetric flow rate for a longer period of time and continues to flow after it has cooled to a viscosity that results in a'a. Arrow indicates "time" at which element 1 stopped flowing. C: element 3 flows for an even longer period of time but being the flow interior, it maintains a low viscosity. When the volumetric flow rate eventually drops and element 3 oozes to the surface it forms pahoehoe. Arrows indicate "times" at which elements 1 and 2 stopped flowing.

The second element of lava is one that became part of the skin of the flow after the lava had traveled a few tens of meters away from the channel. This lava cooled during this movement, and once it became part of the surface crust it cooled even faster. It was in a part of the flow that was still moving rapidly, so unlike the first element it was not allowed to cool through higher viscosities without being disturbed. Because it was forced to flow after it had lost the ability to easily deform, it instead broke apart to form the a'a surface of pahoehoe fragments and clinkers.

The final element of lava is one that remained in the interior of the overflow until the initial movement away from the channel stopped. It underwent some gas loss but minimal cooling during the trip. After the overflow lost its initial momentum, it started to spread because of its own weight; the flowage was accomplished by the still-fluid interior lava. Any lava that broke to the surface during this slow deformation still had a relatively low viscosity and having a low volumetric flow rate, formed pahoehoe. This scenario attempts to portray the significant differences between the conditions on the surface and in the interior of an active lava flow. It retains the idea that the pahoehoe-a'a transition is irreversible for any particular element of lava. It allows, however, for pahoehoe lava to erupt out of a flow that had earlier developed an a'a carapace.

TOOTHPASTE LAVA AND CLEFT STRUCTURES

Although not directly associated with the channel overflows discussed above, clefts (similar to crease structures; Anderson & Fink 1992) and

patches of toothpaste lava found within large a'a flows are also good evidence of the strong contrast between the processes that affect surface and interior lava (Figure 2.14). Toothpaste lava is considered to be lava with the viscosity of proximal-type a'a, but which has not undergone sufficient disruption and cooling to be torn into clinkers (Rowland & Walker 1987). Calculated viscosities for a'a/toothpaste lava range between 7000 and 12,000 Pa-sec, half to one order of magnitude higher than most pahoehoe (Rowland & Walker 1988).

Cleft-like structures consisting of toothpaste lava (Figure 2.14) provide a glimpse of the character of the lava that makes up the core of a proximal-type a'a flow. These structures are either squeeze-ups with axial clefts or pull-apart features, and form during secondary spreading of an already-emplaced flow. The clefts can be 1-2 m deep with surfaces that can be either steeply- or gently-dipping into their axes. The spines that occur on the surface of the toothpaste lava in the clefts are always perpendicular to the long axes of the clefts, are formed as pasty lava is pulled apart during spreading, and are indicators of the direction of opening. This direction varies depending on where the cleft develops within the flow. Those near the margins tend to be parallel to the margins because secondary flowage here is dominated by lateral spreading. In more medial positions, secondary flowage is usually in the downhill direction so that the clefts develop their long axes perpendicular to this.

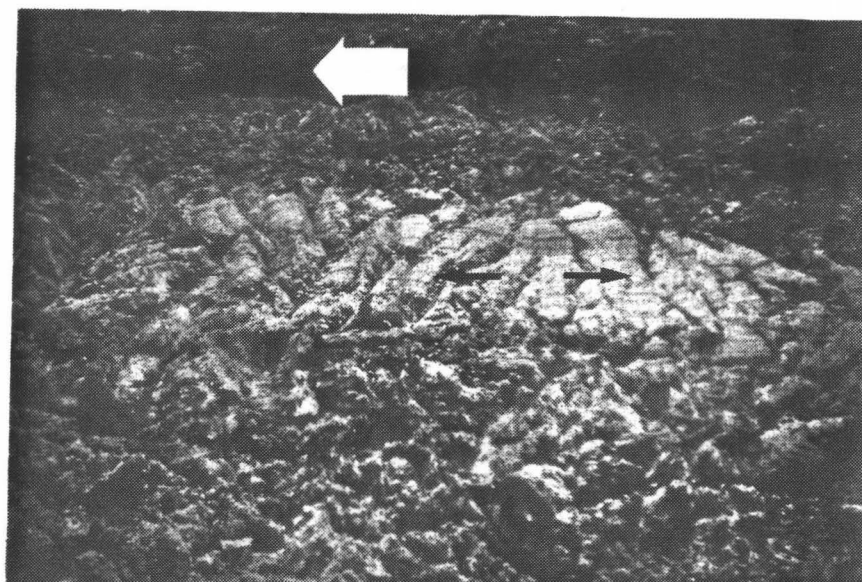


Figure 2.14. Photograph of a toothpaste lava cleft within a portion of the Mauna Loa 1984 a'a flow. The small arrows show the opening direction of the cleft, and the large arrow indicates the overall flow direction.

IMPORTANCE OF CHANNEL OVERFLOWS

In Hawaii, pahoehoe lava can in general be found in three locations: 1) near vents; 2) forming tube-fed flows; and 3) along the channels of flows that are often otherwise mostly a'a. Near-vent pahoehoe contains a large proportion of gas bubbles, which when they coalesce form the hollow voids of "shelly" pahoehoe (e.g. Swanson 1973). In Hawaii, tube-fed pahoehoe is usually erupted at low volumetric flow rates (Rowland & Walker 1990), and only sometimes, when encountering a steeper slope does it make the transition to a'a. In most cases, however, tubes develop over steep slopes; some of the Mauna Ulu flows (Kilauea volcano, 1969-1974) maintained their tube-fed pahoehoe nature during and after flowing over the $\sim 40^\circ$ slope of the Hilina Pali fault scarp (Swanson *et al* 1979; Tilling *et al.* 1987).

Pahoehoe overflows associated with high volumetric flow-rate (a'a-producing) lava flows are always closely associated with lava channels. Although not as well-insulated as a lava tube, a well-developed channel does provide an efficient pathway for flowing lava. Flowing at velocities of up to a few tens of km/hr, lava can travel tens of km still maintaining some of its near-vent attributes such as high gas content and temperature. The requirements for the pahoehoe-to-a'a-to-pahoehoe transition described above are a large overflow that quickly loses its initial momentum; if the rapid flow continues for very long, the interior lava also loses the ability to deform easily and no "second generation" pahoehoe can form. The

overflows from high volumetric flow-rate channels are therefore best suited for forming the double-transition lavas described in this chapter.

CONCLUSIONS

I have described a number of flows and flow features that illustrate the significant differences between the interiors and surfaces of active flows (e.g. Fink & Fletcher). These lead to different reactions to the stresses imposed during the flow emplacement process. In certain situations, namely high volumetric flow-rate overflows from large channels, they can lead to the appearance of pahoehoe forming from a'a. The low viscosity allows the interior lava to withstand the high volumetric flow rate long enough for the initial momentum to dissipate. The interior of the lava is then still fluid enough to form pahoehoe during the low volumetric flow-rate deformation of the emplaced overflow.

CHAPTER III

THE FORMATION OF CIRCULAR LITTORAL CONES

SUMMARY

A study is presented of a number of pyroclastic cones along the southwest coast of Mauna Loa volcano, Hawaii. These features tend to have a common structure, namely an early-formed circular outer rim composed mostly of scoria and lapilli (with some dense spatter and angular lithic fragments), and one or more later-formed inner rims composed almost exclusively of dense spatter. In some examples, the spatter activity fed short lava flows that ponded within the outer rims.

These cones appear to be littoral in origin based on their coastal locations, field relationships, chemistry, and paleomagnetic considerations. Their overall structure, however, contrasts with that of "standard" Hawaiian littoral cones (exemplified by Pu`u Hou and Sand Hills on the Island of Hawaii) mainly in that there is (or once was before erosion) a complete circle of pyroclastic deposits (instead of half cones on either side of the flow). Further they are associated with tube-fed pahoehoe flows instead of a'a. These cones are closely associated with large lava tube/channel systems that had calculated volumetric flow rates of 1000-5600 m³/sec. The vigorous mixing of large volumes of lava and water at a point inland from the coast was required to form them. It is postulated that an initial flow of lava into the ocean built a lava delta having a base of hyaloclastite. Collapse of the active tube into the wet underlying hyaloclastites allowed

sufficient mixing of water and liquid lava, generating strong explosions. These explosions broke through the top of the flow field and built up the outer ejecta rims on the solid carapace of the lava delta. The mixing ratios of lava and water varied generating both spatter and fine lapilli. Eventually the supply of water diminished and the explosions declined in intensity to low spattering. This late-stage activity filled the initial pyroclastic rings with spatter and/or lava.

INTRODUCTION

Littoral cones develop around secondary or rootless vents as a result of steam explosions that take place when lava flows into the ocean (e.g. Moore & Ault 1965; Macdonald 1972; Fisher & Schmincke 1984). Secondary vents formed by lava flowing into lakes, streams, or marshes are not littoral cones *sensu strictu* but are closely related in origin (e.g. the "pseudocraters" of Iceland; Thorarinsson 1953; Morrissey & Thordarson 1991; Thordarson & Self 1993). On the island of Hawaii there are about 50 littoral cones along the coastlines of Mauna Loa and Kilauea volcanoes (Moore & Ault 1965). Three of the largest formed during the 1840 eruption of Kilauea and the 1868 and 1919 eruptions of Mauna Loa, all of which were associated with channelized high discharge-rate flows. Additionally, small littoral deposits were formed during the tube-fed pahoehoe eruptions of Mauna Ulu and Kupaianaha (Kilauea) in 1969-74 and 1986-91, respectively (e.g. Moore *et al.* 1973; Peterson 1976; Heliker & Wright 1991;

Thordarson & Self 1991; Sansone & Resig 1991a; 1991b). The littoral cones formed during the Kupaianaha phase were rarely >2 m high, and developed on the lava bench just inland of the ocean entries.

When a flow enters the ocean, the hot and liquid lava rapidly converts water into steam, which may expand non-explosively (passively) or explosively depending on the rate at which heat is transferred from lava to water. Explosive vaporization of water fragments the lava leading to accumulation of volcanoclastic debris. Water can also come into contact with flowing lava within the lava-tube system of pahoehoe flows and produce explosions landward of the actual ocean entry. In most cases explosions are small and no significant pyroclastic cones develop. Occasionally, however, substantial cones are constructed. The most often cited form of a Hawaiian littoral cone consists of two half cones approximately equal in size on either side of the lava flow that led to their formation (e.g. Fisher 1968; Fisher & Schmincke 1984; Figure 3.1). Additionally, they are usually considered to be associated with a`a lava flows (Macdonald 1972; Macdonald *et al.* 1983). With an a`a flow, even though material may be thrown out in all directions from the point of the explosions, any fragments that land on the flow itself are carried into the ocean. They can then be redistributed by currents either offshore or along the coast to form beaches.

This chapter describes several cones, previously described as littoral (Moore & Ault 1965), that consist of more or less complete pyroclastic cones instead of pairs of half cones, and they are related to tube-fed pahoehoe rather than a`a lava.

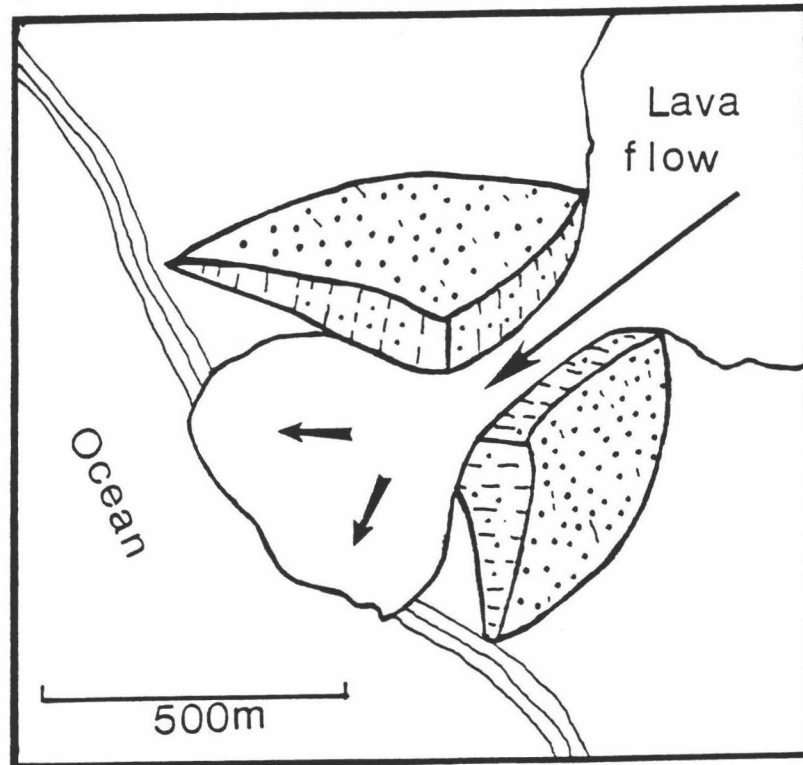


Figure 3.1. Diagram of a "standard " littoral cone (from Fisher & Schmincke 1984). Note that two half cones (stippled) form on either side of the flow.

THE FIELD AREA

The field area consists of the southwest coastline of the island of Hawaii (Figure 3.2) from near Ka Lae (South Point) to the northernmost 1950 Mauna Loa lava flow. In the southern portion the land surface slopes gently to the coastline, with a near-horizontal ($\sim 1^\circ$) coastal terrace up to 3 km wide. Littoral cones are common in this area, and 10 clusters of them were mapped by Moore & Ault (1965), although one of these, Pu`u Mahana on the southeast coast, is a primary Surtseyan vent rather than a littoral cone (Walker 1992). One of the largest littoral cones in the area is Pu`u Hou (actually a complex of three half cones), which formed when one of the flows of 1868 entered the ocean (Fisher 1968). The group of cones within the Pohue Bay flow (Jurado *et al.* 1991) is distributed along about 3 km of coastline and consists of at least 6 cones in various states of erosion and burial. The olivine-phyric Pohue Bay flow, which consists mostly of tube-fed pahoehoe on the coastal terrace, was considered 740-910 years old by Lipman & Swenson (1984). However, paleomagnetic work (see below) gives an age closer to 2700 years. The two northernmost members of this group (Pu`u Ki and the informally named Three-rim Cone) are presented in detail. Seven km north of the Pohue Bay group is another cluster of cones, the largest of which is Pu`u a Pele. About 25 km up the coast from the Pohue Bay group the slopes of the volcano become steeper, and the coastal terrace narrows to several hundred meters wide (or at places is not present at all). `Au`au cone (the third cone that is described in detail) is located almost 40 km up the coast from the Pohue Bay group, and is situated on

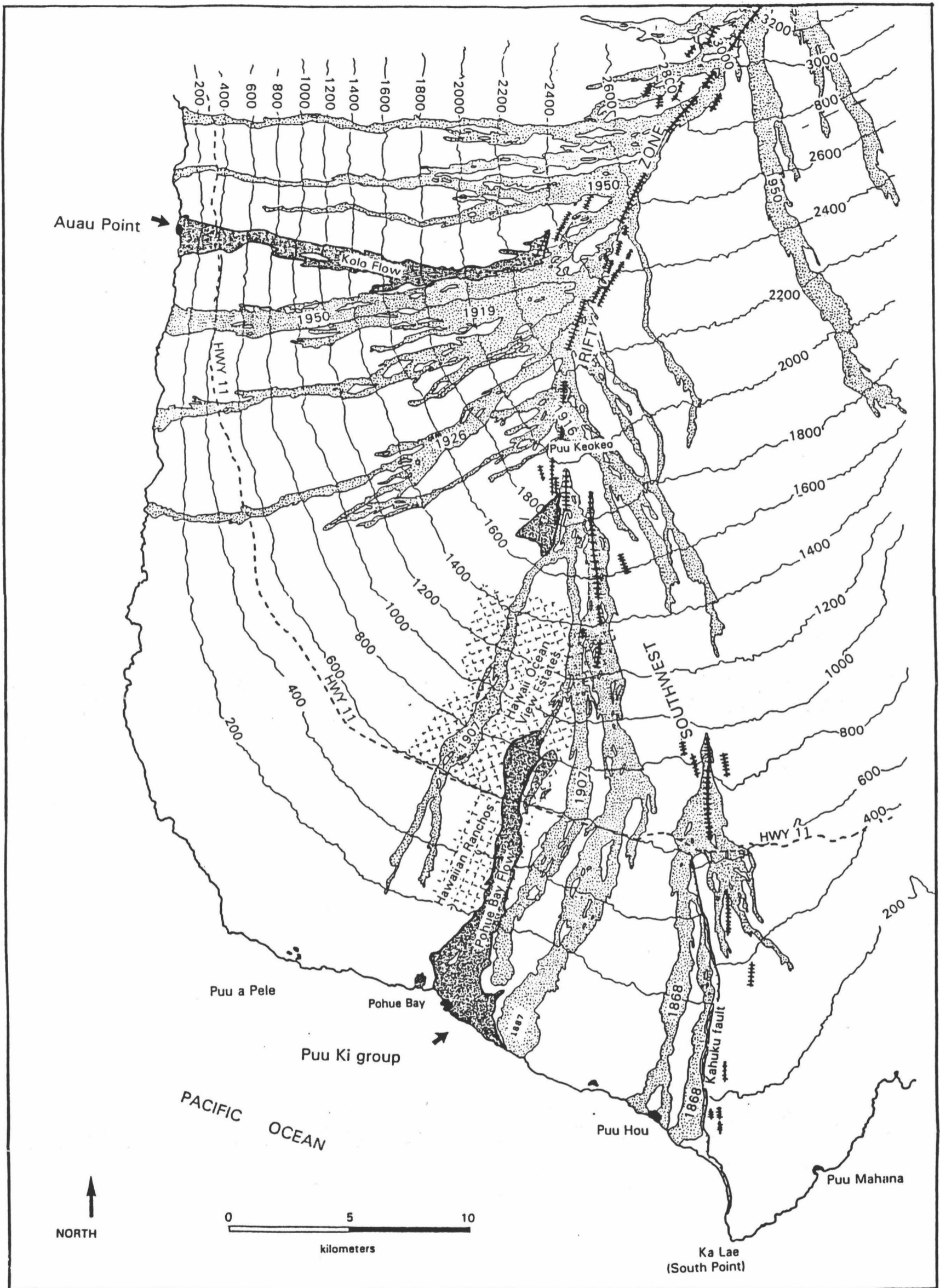


Figure 3.2. Location map of historic lava flows of Mauna Loa's SW rift (light stipple) and the prehistoric Kolo and Pohue Bay flows (darker stipple). Arrows indicate areas studied in detail. Traced from Lipman & Swenson (1984). Contour interval 200m. Elevation in meters above sea level.

one of these narrow coastal terraces. It is ~2 km north of the northern margin of the southernmost flow of 1950, near the center of the ~750 year old Kolo flow (Lipman & Swenson 1984; Figure 3.2).

The climate in the study area is dry and hot and vegetation consists only of scattered bushes and grass. Wave-cut coastal exposures are completely non-vegetated, and access to the cones is easy. Some cones, however, are on private land and require prior permission to visit.

DESCRIPTIONS OF THE CONES

The cones of the Pohue Bay flow area (the three-rim cone and main Pu`u Ki cluster) and the `Au`au cone of the Kolo flow have, in general, the same structure, namely an outer rim of scoria and lapilli (with scattered blocks and bombs) surrounding one or more inner rims of dense spatter and/or ponded lava. Each, however, presents specific relationships that help to piece together the mechanism of circular littoral cone formation.

Three-rim cone

The first example is located ~2 km southeast of Pohue Bay and has been informally named the Three-rim Cone. The largest rim remnant is crescent-shaped (concave towards the ocean), about 300 m long parallel to the coast and about 80 m wide perpendicular to the coast (Figure 3.3). The highest point is roughly in the middle of the crescent and has an elevation of ~23 m above the surrounding area. The "arms" of the crescent slope to the level

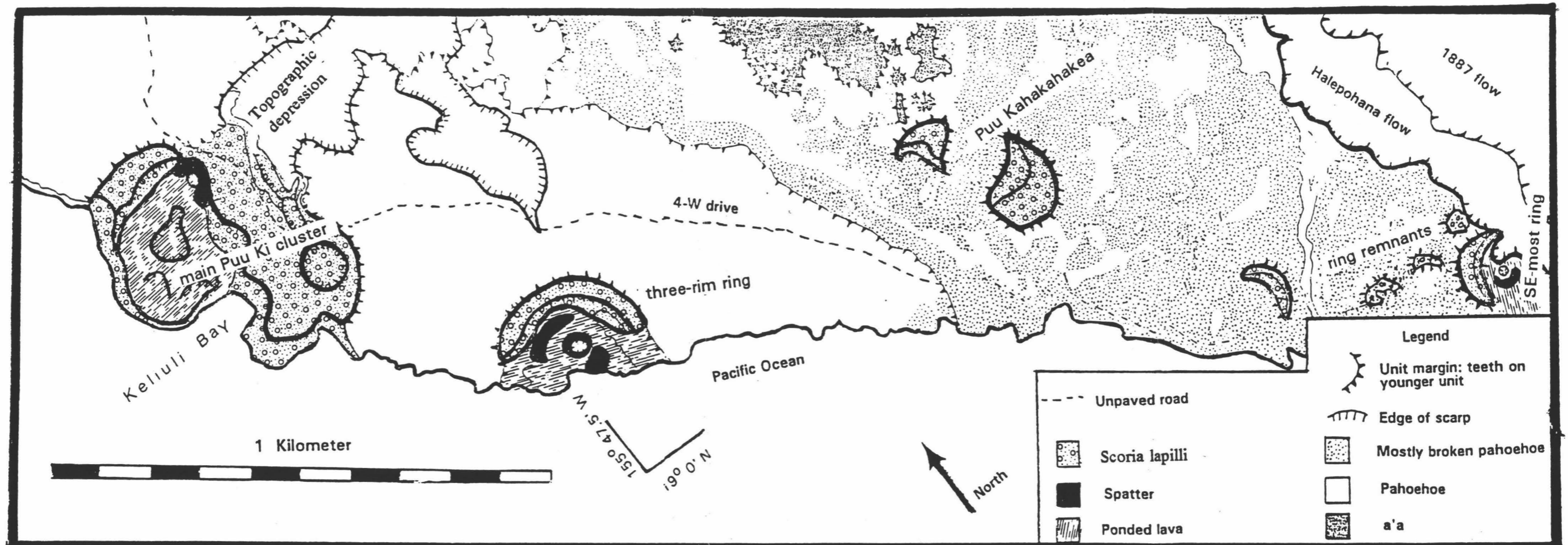


Figure 3.3. Detailed geologic map of the coastal cones within the Pohue Bay flow.

of the surrounding surface at both ends (Figure 3.4). Pahoehoe lava of the Pohue Bay flow wraps around and overlies the landward side of the crescent and slopes ocean ward ending at a low sea cliff ~10 m high. Although this outer rim is not complete now, it is inferred to have been upon formation (see below) and has since been eroded by wave action.

The main outer rim consists mostly of fine lapilli with numerous blocks and bombs up to a meter in diameter. It is poorly lithified and poorly stratified into layers that roughly parallel the outer surface. These layers are truncated by and poorly exposed in the inner surface. The layers of lapilli are 10-20 cm thick and partially palagonitized. There are also a few layers of coarser spatter-like material that comprise more resistant layers of the main rim. Blocks and bombs up to a meter across are commonly found within the lapilli layers. Most of the inner face of the main outer rim consists of wind-blown material which in places has formed a duricrust.

The second and third (inner) rims of the three-rim cone are distinctly different from the outer rim. They are only a few m high and consist entirely of large dense spatter. They define the locations of spatter vents that were active during the eruption. Field relations show that the two inner rims were complete cone structures upon formation, but are now partially truncated by the sea cliff. The original diameter of each was about 150 m. Besides these inner spatter rims, much of the area enclosed by the outer rim consists of lava that flowed from these spatter vents and ponded in what must have been a closed depression formed by the once-complete outer rim. Near the center of the main ponded lava is a small collapse pit indicating subsidence at the end of the activity. The spatter and flows from the inner

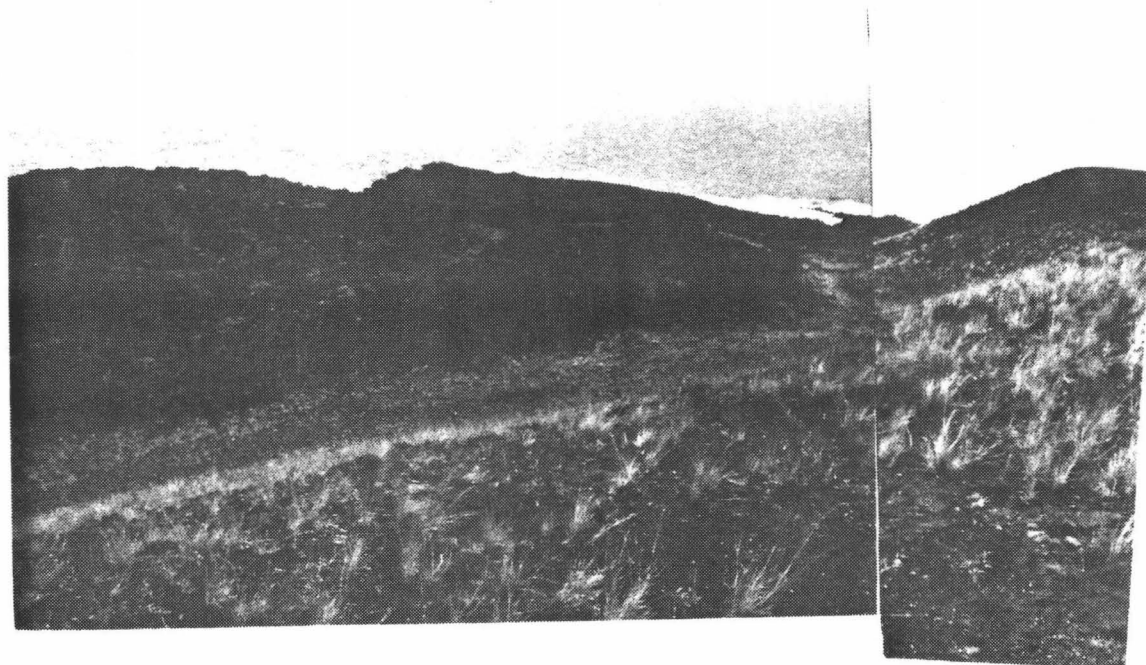


Figure 3.4. Photograph of the three-rim cone (looking ocean ward) showing the outer rim formed of lapilli and spatter (with grass), an inner rim formed of spatter, and a central spatter vent (both unvegetated).

rims overlie the Pohue Bay flow at the NW and SE ends of the main rim (Figure 3.3).

The spatter lumps of the inner rims average about 20-30 cm in size, although some are as large as 1.5 m across. A few of them are ribbon-like, about 10 cm wide and up to 3 m long. The spatter is for the most part confined to the inner rims and the ponded zone but scattered spatter can be found on the inner and outer slopes and crest of the main rim. Importantly (see below), a few spatter lumps were also thrown over the main rim to land on the surrounding Pohue Bay lava.

The sequence of the three-rim cone area is: 1) the main rim of lapilli is the oldest unit and it can be traced in the sea cliff sloping to sea level under the Pohue Bay flows; 2) the tube-fed pahoehoe of the Pohue Bay flow overlaps the main rim, banked against its entire outer perimeter to a height of 20 m above sea level; 3) the spatter and lava of the inner rims overlie both the main rim and the Pohue Bay flow.

Pu`u Ki

About 300 m NW of the three-rim cone is the main Pu`u Ki cluster. It consists of two cones and a buried remnant of a third (Figure 3.3). The southernmost of these is a cone with an outer diameter of ~200 m and a rim about 20 m above the surrounding surface of Pohue Bay lava. It is almost perfectly circular with a crater ~25 m deep (Figure 3.5). Exposed in the walls of the crater are numerous layers of spatter and large cored bombs, most of which have welded to form coherent units 1-2 m thick.

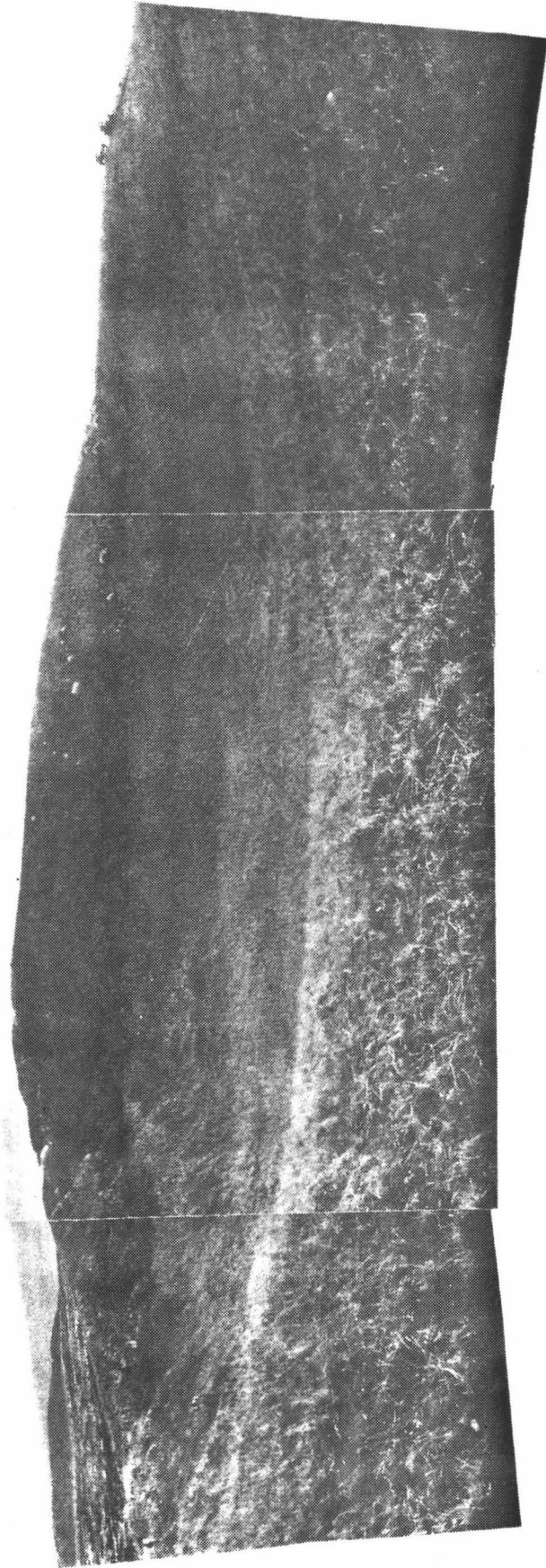


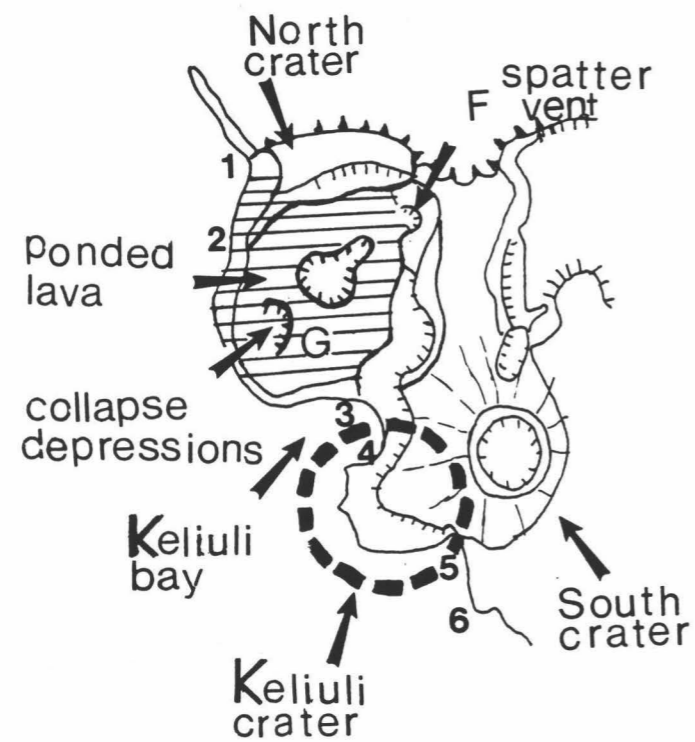
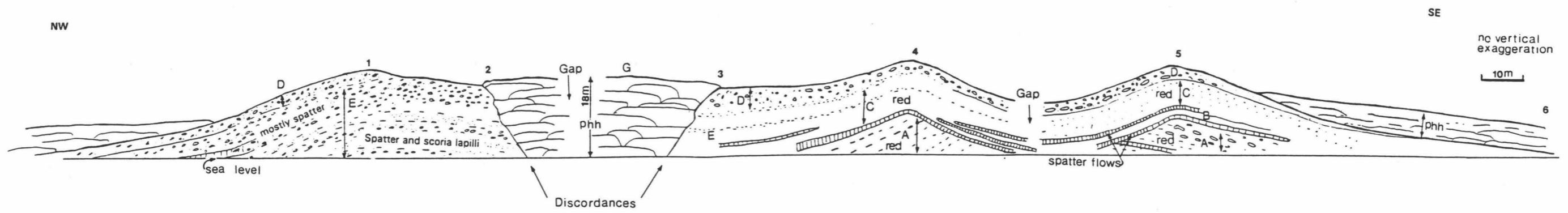
Figure 3.5. Photograph of S-most cone in the main Pu`u Ki cluster.

Lapilli-sized material in this southernmost cone is relatively scarce, being mostly concentrated near the top of the section.

The northernmost cone of the main Pu`u Ki cluster is a structure much like the three-rim cone in that it consists of a higher outer rim of mostly lapilli, bomb, and block-sized material surrounding inner deposits of dense spatter and ponded lavas. The highest elevation point on this outer rim is 44 m above sea level, ~20 m above the surrounding lava, and the rim diameter is about 450 m.

The structure of this main cluster is well exposed in the coastal cliffs, and a descriptive traverse from NW to SE is presented (Figure 3.6). At the NW-most exposure (location 1) the pyroclastic layers roughly parallel the ground surface (units D and E), dipping first to the north then south as they pass over the axis of the rim. To the north they are overlain by Pohue Bay lavas, and to the south they are truncated and unconformably overlain by flat-lying ponded lavas of Unit G (location 2). A small beach has formed here.

A detailed stratigraphic column of location 1 is shown in Figure 3.7. The layers can in general be classified into two types, lapilli-rich and spatter-rich (both of which are olivine-phyric), and they reflect different degrees of explosivity. One of the spatter-rich layers grades away from the cone into a spatter-fed flow extending to the north, and forms the lowest unit in the low sea cliff. This flow has an unusual texture that has been accentuated by wave action owing to the incomplete welding of the spatter lumps. This layer is more welded away from the source. It may be that the spatter lumps were mostly being thrown beyond the rim of the cone (to accumulate faster where the welded flow is now seen), or material was continually



Deposit A comprises the buried rims of the Keliuli Bay crater and consists of scoria, spatter and spatter fed lava flows.

Deposit B Spatter and spatter flows.

Deposit C Scoria fall, spatter in part welded. It contains potato-shaped cored bombs. The South Crater is the source of this deposits (from the SW thinning of the deposits).

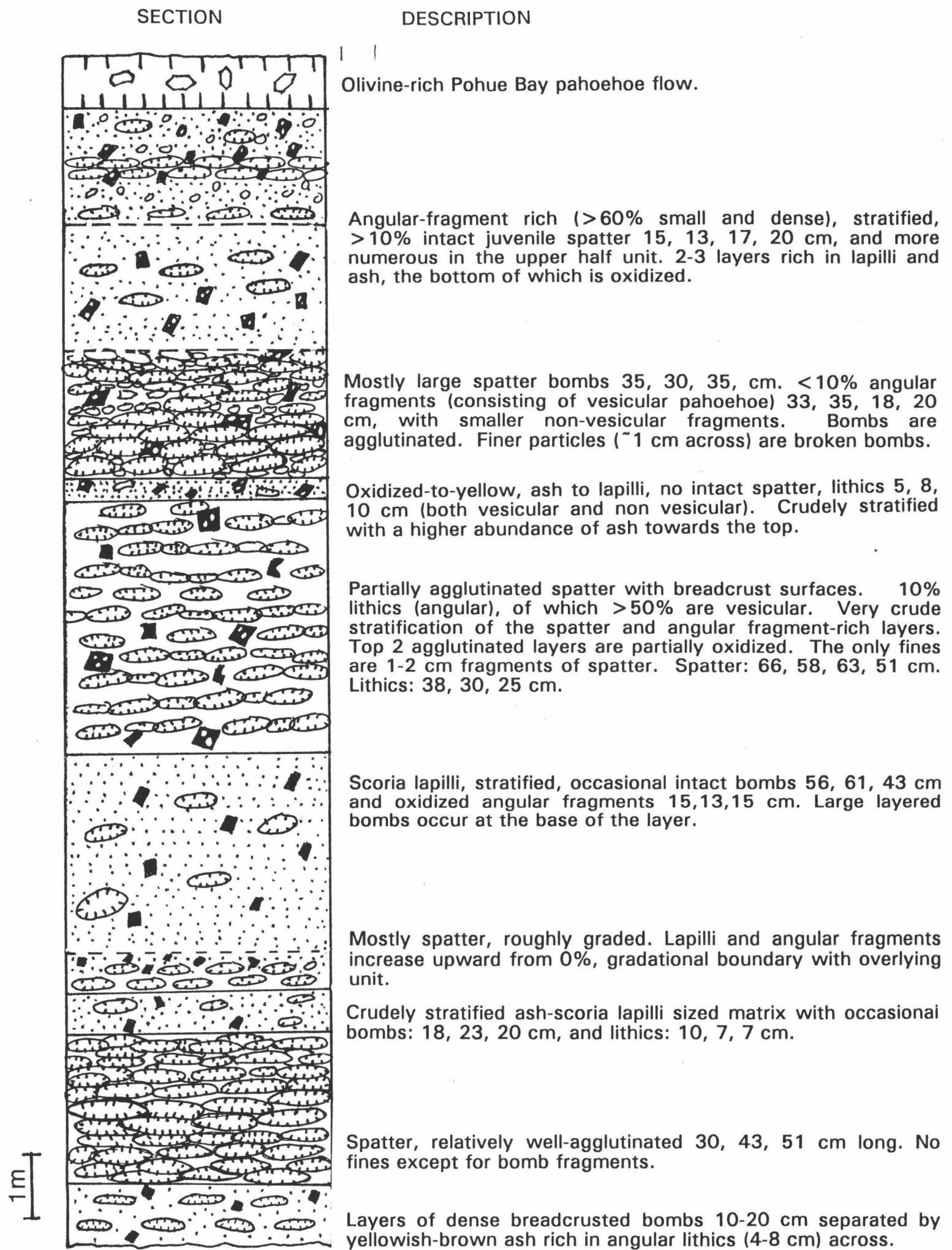
Deposit D High content of fine ash that mantles all the pyroclastic cones and also occurs east of North Crater. It is rich in lithics and represents the most widely spread unit recorded in the Pu'u Ki cluster.

Deposit E At location (3) comprises the wall of North Crater. It mainly consists of spatter and smaller amounts of angular fragments.

Deposit F Very localized spatter, the youngest of all the pyroclastic deposits of the Pu'u Ki cluster (see inset map).

Deposit G Ponded lavas.

Figure 3.6. Cross-section of the main Pu'u Ki cluster as viewed from offshore.



LEGEND:

- | | | | |
|-----------------------|--|------------------------|--|
| bread crusted spatter | | vesicular fragment | |
| spatter fragment | | non vesicular fragment | |
| sandy ash | | | |

Figure 3.7. Stratigraphic column of the deposits exposed at the N end of the main Pu'u Ki cluster (D and E of Figure 3.8).

sloughing off the cone to form the spatter-fed flows, and the process was interrupted (and is now exposed) by the sudden return to violent explosions to form the next overlying layer of lapilli-sized material.

In addition to lapilli and spatter, all the layers contain abundant angular fragments of both vesicular and non-vesicular olivine-rich lava. Some of these fragments have densities as high as 3.4 g/cc (measured from sawn blocks). The largest of these are concentrated in the uppermost pyroclastic layers, are up to 2.5 m across (Figure 3.8), and fragments up to 0.5 m in size can be found more than 500 m from the center of the cone. The amounts and types of these angular fragments are different in the lapilli-rich and spatter-rich layers. Lapilli layers contain higher proportions of angular fragments than the spatter layers. Furthermore, a larger proportion of the lithics in the lapilli layers tend to be non-vesicular, although of the same composition.

The next unit (G) to the SE consists of flat-lying ponded lavas. These lavas have a roughly circular outline in plan view, flow units are mostly ~1 m thick, and have a total thickness of about 20 m. These lavas are olivine-phyric vesicular pahoehoe, and some of them contain pipe vesicles. They become more olivine-rich upward in the section. At the northern and southern ends of this ponded lava the lowermost flows can be seen to rest horizontally and unconformably on the inward dipping truncated surface of pyroclastic layers (locations 2 and 3; Figure 3.9).

This area of ponded lava contains two collapse pits (Figure 3.10), the larger seaward one is ~100 m in diameter and ~5 m deep, and the smaller landward one is ~20 m in diameter and also ~5 m deep. Both of these pits

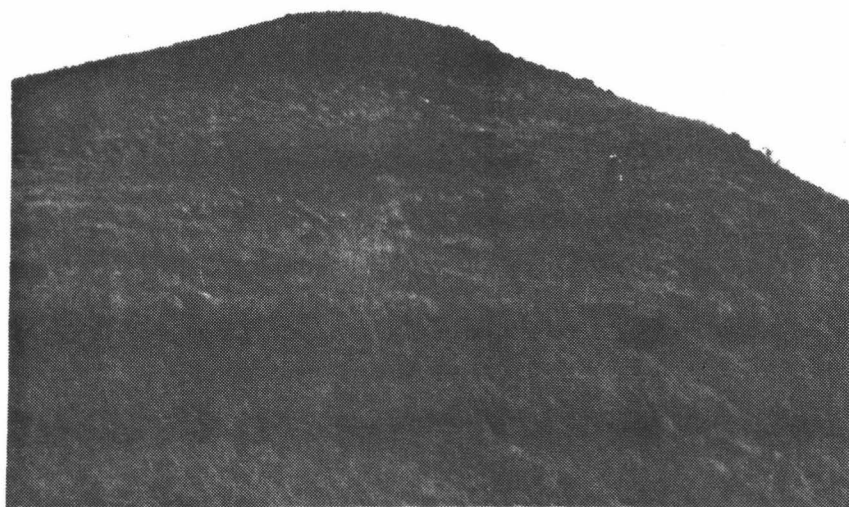


Figure 3.8. Photo of the main Pu`u Ki cluster surface showing giant angular blocks scattered on top (see person for scale).

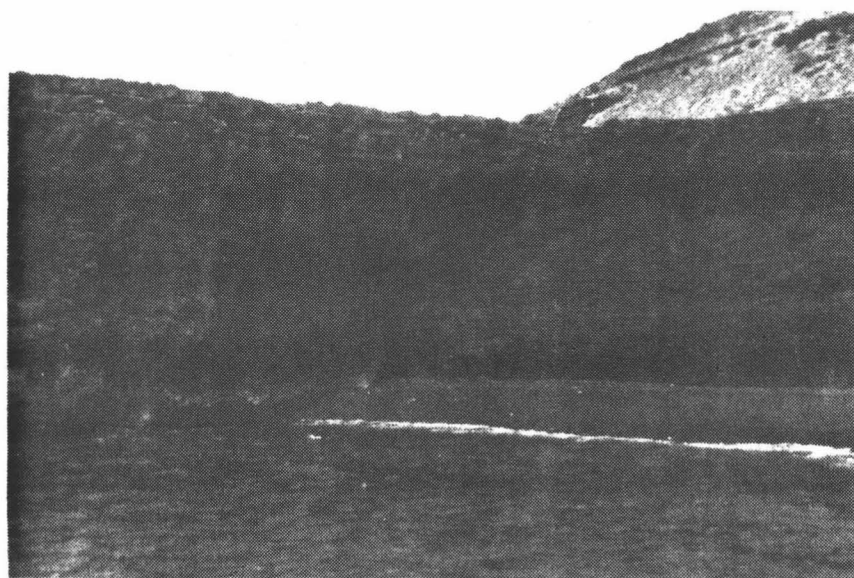


Figure 3.9. Contact between the ponded lavas and the pyroclastic rim of N-most cone in the main Pu`u Ki cluster (units G and C of Figure 3.8).

have near-vertical scrape marks on their walls indicating that the inner parts subsided. A low rim of dense spatter occurs near the landward pit (Figure 3.3). It is 1-2 m high, and continuous with a thin layer of spatter that mantles the main cone at this location. This spatter has the same characteristics as that which makes up the inner rims of the three-rim cone.

The next exposure SE-ward forms Keliuli Bay (location 4). This exposure is similar to the NW-most one; layers of lapilli-rich and spatter-rich pyroclastics form a truncated surface overlain by ponded lavas of Unit G to the NW (location 3). These layers arch over and flatten out to the SE. A number of them grade into spatter-flows. The axes of these arching layers are truncated by the sea cliff at the head of Keliuli Bay, and trend seaward, indicating the pre-erosion seaward extension of this cone. Combined with the ponded nature of Unit G, this seaward extension is strong evidence that this structure once formed a complete cone. Also exposed at Keliuli Bay is a remnant of an earlier cone. It consists of about 15 m of oxidized spatter-like pyroclastic layers dipping NW and truncated by a SE-dipping surface. This remnant (unit A) is termed the Keliuli cone, and has been mantled by the more than 20 m of pyroclastics that make up the bulk of the exposure and parallel the surface of the cone (Figure 3.11).

One of the welded spatter flows forms the peninsula just SE of Keliuli Bay (at "Gap" in profile, figure 3.6), and extends around to the next small indentation of the coast. In this next small bay (location 5) is found a thick sequence of oxidized and welded scoria (unit C) overlying what appears to be the southern half of the Keliuli cone. Here, however, the layers of the Keliuli cone dip SE and are truncated to the NW. The uppermost layers

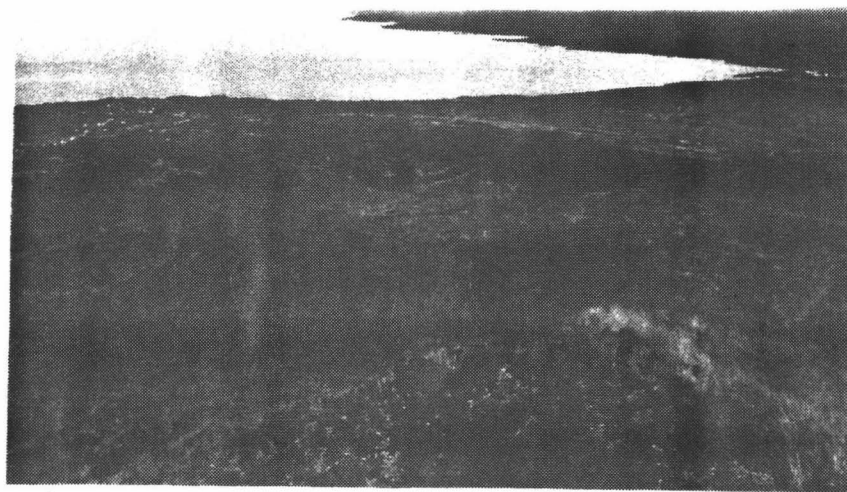


Figure 3.10. Photo of the surface of the ponded lava (unit G of Figure 3.8) at the main Pu`u Ki cluster, showing collapse structures.

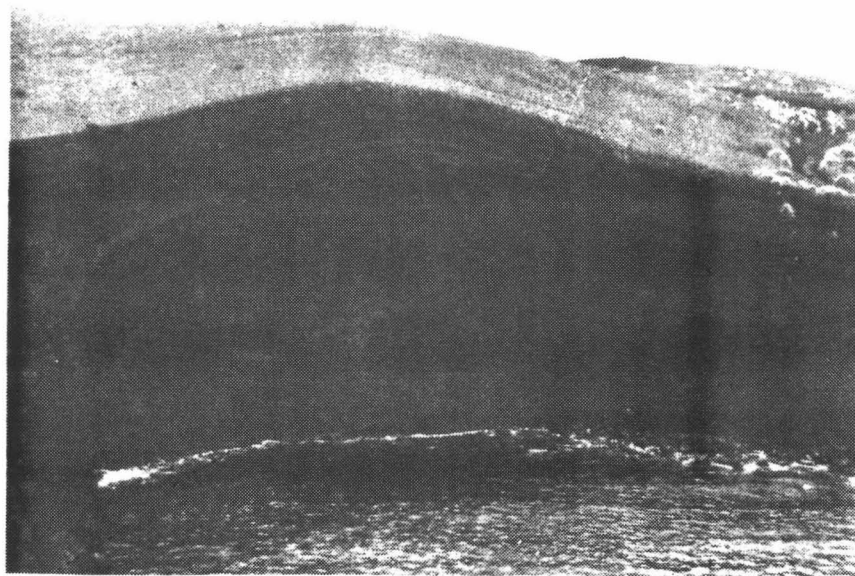


Figure 3.11. Photo of the N Keliuli cone remnant buried by pyroclasts from the main Pu`u Ki cluster (units A and E of Figure 3.8).

(units C and D) drape this remnant, and are overlain by Pohue Bay lavas in much the same manner as those seen in the NW-most exposure. The sequence of cone formation within the main Pu`u Ki group is: 1) the Keliuli cone; 2) southernmost (complete) cone (not directly exposed in the coastal section); and 3) the northernmost cone. Unit D covers the entire surface of the area, is consistently fine lapilli-sized, and contains the highest number of large lithics.

At location 1 the lapilli scoria tends to dominate, comprising most of seven of the ten most discernible layers (Figure 3.7) and these layers are for the most part neither welded nor oxidized; most of the material is dark gray. At location 5, however, dense bomb-sized scoria and ribbon-like spatter predominate, forming massive welded layers a few meters thick, most of which have been oxidized to a very bright red. A few small cored bombs can be found in this unit, and each core is a non-oxidized fragment of olivine-rich basalt.

As at the three-rim cone, the sequence consists of an early-formed outer rim of pyroclasts surrounding ponded spatter-fed lava. At the northernmost Pu`u Ki cone the amount of ponded lava is significantly greater than at the three-rim cone. Although neither is any longer a complete cone, the ponded lavas must have had something to pond within, and a map view allows the once complete cones to easily be reconstructed. The topmost Pohue Bay lava overlies part of the main Pu`u Ki cluster but spatter bombs from the three-rim cone are found on its surface, suggesting that the three-rim cone is younger than the main Pu`u Ki cluster.

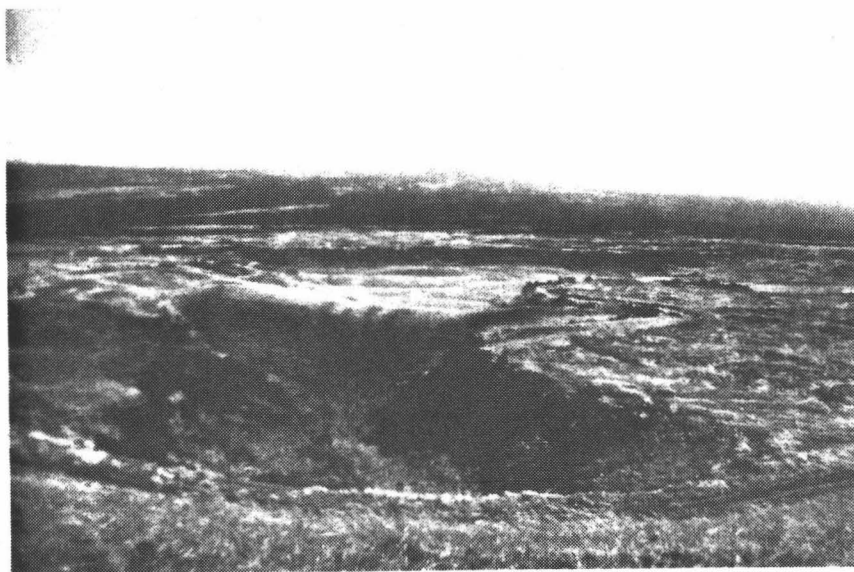


Figure 3.12. Photograph of the depression inland from the main Pu`u Ki cluster. This depression is 4-5 m deep.

A prominent depression occurs immediately inland from the main Pu`u Ki cluster (Figures 3.3 & 3.12). This depression has an area of about 0.15 km² and averages 4-5 m deep. It is formed of two branches with channel-like extensions that point in the direction of the three rim cone and main Puu Ki cluster. It has a relatively flat floor and its walls consist mostly of slabs of pahoehoe that have been tilted inward. There are places where the inner surface obviously subsided relative to the walls and produced scrape marks in the still-plastic lava. This depression most likely represents a collapsed lava rise (Walker 1991). The lava rise had a minimum calculated volume of ~500,000 m³ prior to draining; its possible significance to formation of the Pu`u Ki cones is discussed later.

`Au`au cone

`Au`au cone occurs at `Au`au Point some 40 km NW of Pu`u Ki (Figure 3.2). Its setting differs from the cones described above in that there is a very steep slope inland and only a narrow coastal terrace. The structure of `Au`au cone (Figure 3.13), however, is essentially identical to that of the three-rim cone and Pu`u Ki. It consists of an outer rim of lapilli and bomb-sized scoria and an interior of dense spatter and ponded lava. The outer rim stands 15-20 m above the surrounding Kolo lava flow and reaches a height of about 30 m above sea level. It is about 200 m in diameter and consists of lapilli-sized poorly bedded and unconsolidated pyroclastics. There are abundant spatter layers. There are also many bombs and blocks, some of which are up to a meter in diameter, intercalated within the lapilli and spatter layers.

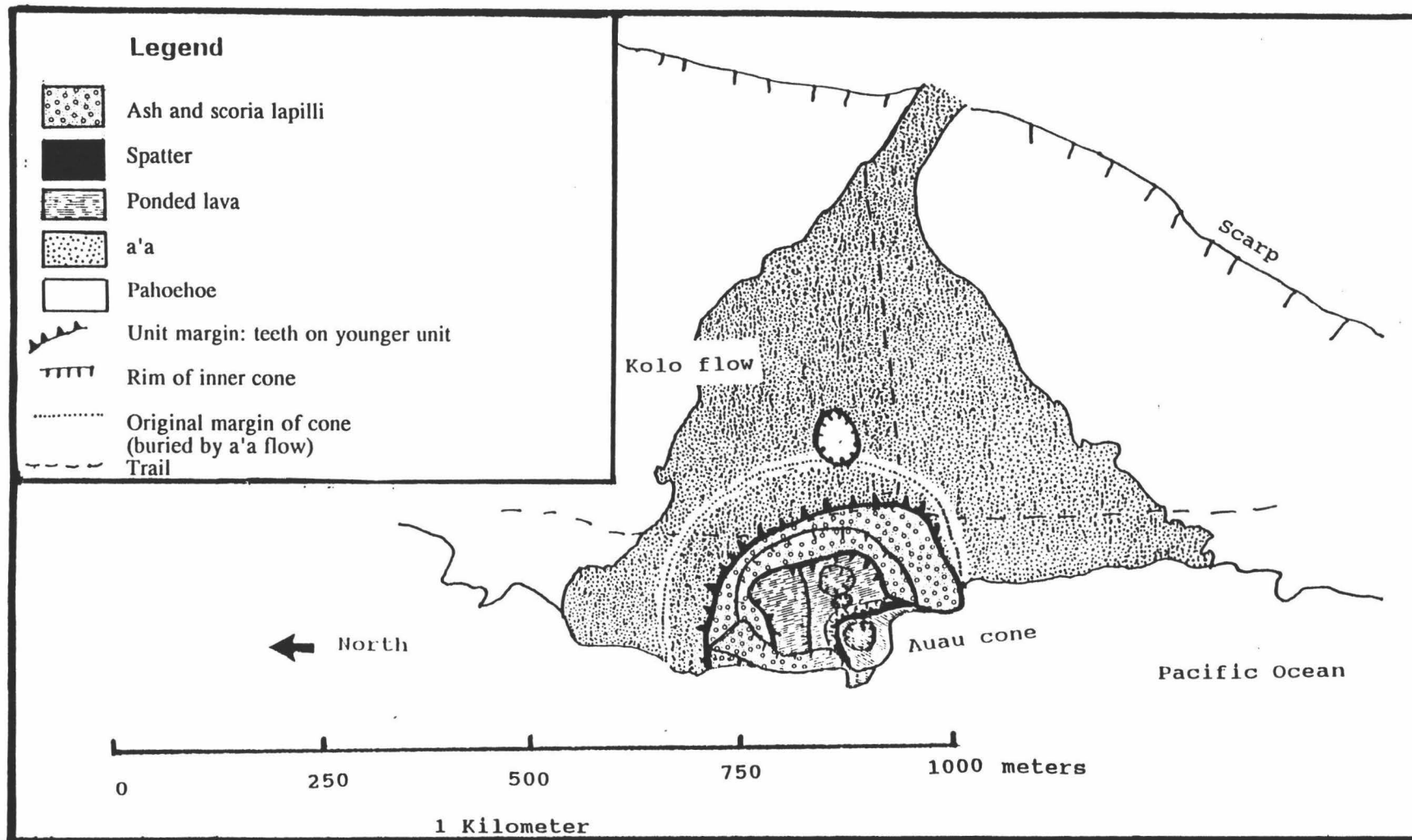


Figure 3.13. Detailed geologic map of the 'Au'au cone located within the Kolo flow.

Surrounded by this outer rim is ponded lava, which in the sea cliff is ~15 m thick and consists of flows 1-2 m thick. Most of this ponded lava is pahoehoe but the top flow is a`a with occurrences of toothpaste lava. Two minor collapse pits are found in the N part of the ponded lava flow. `Au`au cone differs from the two previous examples in that there are two ocean-facing scarps. The N one is relatively straight, extending across 3/4 the coastal exposure of the cone and consisting of cross-sections of the northern arm of the outer rim and ponded flows that have been exposed by wave action and/or collapse. At the S end of this, the scarp curves inland to form a strongly arcuate bite (Figure 3.14). From the base of this arcuate scarp extends a lava flow that forms a small peninsula sloping to sea level. The face of the arcuate bite as well as the S half of the main outer rim are mantled by a layer consisting of dense spatter that ranges up to a meter in thickness.

`Au`au cone occurs within the Kolo flow (Lipman & Swenson 1984) which is mostly pahoehoe but several later surges of a`a occurred. One of these apparently re-occupied the main tube and surfaced within the inner part of the cone to form the thin a`a/toothpaste flow that covers the topmost inner ponded lava and spatter layers. Within the cone this a`a flow is mostly <1 m thick, and it issued from a jumbled and upraised area in the southern part of the cone floor, which bears evidence that this last episode of lava issuing from the tube involved the forcible explosion of large solid blocks from within the tube. The a`a/toothpaste lava formed numerous small flows that issued from boccas. It covered the spatter layer generated by the collapse of the arcuate scarp, lapped against the main

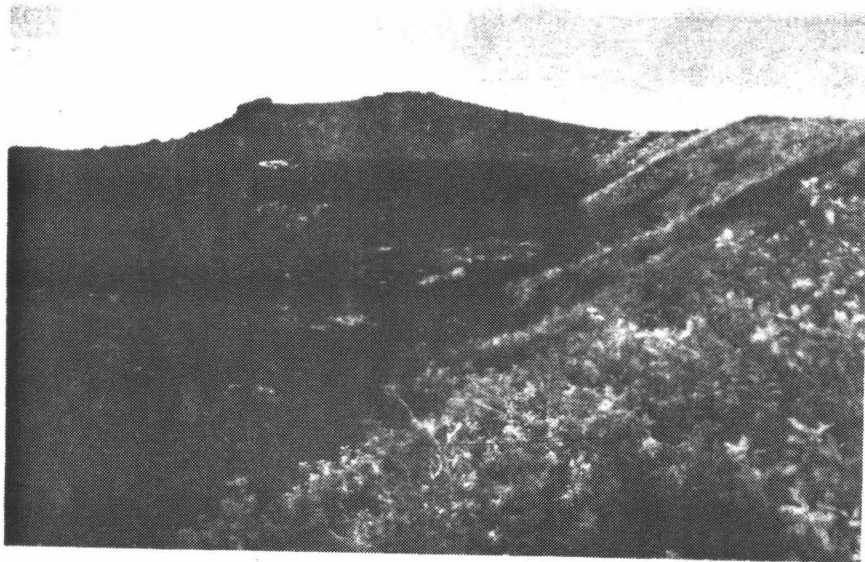


Figure 3.14. Photo of the Au`au cone showing an outer rim of pyroclastics (with grass) filled with ponded lava and a thin cover of toothpaste lava (unvegetated).

cone, and flowed over the face of the arcuate scarp to mantle the peninsula of lava.

The same lava that produced the last a`a within the cone also formed an upraised blister-like structure just outside the main rim. The top surface of this blister consisted of the pahoehoe lava associated with the formation of the main cone as well as a thin layer of outer rim lapilli. Short lava flows issued from the base of this blister when it was inflated. Finally, the blister collapsed and the top surface was displaced downward to form the present floor of a pit. The short lava flows of a`a and toothpaste lava today appear to have emanated from relatively narrow piles of rubble rimming the pit, but this is unlikely. This a`a/toothpaste lava clearly post-dates the main outer rim, but by how long is not clear. The main `Au`au rim was formed by fluid lava as shown by the nature of the ponded lavas and the spatter. The a`a came along later in the eruption and was not involved in the formation of `Au`au cone. An even later episode of a`a bifurcated around `Au`au cone (Figure 3.13).

The pyroclastic unit that comprises the main rim can be followed S in the low sea cliff sandwiched between pre-Kolo or early Kolo flows and the latest a`a. 350 m away it is 20-30 cm thick and rests on clinker of a thick a`a flow that extends southward. It is at this point that the latest a`a flow dies out so that the ash makes up the surface. The transition from a`a-covered to ash-covered surface is made obvious by an increase in the amount of vegetation.

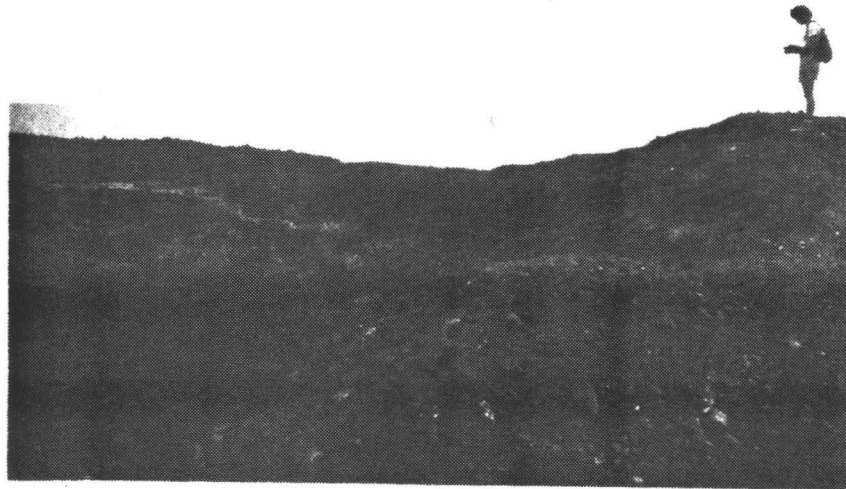


Figure 3.15. Photo of the SE most cone of the Pu`u Ki group showing an outer rim of pyroclastics (right) and ponded lavas within (left).

Summary of cone structures

In summary these three cone complexes have the following structures in common: 1) an outer rim of lapilli to bomb-sized scoria and spatter that either still is or was once a complete cone, and 2) one or more inner rims of dense spatter and associated lava that ponded within the cones. An additional example of the same structure is the SE-most cone of the Pohue Bay group near the toe of the 1887 flow (Figures 3.3 & 3.15). The two structural components indicate very different eruptive vigors that produced deposits that resemble those of both Hawaiian and hydrovolcanic activity. Their origin is considered in the next section.

POHUE BAY CONES: LITTORAL OR PRIMARY

Although it is clear that water was involved in the formation of these cones, it is not clear whether they are primary (vents) or secondary (littoral) structures. Secondary cones in Iceland are similarly difficult to distinguish from primary vents (T Thordarson pers. comm.). In this section the features of these cones and their relationships to the surrounding lavas are discussed in order to determine their origin.

Proximity to coastline

All the studied structures occur at the coastline. This is not sufficient evidence to determine the origin of the cones described here because

phreatomagmatic eruptions from primary vents can also occur at or near the coast (e.g. Kapoho cone, Holcomb 1987; Pu`u Mahana, Walker 1992).

Location with respect to rift zones

Most flank eruptions during the tholeiite stage of Hawaiian volcanoes take place from narrow and well defined rift zones (e.g. Macdonald *et al.* 1983). An exception to this is the group of radial fissures that occur around the N and NW sectors of Mauna Loa (Lockwood & Lipman 1987) and consist of linear vents of spatter and cinder oriented radially to the Mauna Loa caldera. One of them erupted in 1877 within Kealakekua Bay (Moore *et al.* 1985; Lockwood & Lipman 1987). The cones discussed in this chapter might be considered to be in this category because of their distance from the rift zones but `Au`au cone and especially the Pu`u Ki group are considerably south of the zone of mapped radial rifts. Furthermore if primary, the Pu`u Ki group (aligned parallel to the coast), is decidedly non-radial with respect to the Mauna Loa caldera.

`Au`au cone is not located near to either of Mauna Loa's rift zones but the Pu`u Ki group occurs within 15 km of the SW rift of Mauna Loa. This rift has a distinct bend at Pu`u o Keokeo, at an elevation of about 1800 m (Figure 3.2; Lipman 1980a; 1980b). If the line of the upper part of the rift is extended seaward, it intersects the coastline at the location of Pu`u A Pele, only a few km NW of Pu`u Ki. This suggests the possibility that the cones are primary and lie on a now-extinct part of the SW rift, implying that the present lower portion of the rift has migrated east from an original straighter line. There are, however, no known vents between Pu`u o

Keokeo and the Pu`u A Pele group nor is there a topographic ridge there. There is thus no evidence that Puu Ki lies on a rift zone. Furthermore, it is more likely that the middle portion of the SW rift zone has been moving W due to the expansion of Kilauea's SW rift, rather than the lower portion moving E (Lipman 1980a; 1980b). This would mean that the position of the lower rift zone relative to the Pu`u Ki group has remained the same, and the separation by ~15 km supports the rootless origin of the cones.

Presence of dense angular fragments

At all the cones, angular blocks are included in the deposits, They are up to >1 m across (Figure 3.8), and almost all are olivine-phyric. Some of these have a glass-like surface which resembles a coating of lava. Many are almost totally non-vesicular, but some of them grade into more vesicular lava that appears to have been fluid at the time it was erupted. The origin of these blocks included in the pyroclastic layers is problematic because accidental lithics are common in primary hydrovolcanic deposits, but are not usual at rootless vents.

These blocks are not accidental because they represent completely degassed lava associated with the that which formed the cones. Petrographically the angular blocks are identical to both the Pohue Bay flow and the dense spatter of the inner rims. I suggest two possibilities. The first is that the angular blocks formed from lava that spent time cooling and degassing in some sort of storage reservoir within the associated pahoehoe flow. Such lava probably never flows on the surface because of its high density, which in these examples is augmented by accumulated olivines.

The second possibility is that the blocks are fragments of spatter that degassed during one or more cycles of ejection and sliding back into the explosion vent. In either case the angular fragments are not, by definition, accidental lithics because they are from the same flow. Further support for this idea was provided by the recent littoral explosions at Kamoamo, Kilauea. Numerous angular blocks of dense non-vesicular lava are reported to have littered the area around the small spatter vent that formed (T. Mattox, pers. comm.). Unfortunately none were collected and the area was soon buried by later flows.

Pyroclastic considerations

As noted above there are in general two types of pyroclastic material found at these cones, the lapilli-sized material that makes up the bulk of the outer rims and the dense spatter that is either found in layers within the outer rims or forms the inner rims and feeds the ponded lava. The finer material indicates that water was involved in the eruptions, but does not indicate whether the cones are primary or secondary. However, close examination shows that most of the finer grains are angular, non-vesicular, and contain fractured olivines. Such fractured olivines have been used by Walker (1992) to differentiate secondary and primary deposits. This is because explosive fragmentation of solid or almost solid lava is likely to cause fracturing across mineral grains whereas in a primary eruption, the lower viscosity of the erupting lava allows deformation to be concentrated in the fluid, preserving the integrity of the phenocrysts.

Grain size parameters

Sieved samples from Pu`u Ki and `Au`au cones are plotted (Figure 3.16) in conjunction with samples of two known littoral cones (Sandhills and Pu`u Hou). The Pu`u Ki samples fall mostly in the Surtseyan field of Walker and Croasdale (1972), however, the coarser material was not sieved because it was too coarse and too welded. It would probably have fallen in the Strombolian field (coarser and better-sorted than Surtseyan). The Sandhills, Pu`u Hou, and `Au`au samples fall on the border between Strombolian and Surtseyan fields. Littoral explosions vary greatly depending on the ratio of water to magma, and can resemble both Strombolian and Surtseyan eruptions. Thus although useful for differentiating primary (dry) Strombolian deposits from primary (wet) Surtseyan deposits, Figure 3.16 does not show a relationship that can be used to differentiate wet primary from wet secondary deposits.

Density

Littoral pyroclasts are degassed relative to primary pyroclasts because their source is lava that has degassed during flow on the surface as well as the vent. The degassed nature of the pyroclasts considered here can be determined from sieved samples, sawn blocks, and sulfur contents.

Plots of class density vs. sieve aperture size (Figure 3.17) shows that the pyroclastic deposits of the Pohue Bay and Auau cones reach a relatively constant density for grains smaller than 2-3 mm. The deposits of primary vents, however, show continuous density increases with decreasing grain size because the big fragments contain many vesicles and the smaller ones

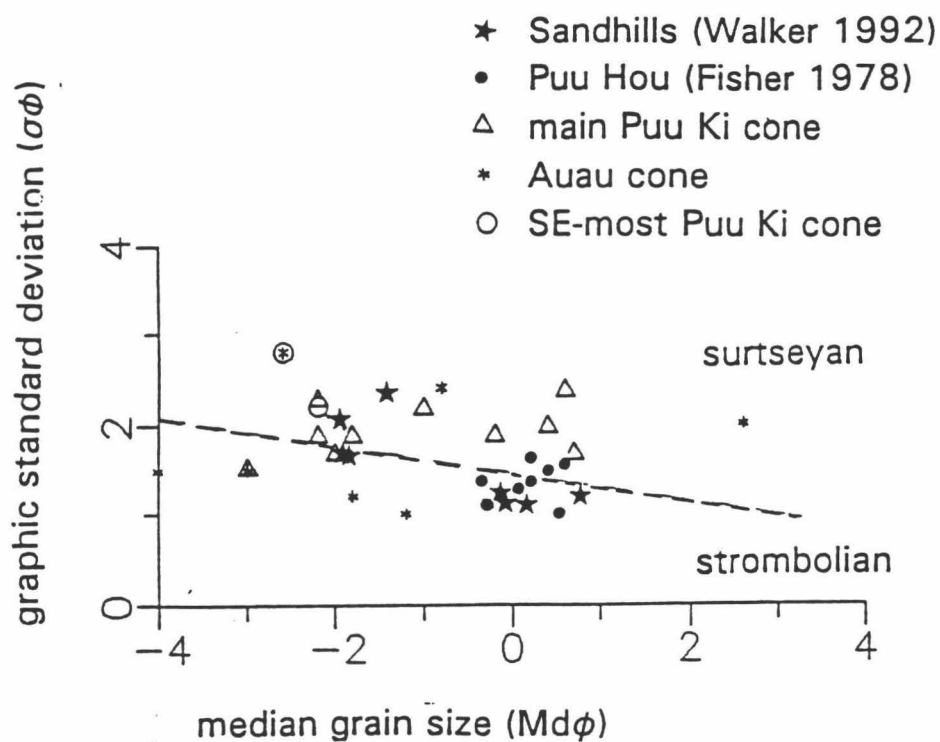


Figure 3.16. Plot of graphic standard deviation ($\sigma\phi$) against median grainsize ($Md\phi$) of sieved samples of single beds. Dashed line delineates approximate boundary between Surtseyan and Strombolian fields (Walker & Croasdale 1972). Littoral cone samples straddle the Surtseyan-Strombolian boundary.

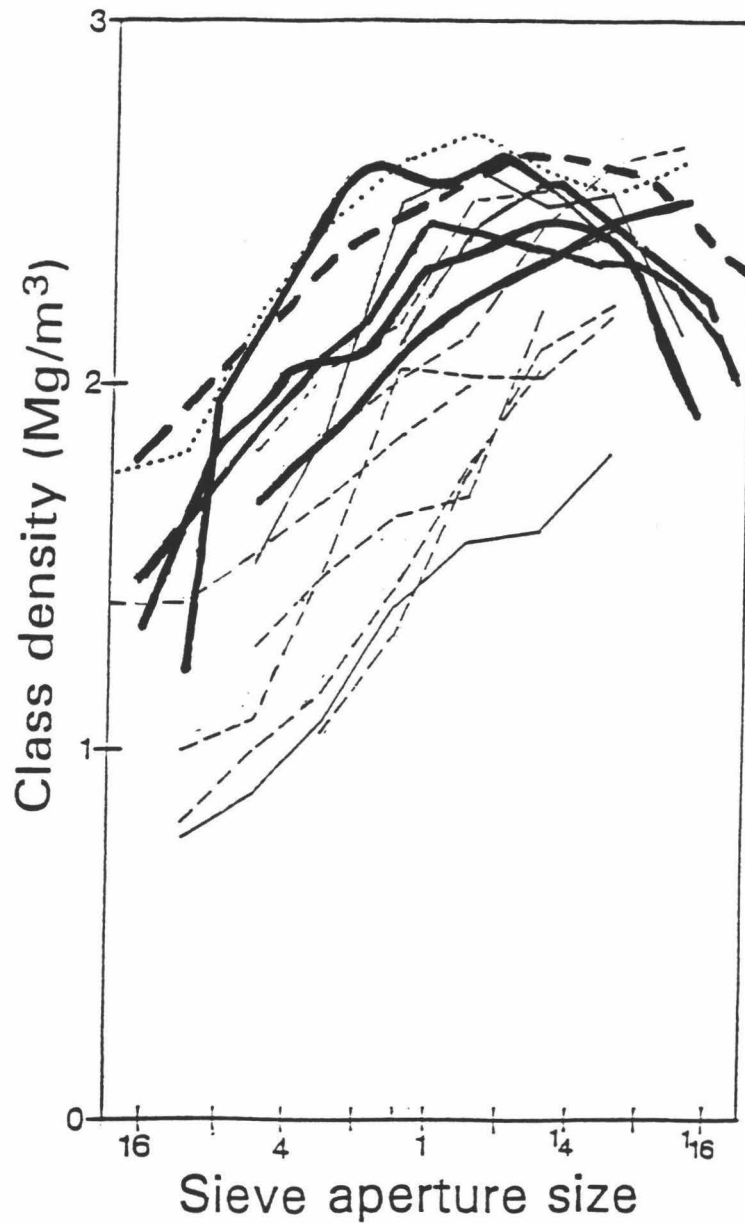


Figure 3.17. Class densities of sieved samples, as they vary with grainsize, for Pu`u Ki (heavy lines), Auau cone (dashed heavy line), Sandhills (dotted line). Also plotted are a number of other basaltic pyroclastic deposits from Walker 1992: Surtseyan ash cones (solid lines), Strombolian cinder cones and plinian deposits (dashed lines). This graph shows that littoral deposits (Pu`u Ki and Sandhills) have higher densities for all grainsizes.

are mostly vesicle-wall fragments. In most littoral vents, the lava has degassed during flow from the vent, thus breaking it into smaller and smaller particles does not have a strong effect on particle density. This relationship was used by Walker (1992) to differentiate the pyroclasts of Pu`u Mahana (a Surtseyan tuff cone) from the Sand Hills (a littoral deposit). When the class density is plotted against sieve aperture, Pu`u Ki falls in the denser end of the range (Figure 3.17).

By measuring and weighing sawn blocks, the density of the three-rim cone, Puu Ki, and Auau spatter averages 1.5 g/cm^3 . This compares to 0.8 g/cm^3 for the densest olivine-rich spatter from Puu Puai, a primary vent of Kilauea Volcano. The Pohue Bay flow presents a spectrum of decreasing gas content from the uphill channel overflows (1.1 g/cm^3) to the coastal flows and spatter (1.5 g/cm^3) to the angular fragments (3.4 g/cm^3). This decrease in vesicularity toward the cones is not consistent with them being primary vents.

Additional evidence of degassing comes from determining the amount of unexsolved volatiles. Initial sulfur contents of Hawaiian magma has been determined to be about 1300 ppm (Harris & Anderson 1983). During eruptions the S decreases to around 700 ppm (Moore & Fabbi 1971). Surface flows eventually contain from 50 to 200 ppm S (Moore & Fabbi 1971; Swanson & Fabbi 1973; Sakai *et al.* 1982). The S contents of cones and lavas of the Pohue Bay flow range between 30 and 140 ppm (Table 3.1), showing that the lava is degassed considerably from its probable original value, and probably not of vent or near-vent origin.

Table 3.1 Chemical data

sample	SiO ₂	TiO ₂	Al ₂ O ₃	Fe ₂ O ₃	FeO	MnO	MgO	CaO	Na ₂ O	K ₂ O	H ₂ O+	H ₂ O-	P ₂ O ₅	F	Cl	CO ₂	S	total	Na ₂ O + K ₂ O	
36a	50.7	2.09	12.3	12.4	9.06	0.17	10.7	9.29	2.19	0.48	0.28	0.13	0.27	0.03	0.008	0.39	0.01	101.438	2.67	
94	50.5	1.97	13.5	11.9	8.76	0.17	7.71	10.2	2.68	0.41	0.17	0.29	0.24	0.03	0.82	0.03	0.08	100.70	3.09	
95	51.5	2.0	13.3	12.1	8.0	0.17	7.87	10.1	2.12	0.40	0.26	0.21	0.26	0.06	0.011	0.07	0.01	100.441	2.52	
96	50.5	1.88	12.6	12.2	8.91	0.17	10.2	9.51	2.07	0.37	0.24	0.11	0.24	0.05	0.028	0.09	0.01	100.268	2.44	
97	50.4	1.85	12.4	12.4	9.16	0.17	11.1	9.18	1.96	0.37	0.32	0.22	0.24	0.04	0.036	0.09	0.02	100.796	2.33	
98	51.7	2.02	13.4	12.1	9.34	0.17	7.85	10.1	2.2	0.39	0.31	0.17	0.24	0.03	0.013	0.14	0.01	100.843	2.59	
99	50.1	1.8	12.0	12.4	8.65	0.17	12.1	9.14	1.88	0.36	0.25	0.15	0.23	0.03	0.006	0.06	0.01	100.686	2.24	
102	51.2	2.01	13.3	11.7	5.44	0.16	8.0	10.3	2.24	0.45	0.12	0.16	0.25	0.03	0.006	0.07	0.01	100.006	2.69	
17	53.0	2.44	13.8		11.5	0	6.24	10.2	2.38	0.50			0.30				0.004	100.364	2.88	
18	52.6	2.26	14.1		11.2	0	6.35	10.7	2.36	0.46			0.25				0.003	100.283	2.82	
19	52.7	2.25	14.9		10.1	0	6.59	10.6	2.62	0.49			0.31				0	100.56	3.11	
20	52.2	2.39	13.9		10.8	0	6.45	10.2	2.55	0.52			0.32				0.004	99.334	3.07	
22	51.8	2.34	14.0		11.1	0	6.22	10.3	2.29	0.46			0.26				0.006	98.776	2.75	
25	52.1	2.18	14.2		10.9	0	6.55	10.7	2.26	0.42			0.27				0.013	99.593	2.68	
26	51.1	2.26	13.9		11.5	0	6.57	10.5	2.44	0.46			0.28				0.006	99.016	2.90	
29	51.6	2.22	14.2		11.2	0	6.54	10.5	2.25	0.44			0.25				0.012	99.212	2.69	
30	52.3	2.38	13.5		11.5	0	6.37	10.4	2.28	0.47			0.29				0.009	99.499	2.75	
37	51.9	2.23	13.6		11.4	0.18	6.53	10.6	2.44	0.44			0.30				0.005	99.625	2.88	
32	52.0	2.24	13.9		11.5	0	6.55	10.5	2.42	0.46			0.28				0.014	99.864	2.88	

sample	Nb	Rb	Sr	Zr	Y
36a	18	10	305	154	32
94	12	10	310	126	22
95	16	10	320	138	28
96	14	10	300	128	24
97	12	12	290	128	30
98	13	10	310	138	27
99	14	10	275	122	25
102	12	10	320	124	22

Table 3.1. Chemical data for the Pohue Bay flow and cones. Samples 36a to 102 are whole-rock analyses, and were collected by Jack Lockwood. Samples 17 to 32 are glass analyses, and were collected and analyzed by Dave Clague.

Cone morphology

Shape

A closed rim of pyroclastics implies a point source of explosions and is most often associated with primary vents since the "standard" Hawaiian littoral cones occur in the form of pairs of non-circular half cones. However, the rootless cone groups of Iceland are known to be secondary vents and they possess closed rims (Thorarinsson 1953; Thordarson & Self 1993). Additionally, the recent littoral explosions at Kilauea produced a circular spatter cone about 10 m in diameter (Figure 3.18). Thus a complete cone of pyroclastic material does not *a priori* indicate a primary vent.

Rim diameter/base diameter ratios

Figure 3.19 is a plot of rim diameter/basal diameter vs. basal diameter for various volcanic edifices measured from topographic maps and from the data of Wood (1979). The data separate roughly into "wet" and "dry" fields. The wet deposits occupy the upper part of the diagram whereas the dry deposits occupy the lower part of the diagram. A sub-horizontal line separates the two fields.

The dry field includes tholeiitic spatter cones and cinder cones of Kilauea and Mauna Loa, Mexican ash cones (from the Michoacan-Guanajuato monogenetic field), Mauna Kea cinder cones (alkalic), and Icelandic rootless cones (the larger Icelandic rootless cones have similar dimension ratios to phreatomagmatic vents; T. Thordarson pers. comm.). The wet field includes the cones described in this chapter plus primary tholeiitic and

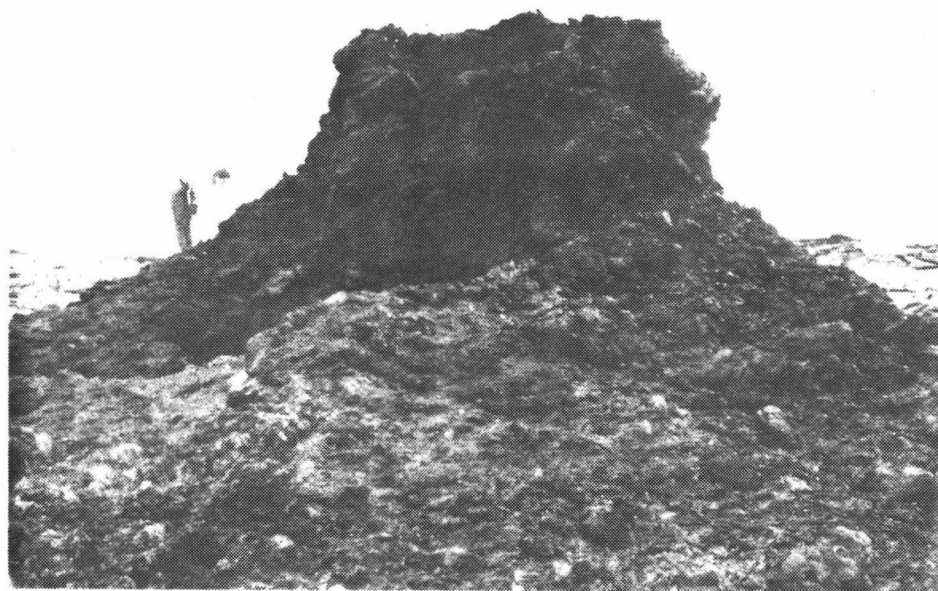
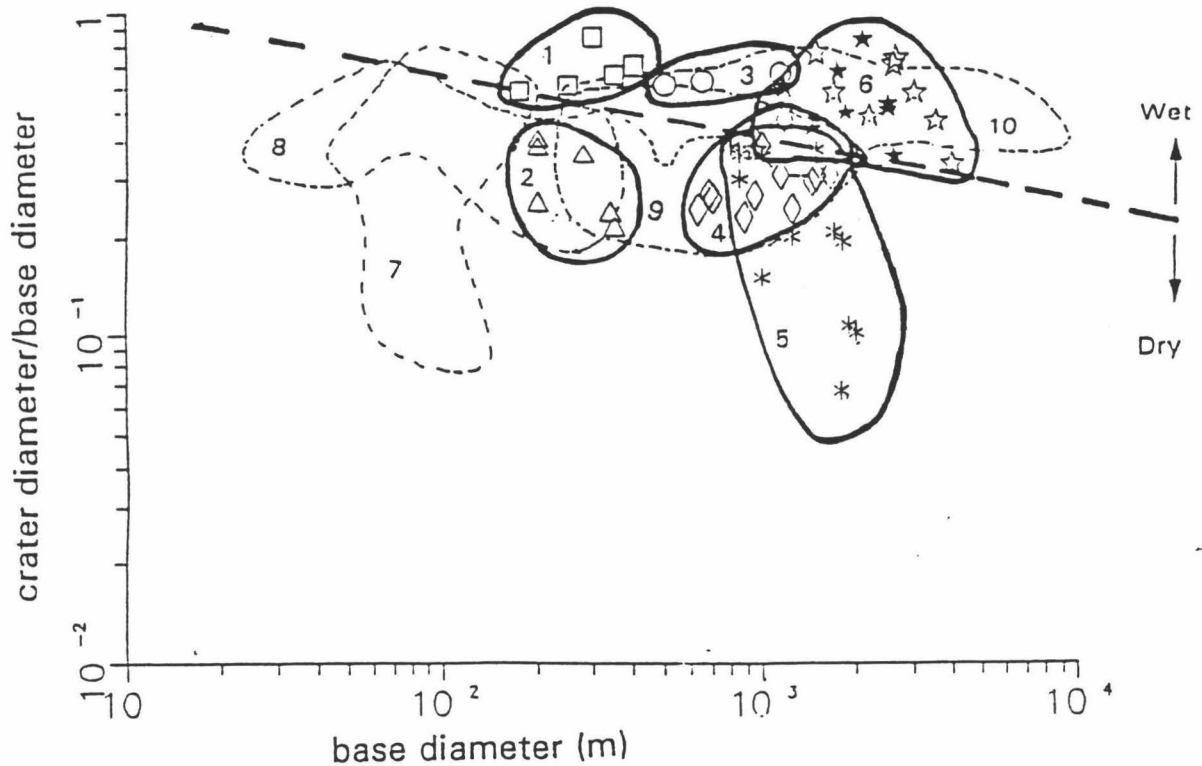


Figure 3.18. Photograph of the littoral cone formed at Kamoamoa, Kilauea on Nov. 24, 1992 (in about 20 minutes), 40 m inland from where a lava tube entered the ocean. Photo by S. Self.



- 1 Pu'u Ki and Auau cones (squares)
- 2 Mauna Loa cinder cones (triangles)
- 3 Hawaiian Tholeiitic surtseyan rings (circles)
- 4 Mexican ash cones (diamonds)
- 5 Mauna Kea cinder cones (astarisks)
- 6 Honolulu volcanic series (filled stars) and Mexican (Michoacan-Guanajuato monogenetic field) maars (open stars)

From Wood 1979:

- 7 Spatter cones
- 8 Rootless cones
- 9 Cinder cones
- 10 Maars

Figure 3.19. Graph of cone basal diameter vs. the ratio of crater diameter to cone basal diameter (after Wood 1979). Note that the data can be divided vertically (heavy dashed line) into wet and dry fields; wet eruptions produce wider craters for a given basal diameter (shown schematically by stippled profiles). Note also that horizontal variation correlates with magmatic gas content (i.e. tholeiites to the left and alkalic basalts to the right).

alkalic phreatomagmatic cones, rings, and maars. Figure 3.19 illustrates that in general the addition of water to a "dry" eruption results in a vent structure with a much larger crater for a given overall diameter. The cones considered here have the form of phreatomagmatic vents but they are composed largely of spatter. The explosions were strong and shallow enough to distribute the pyroclasts widely but not strong enough to fragment them to a great degree.

Within the wet field position along the x-axis is determined by the absolute volume of magma or lava that interacts with water. The Pohue Bay and `Au`au cones are almost an order of magnitude smaller than primary phreatomagmatic vents. This is because even though the volume of the eruption as a whole may be comparable with that at a Surtseyan vent, not all of the lava reaches the coast and not all of that interacts with water.

Relationships between cones and flows

Relationships between cones and associated flows provide evidence to the cone origins. If the cones and flows can be tied to the same eruption, then the littoral origin is more likely. Field relationships, chemistry, petrography, and paleomagnetic techniques were used to address this question.

Field relationships

The Pohue Bay flow, which has a source some 10-15 km upslope (Lipman & Swenson 1984), overlaps the outer rim of the three-rim cone. However, there are numerous blobs of spatter from the inner rims of the



Figure 3.20. Photograph of a spatter bomb lying on the Pohue Bay flow. It flew 200 m from its source (the spatter rim inside the outer rim).

three-rim cone that lie on the Pohue Bay flow (Figure 3.20). This indicates that spattering from these vents was taking place *after* the emplacement of (at least this part of) the Pohue Bay flow. Thus the outer rim, the Pohue Bay flow, and the inner rims are tied together into one event, and because the source of the flow is not the three-rim cone, the cone must be secondary.

Chemistry

Samples of both flow and cone material (Figure 3.21) were collected for whole rock chemical analysis, and analyzed by XRF at the USGS Branch of Geochemistry in Menlo Park California. In addition, numerous chemical analyses of cone deposits were kindly provided by DA Clague of the US Geological Survey.

Figure 3.22 plots magnesium values against sodium plus potassium, phosphorus, and titanium oxides from the whole rock and glass analysis. Within analytical error, all samples of both cones and flows show a co-magmatic trend. This supports the idea that the Pohue Bay flow and the Pu'u Ki cones belong to the same eruption. One whole rock analysis was sampled from a separate younger flow to the N (the Kipuka Kanohina flow) and consistently plots off this trend. This provides a good comparison because it shows that although two lavas may come from the same rift zone on the same volcano, they can be distinguished chemically.

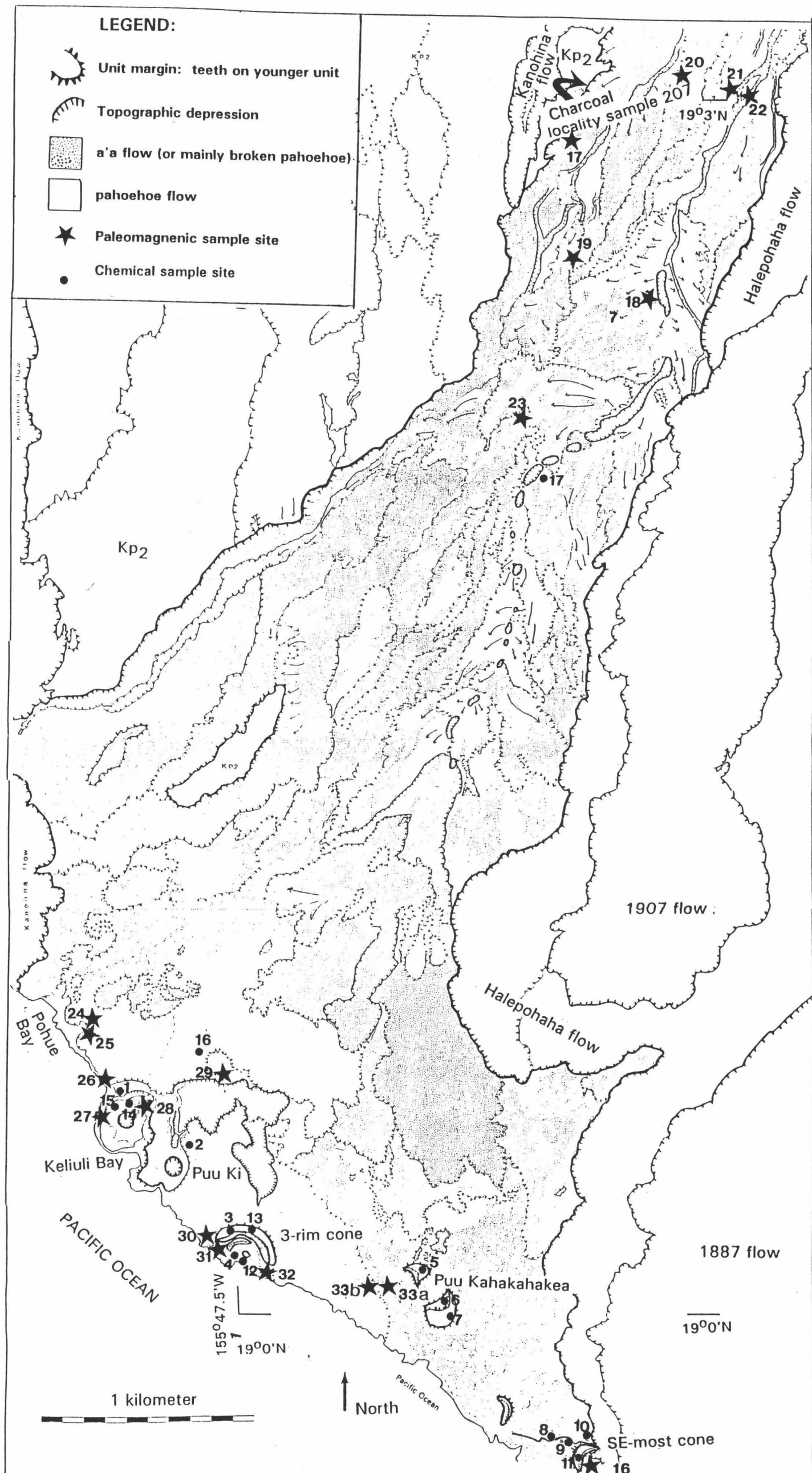


Figure 3.21. Location map of paleomagnetic and chemical sample sites within the Pohue Bay flow and associated cones.

Pu`u Ki Data

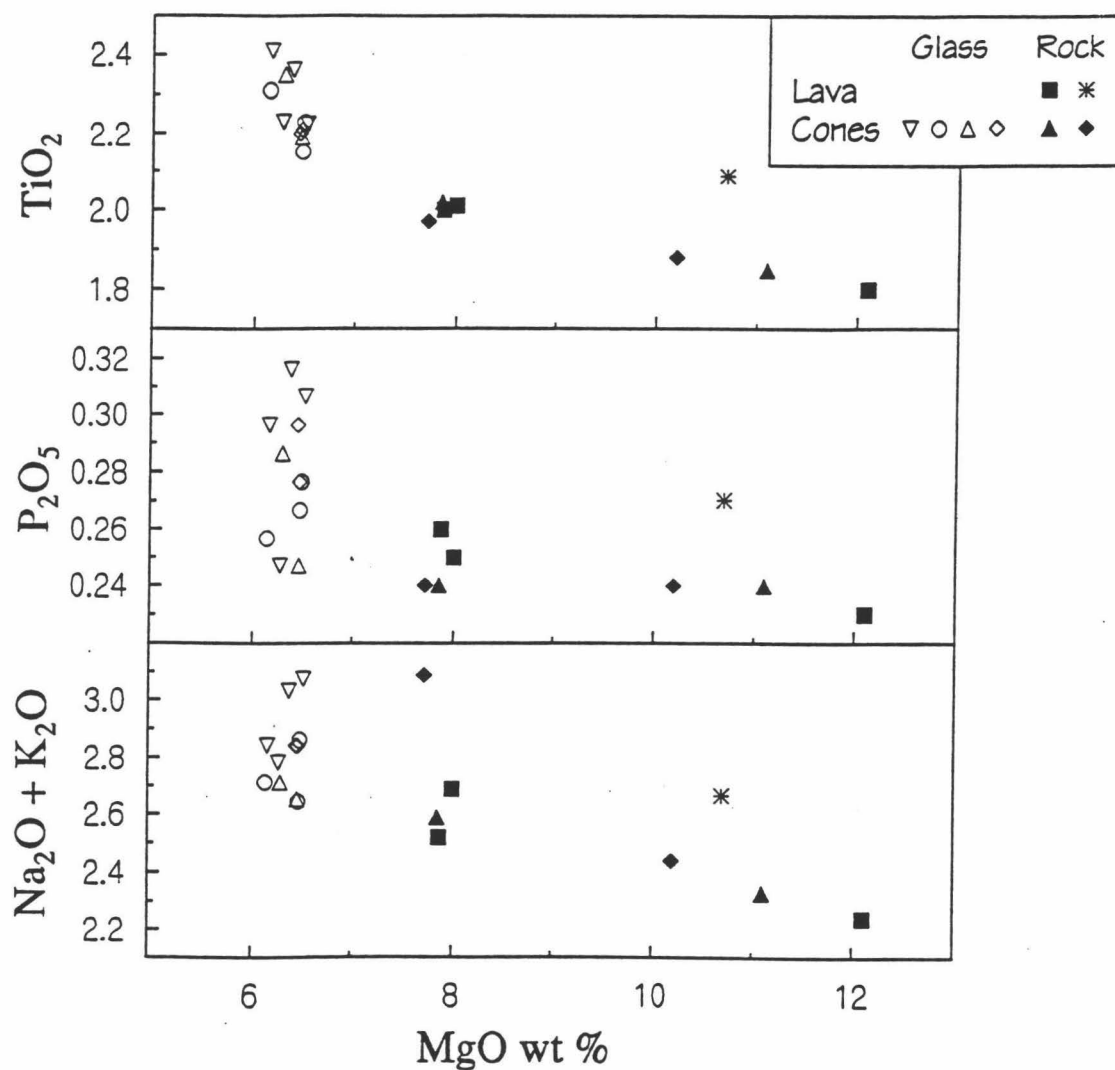


Figure 3.22. Chemical data for Pohue Bay flow and Pu`u Ki cones. *Squares*: Pohue Bay flow (whole-rock only), *asterisk*: whole rock sample from the Kipuka Kanohina flow, *triangles*: three-rim cone pyroclastics, *diamonds*: main Pu`u Ki cone pyroclastics, *inverted triangles*: SE-most cone of the Pu`u Ki group (glass only), *circles*: Pu`u Kahakahakea (glass only). Glass samples were collected and analyzed by D. Clague, whole rock samples were collected by J. Lockwood and analyzed by N Elsheimer, D Siems, E Bell, T Fries, and B King. Figure produced by J. Sinton.

Petrography

Thin sections of the Pohue Bay flow, dense spatter from the inner rims, and the angular fragments within the outer rims show identical mineralogies and differ only in their vesicularity. All are olivine-phyric with rare orthopyroxene, and the main textural differences are due to the size of vesicles and plagioclase crystals (which range from groundmass laths to euhedral crystals ~ 1 mm long). Thin sections of other flows in the field area show a wider range of textural differences but they are not sufficient to differentiate these flows from the Pohue Bay lava.

Paleomagnetism

A detailed paleomagnetic and rock-magnetic study of the Pohue Bay flow and cones was undertaken to investigate their relationship. The relatively slow rates of paleosecular variation (PSV) observed for Hawaii during the past millennia (e.g. Doell and Cox, 1971; 1972) limits the potential utility of paleomagnetic methods. Holcomb *et al.* (1986) observed a variable PSV rate around 4.5° per hundred years for the past 3000 years. This gives a practical limit for the time resolution possible and it also means that high precision (low angular dispersion) both within and between site mean results is required for the study. Detailed paleomagnetic studies of single flows that require this precision have been rarely attempted (e.g. in Iceland). In the next paragraphs a detailed paleomagnetic study of the Pohue Bay flow and cones is presented.

An average of 12 samples were drilled in each of 20 sites in the Pohue Bay flow both upslope and on the coastal flat, as well as from the ponded

Table 3.2

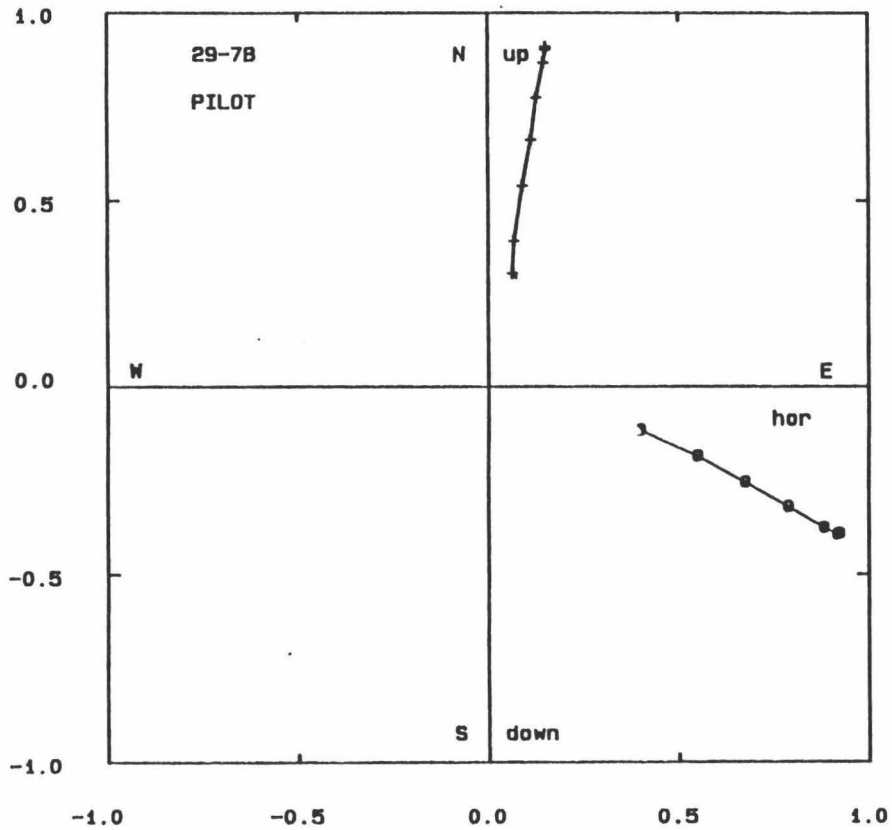
PALEOMAGNETIC SITE LOCATIONS

site #	lava type	area	elevation	field description
15	spongy phh	off map	415 m	channel overflows
16	phh	within cone	4 m	lava ponded in cone
17	a'a	upslope	268 m	channel overflow
18	phh	upslope	244 m	channel overflow
19	a'a edge	upslope	232 m	younger flow
20	a'a	upslope	308 m	younger flow
21	phh	upslope	317 m	channel overflow
22	toothpaste-a'a	upslope	317 m	filling up channel
23	transitional	upslope	189 m	comes out from sheet phh
24	phh	downslope	18 m	surrounds cones
25	phh	downslope	19 m	squeeze out from 24
26	phh	downslope	10 m	Sea cliff, same as 24 and 25
27	phh	within cone	10 m	bottom flow ponded in cone
28	phh	within cone	24 m	last overflow from collapse pit
29	phh	downslope	24 m	old flow
30	phh	downslope	6 m	surrounds cone
31	phh	within cone	2 m	erupted within cone
32	phh	within cone	9 m	erupted within cone
33A	toothpaste	downslope	11 m	flow unit within jumbled plates
33B	phh	downslope	10 m	channel overflow

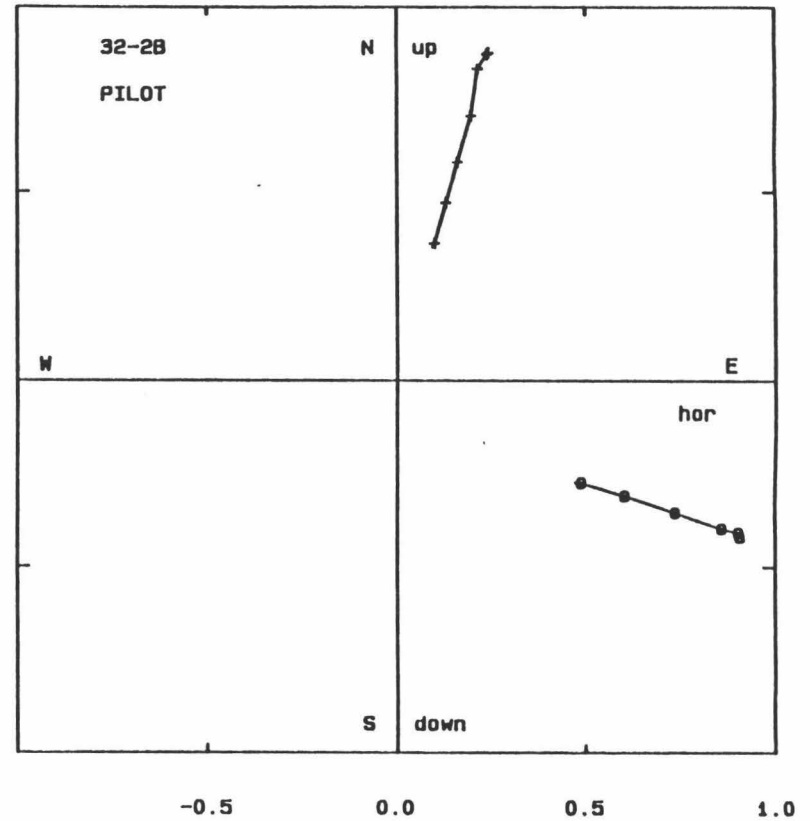
lava inside the cones (Figure 3.21; Table 3.2). Sampling sites were selected so as to avoid problems due to local flow deformation (e.g. inflation under a cooled crust), and subsites (several meters apart) were sampled to detect any local effect in the magnetization directions (e.g. Holcomb et al., 1986). Cylindrical cores 2.5 cm diameter and 10-20 cm long were collected with a gasoline-powered portable drill and oriented *in situ* with magnetic and solar compasses. A total of 530 specimens 2.5 cm long were later sliced from these oriented cores.

The direction and intensity of natural remanent magnetization (NRM) of all specimens were measured with a spinner fluxgate magnetometer. NRM intensities range from 311 to 2666 $\times 10^{-3}$ A/m. Low-field magnetic susceptibility showed large between-site variation, with mean values from 171 to 3915 10^{-4} SI units. Site-mean NRM declinations range from 358.7° to 15.6° and inclinations from 34.2° to 17.1°. Angular dispersions as indicated by α_{95} and k parameters (Fisher 1953) varied from 1.4 to 10.1 and 61 to 890, respectively. Site 16 presents the highest dispersion and site 24 the lowest.

The stability and vectorial composition of NRM were investigated for at least one specimen of each sample by detailed step-wise alternating field (AF) demagnetization, using a Schonstedt AF demagnetizer. The Characteristic remanence (chNRM) direction was estimated for each sample from the linear segments going through the origin in the corresponding vector (Zijderveld) plots and vector subtraction analysis (Figure 3.23). In general a well-defined component was isolated after removing a small secondary low-coercivity component. Some 10-20% of the initial



Normalized components



Normalized components

Figure 3.23. Vector diagrams of demagnetization by AF. Note that flows (samples 19 and 29) and cones (sample 32) all show one stable component of demagnetization after the first or second step, and this points towards a small secondary viscous (low-coercivity) component.

magnetization intensity still remained after demagnetization in 80-100 mT. Since a detailed definition of magnetization directions was required, all remaining specimens were AF demagnetized using the optimum field range defined from previous results. In some sites all specimens were subjected to detailed AF demagnetization. Mean directions and corresponding Fisher statistics for the characteristic magnetization were calculated by a sequential vector averaging procedure. First, sample mean directions were calculated by giving unit-weight to specimen directions and then site-mean directions were calculated from the corresponding sample directions. For comparison purposes, mean directions were calculated for the magnetic and solar orientations. Sun compass corrected directions are used for the final discussion (Figure 3.24). Site mean directions and statistical parameters are summarized in Table 3.3. Most site-mean directions show a small angular dispersion, with α_{95} between 1.4 (site 24) and 6.1 (site 31; Table 3.3).

Magnetic carriers in the samples were investigated by the coercivity spectrum characteristics from AF demagnetization and isothermal remanent magnetization (IRM) analysis. One specimen per site was given an IRM in steps with a pulse magnetizer up to maximum fields of 2.5 Tesla. After-saturation fields were applied in an opposite direction (Figure 3.25). Samples saturated in low fields, between 0.2 and 0.5 Tesla, indicating the predominance of titanomagnetite minerals. From available results (AF coercivity, low-field susceptibility, Q-coefficients, IRM acquisition curves, angular dispersion of NRM and chNRM and vectorial composition and stability) the characteristic remanence corresponds to a primary

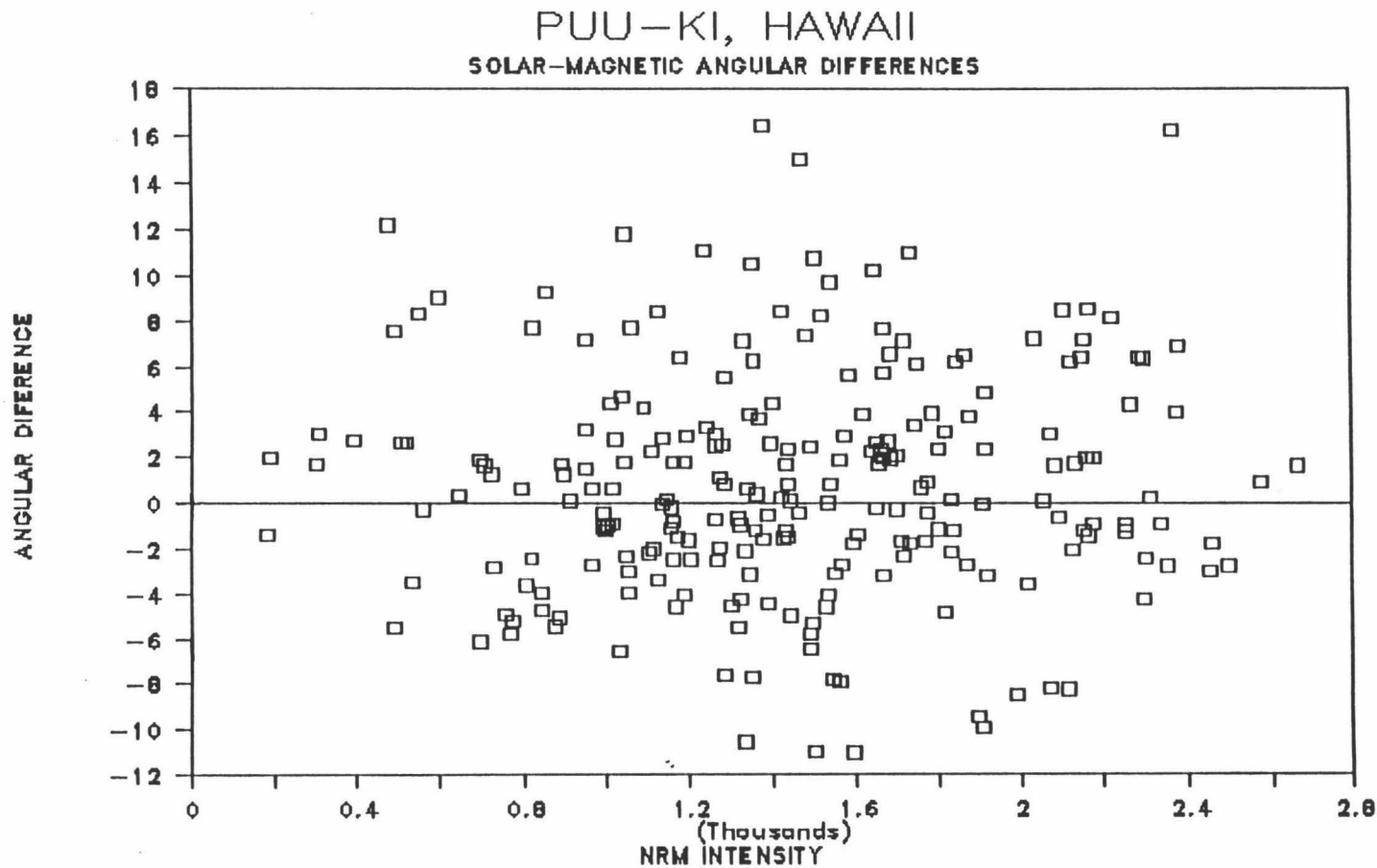


Figure 3.24. Angular dispersions between solar and magnetic azimuths. Notice that dispersions are up to 17 degrees. This is the reason why the magnetic azimuths were not used in the final discussion. Also notice that there is no direct relationship between the angular dispersions and the intensity.

Table 3.3 Paleomagnetic results
 PALEOMAGNETIC RESULTS (MEAN DIRECTIONS)

Site	Dec. (°)	Inc. (°)	K	α_{95} (°)	R	n
15	11.1	23.9	464.4	2.1	10.9785	11
16	355.1	17.1	123.2	5.0	7.9432	8
17	11.4	16.6	249.5	2.8	11.9559	12
18	15.4	20.4	116.4	4.2	10.9141	11
19	12.0	25.3	169.4	3.2	12.9292	13
20	10.9	29.8	206.4	3.0	11.9400	12
21	8.4	27.0	295.5	2.7	10.9662	11
22	5.6	14.2	211.7	3.0	11.9480	12
23	11.4	18.7	115.0	4.1	11.9043	12
24	9.2	22.3	908.2	1.4	11.9879	12
25	10.5	31.3	363.9	2.4	10.9725	11
26	8.5	26.1	237.0	2.9	9.9670	10
27	15.7	25.5	679.7	1.8	10.9853	11
28	10.4	20.7	278.6	2.7	10.9641	11
29	12.0	19.3	361.2	2.3	11.9695	12
30	10.8	26.2	183.6	3.2	11.9401	12
31	12.4	30.0	56.4	6.1	10.8227	11
32	12.8	24.4	271.2	3.1	8.9705	9
33A	10.3	18.3	279.7	2.4	13.9535	14
33B	8.7	25.6	2813.1	1.7	3.9989	4
all sites	10.1	23.2	170.1	2.5	19.8883	20

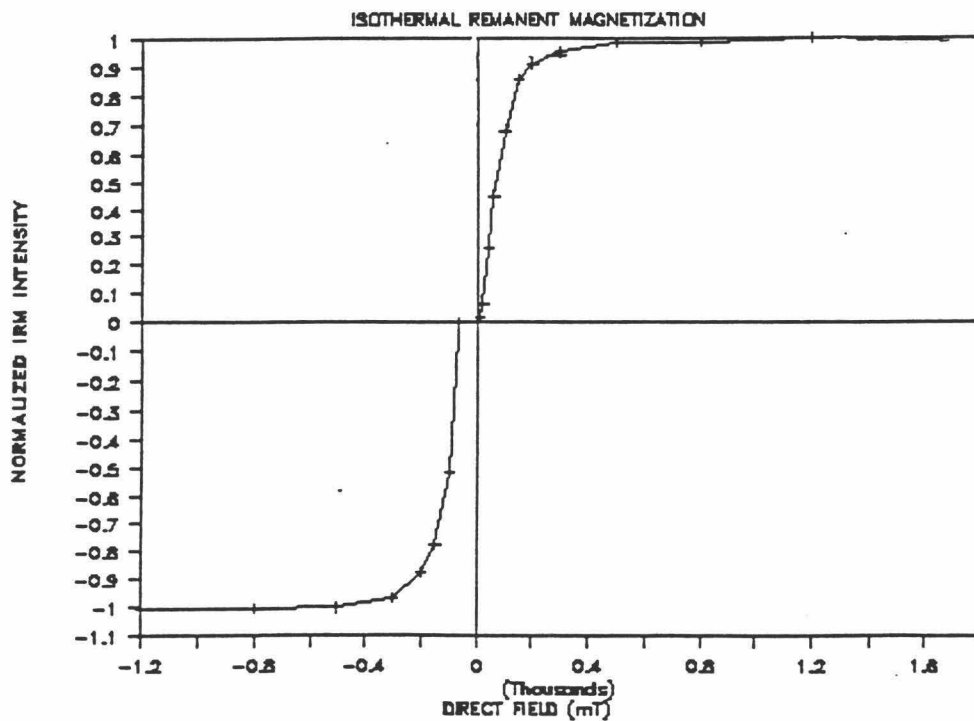
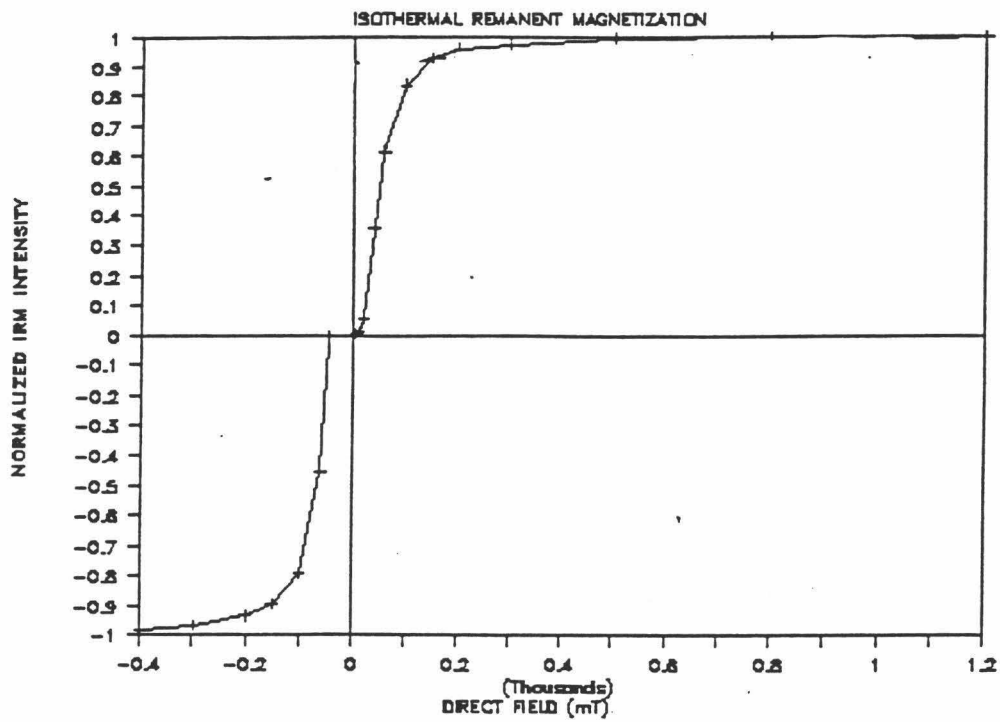


Figure 3.25. Histerises diagrams of the isothermal remnant magnetization. Note that the curves saturate below 1 Tesla, indicating that titanomagnetite is the source of the magnetization.

thermoremanent magnetization (TRM) residing in titanomagnetite minerals of single (SD) or pseudo-single (PSD) domain states.

Site mean chNRM directions for the sites in lava flows form a tightly clustered distribution, except that site 22 that falls some degrees off the group (Figure 3.26). Corresponding chNRM directions for the cones also show a well defined group, except that site 16 (Figure 3.26). Overall mean directions for the lava flow and for the cones were calculated using procedures similar to those for PSV analysis (e.g. McWilliams *et al.* 1982; Bohnel *et al.* 1990) incorporating two-tier analysis (Watson and Irving 1957; McFadden 1982) and 'outlier' analysis (McFadden 1980). The overall mean direction for the lava flow sites is Dec = 10.8° , Inc = 23.6° , with $k = 287.4$ and $\alpha_{95} = 2.3^\circ$. Inclusion of site 22 outlier direction does not greatly change the parameters (Table 3.4). The corresponding overall mean direction for the cones is Dec = 12.8° and Inc = 25.2° with $k = 353$ and $\alpha_{95} = 4.9^\circ$ (Table 3.4), which is statistically indistinguishable from that for the lava flows (test after McFadden and Lowes, 1981). Because of the small number of sites in the cones, statistical parameters vary with inclusion of data for site 16, resulting in $k = 81$ and $\alpha_{95} = 8.5^\circ$ but almost the same mean direction is obtained (Table 3.4). To proceed further, the overall mean direction for lavas and cones together shows a small angular dispersion ($k = 301$ and $\alpha_{95} = 2^\circ$) with Dec = 11.2° and Inc = 24.0° . The corresponding PSV estimate is $S_b = 4.4^\circ$. This PSV estimate is considerably lower than that representative for Hawaii (around 11) reported earlier (e.g. Doell and Cox, 1971, 1972; McWilliams *et al.* 1982) and further points out to the short time interval represented by the sites studied here.

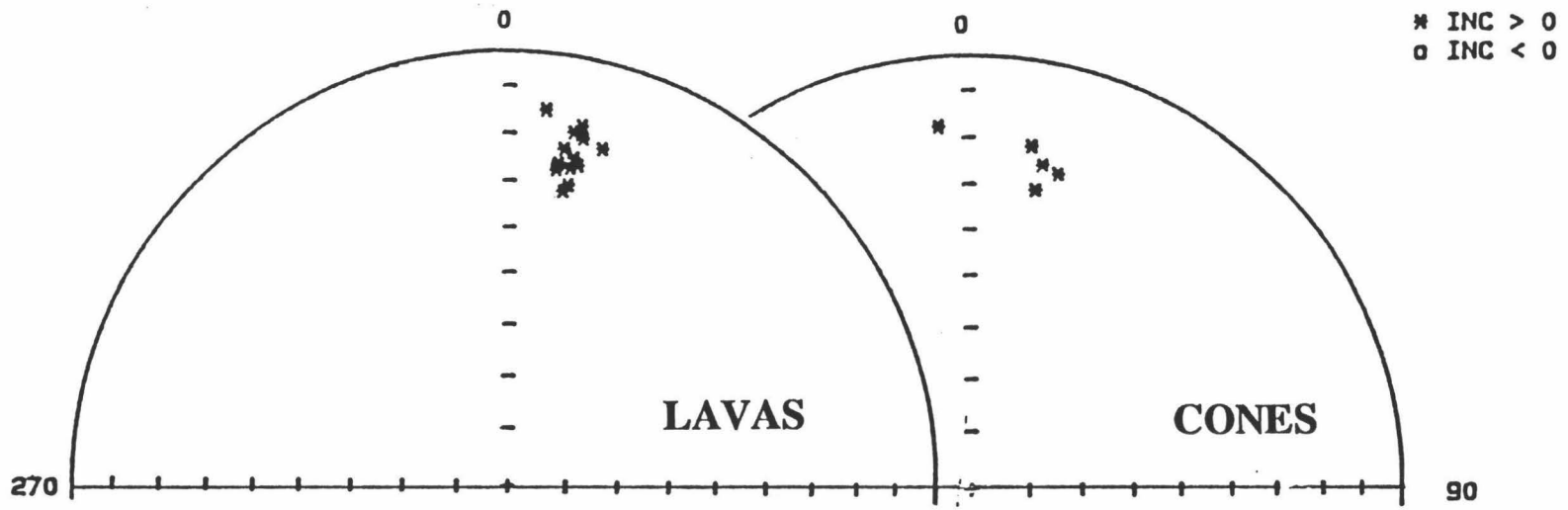


Figure 3.26. Equal area stereograms of flow sites (left) and cone sites (right). Note that in both diagrams all the sites cluster very well with the exception of the outliers (site 22 in the lavas and site 16 in the cones), and that the clusters are in the same location.

Table 3.4
FISHER STATISTICS AND PALEOSECULAR VARIATION CALCULATIONS

	dec (°)	inc (°)	K	α_{95} (°)	R	n	St	Sw	Sb	Sf	eccentricity	dipole moment	axis ratio	alpha	Nmean
all cones	9.1	23.7	81.1	8.5	4.95065	5	9.0	6.8	8.8	8.7	0.94	0.80	3.04	37.2	10.0
cones w/o 16	12.8	25.2	352.6	4.9	3.99149	4	4.3	6.7	3.8	3.6	0.89	0.66	2.21	87.7	10.5
all flows	10.4	23.0	228.5	2.5	14.93874	15	5.4	5.3	5.1	5.0	0.91	0.70	2.38	9.1	11.2
flows w/o 22	10.8	23.6	287.4	2.3	13.95477	14	4.8	5.3	4.6	4.4	0.94	0.79	2.93	19.9	11.2
all w/o 16 & 22	11.2	22.0	301.1	2.0	17.94355	18	4.7	5.6	4.4	4.2	0.90	0.69	2.33	115.3	11.0

Table 3.3. n: number of sites, K and α_{95} : precision parameters, dec: declination, inc: inclination, St, Sw, Sb, and Sf: angular dispersion parameters, axis ratio: ratio of major to minor axis of ellipse approximating the VGP distribution (from Bohnel *et al.* 1990)

Paleomagnetic Data Summary

In summary, the results support that lavas in the cones and Pohue Bay flow present similar paleomagnetic (directional) characteristics and a relatively close age relationship (within the PSV characteristics for Hawaii). The directions from the sites in the lava flows appear to have been drawn from a common Fisherian distribution (McFadden 1980), with the exception of site 22. The site is in the toothpaste lava/a'a flow that fills the upslope channel and could represent either a younger flow or post-cooling deformation within the channel. The number of sites in the cones is too small for statistical discrimination of distribution type; site 16, the SE-most cone, is an outlier. This might be due to a vent anomaly or an older age; the area of the Pohue Bay flow adjacent to the SE-most cones is the oldest mapped (Figure 3.3).

It should be kept in mind that there are limitations in terms of time resolution imposed by the PSV characteristics and the paleomagnetic record of the samples. Holcomb *et al.* (1986) estimated a secular variation curve for Hawaiian lavas that covers the past 3000 years (Figure 3.27) and used this for dating purposes. The Pohue Bay flow had been assigned an age of around 740-910 years BP based on degree of weathering (Lipman and Swenson 1984). The paleomagnetic data (using the mean virtual geomagnetic pole VGP position) can also be compared with the PSV curve to determine an age. This is done graphically in Figure 3.27. The Pohue Bay flow mean VGP falls a few degrees off the curve close to the 2000-2500 years-old segment. An old radiocarbon-dated Kilauea lava sampled by JP Lockwood (locality: Lat: 19°27.62'N, Lon: 155°14.86'W, Elev: 3805')

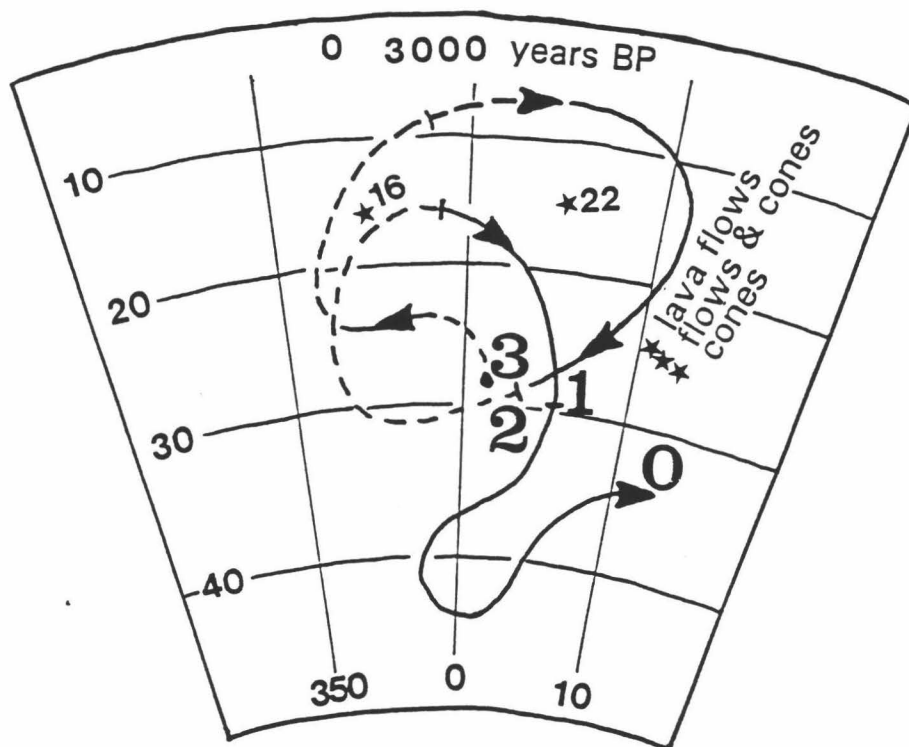


Figure 3.27. Secular variation curve for Hawaii during the last 3000 years (from Holcomb *et al.* 1986). Large numbers indicate ages in thousands of years BP. Stars represent the mean VGP for sites 16, 22, lavas-only (excluding site 22), cones-only (excluding site 16), and lavas-and-cones together (excluding sites 16 and 22). Note that the mean VGP's fall a few degrees off the curve close to 2000-2500 years BP segment.

has very similar paleomagnetic directions (Dec = 8.0° , Inc = 27.9°) to those of the Pohue Bay Flow. Its ^{14}C age is 2770 ± 150 years (JP Lockwood pers. comm. 1993), which corresponds well with the age for the Pohue Bay flow and cones determined from the PSV curve.

A charcoal sample found underneath the Pohue Bay flow (see Figure 3.21 for location) was dated by Accelerator Mass Spectrometer (AMS) at the University of Arizona and gave an ^{14}C age of 305 ± 45 years BP. This date is clearly too young considering that charcoal from ancient Hawaiian archaeological sites on the Pohue Bay flow yielded ^{14}C ages of 595 ± 80 years BP (Soehren 1966).

Summary of Evidence for Littoral or Primary Origin

A comparison of the evidence pertaining to whether the cones described in this chapter are primary or littoral shows that the data lean towards the littoral origin, however, it is not unequivocal (see Table 3.5). If the cones are primary, anomalies in the behavior of Mauna Loa's rift zone plumbing are required, as are simultaneous eruptions from the rift and from vents along the coast (to explain the field relationships). Dense angular fragments resemble accidental lithics but are more likely to be parts of the associated lava. Grainsize parameters indicate that water was involved in the formation of these cones, but cannot be used to determine whether magma or lava was interacting with the water. The cones considered here have the form of primary tuff cones, however, they are composed mostly of spatter. This may be an indication of their non-primary nature. Chemical analyses show that the pyroclastics forming the cones has been largely degassed,

Table 3.5 Balance of littoral and primary evidence

Attribute	if primary	if littoral	Puu Ki and Auau cones	littoral balance
on coastline	sometimes	always	yes	0
on rift zones	most of the time	not necessarily	no	+0.5
angular fragments	expected	possible	yes	-0.5
primary pyroclastic density	low	high	high	+1.0
pyroclastic grain size	see Fig. 16	see Fig. 16	indistinguishable from primary	0
edifice morphology	circular ring	twin cones, circular in Iceland	circular	-0.5
edifice size	big	small	small	+1.0
relationship between flows and cones	not necessarily related	related	related (by field work, chemistry, & paleomagnetism)	+1.0
Sulfur content	high	low	low	+1.0
total littoral balance				+3.5

Table 3.5. Compilation of evidence for primary and secondary origins for the cones considered in this study. In the last column, each item of evidence has been given an arbitrary vote, and the balance is +3.5 in favor of a littoral origin.

strong evidence that they are not vents. Field relationships, chemistry, petrography, and paleomagnetic data all indicate that the cones and flows are coeval. Since the source of the flows is upslope, this also strongly supports a littoral origin for the cones.

DISCUSSION: THE FLOW OF LAVA INTO THE OCEAN

As lava enters the ocean it can either interact explosively or non-explosively, and this is primarily controlled by the rate at which heat is transferred from liquid lava to sea water. Before presenting my scenario for the Pohue Bay and Auau cones, I will describe several well-known examples of lava flows entering the ocean and the resulting lava-seawater interactions. When the 1950 Mauna Loa flow fronts (consisting of clinkery a'a) first entered the ocean, huge steam clouds were generated but not much littoral ash was observed (Finch & Macdonald 1950). There are, however, small littoral cones associated with the 1950 flows (Macdonald & Abbot 1970) and their formation may have been initially obscured by the steam. These flows were some of the fastest ever observed in Hawaii with flow-front velocities of 660-9300 m/hour and volumetric flow rates of 30-1000 m³/hour (Rowland & Walker 1990). Well-developed channels very quickly extended to the coastline so that the lava entering the water thereafter consisted of the relatively smooth-surfaced channel interior. The quiet entry of an exceptionally high volume of lava into the ocean was noted as remarkable (Macdonald & Finch 1950; Macdonald 1972).

During the 1969-1974 Mauna Ulu eruption, both pahoehoe and a'a entered the ocean (Moore *et al.* 1973; Moore 1975; Peterson 1976). A narrow a'a flow with a volumetric flow rate of 140-400 m³/hour entered the ocean in June 1969. It maintained its continuity several hundred meters under water, and no littoral explosions or debris were reported (Moore *et al.* 1973). Later in the Mauna Ulu eruption, tube-fed pahoehoe with volumetric flow rates between 3 and 4 m³/sec entered the ocean numerous times. These flows formed lava deltas which consisted of pahoehoe lava above sea level overlying forset layers consisting mostly of hyaloclastite formed by small littoral explosions, as well as pillow lavas and broken fragments of pillows (Moore *et al.* 1973).

Lava deltas also formed during the tube-fed pahoehoe episodes 48 and 51 of the Puu Oo/Kupaianaha eruption (Heliker & Wright 1991; Mattox *et al.* 1992). The volumetric flow rates were <5 m³/sec. At most times the ocean entry consisted of numerous slow-moving toes cascading over a low sea cliff or lava bench, and steam explosions were minimal. Due to the unconsolidated base the lava delta collapsed repeatedly (Heliker & Wright 1991; Moulds *et al.* 1990), and larger feeder tubes erupted directly into the water. The same overall volumetric flow rate into the ocean was suddenly taking place from one or two larger streams; both the vigor of the steam explosions and the amount of comminuted flow material that was thrown out increased immediately. The littoral cones produced during this activity were mostly less than a few meters high, and developed at the edge of the lava bench above the ocean entry.

A recent event at the Kamoamoao ocean entry was rather different (November 1992; T. Mattox pers. comm.). Shortly after a bench collapse event strong explosions tore open the flow carapace about 40 m inland from the ocean entry and incandescent lava was thrown up to 100 m high. The initial explosions produced fine material that the wind blew out to sea. The last explosions were less violent and produced a secondary vent structure a few meters high constructed of dense spatter (Figure 3.18).

The 1840 Kilauea a'a flow ($94 \text{ m}^3/\text{sec}$) produced the Sand Hills half cones (Walker 1992). Out of the three arms of the 1868 Mauna Loa channel-fed pahoehoe and a'a flow that reached the ocean ($95 \text{ m}^3/\text{sec}$), one produced the three Puu Hou half cones (Fisher 1968). The Pohue Bay tube-fed pahoehoe flow ($1000\text{-}4000 \text{ m}^3/\text{sec}$; Jurado-Chichay & Rowland 1993) produced numerous circular littoral cones.

In conclusion from these examples, lava-water interaction produces a large range of explosivity when a flow enters the ocean. Neither volumetric flow rate nor lava type is a good predictor of the nature of lava-water interaction. Therefore, other variables and processes have to be considered in order to explain the nature or occurrence of explosive lava-seawater interaction.

If the lava is tube-fed pahoehoe, pillow lavas form under water. The rapidly-developed chilled skin physically prevents contact between water and liquid lava except at small spreading cracks (Moore 1975). A thin layer of steam develops around each pillow and helps to insulate the pillow (Moore *et al.* 1973; Moore 1975; Mills 1984). When the mixing of lava and water is increased, either when a tube empties directly into the ocean after

bench collapse or when a large wave washes lava into a coastal skylight, the explosivity of the lava-water interaction is increased. The littoral deposits formed by this activity constitute much of the lava delta and occasionally produce small littoral cones.

In the case of an a'a flow with a thick clinker carapace, a thermal gradient exists from ambient to incandescent lava temperature (~1140°C). Infiltrating water would be expected to boil long before it reached the incandescent lava (i.e. when it reaches the 100° isotherm) and the high permeability of the clinker would allow the steam to escape passively (T. Thordarson pers. comm.). The Sand Hills case, however, indicates that strong littoral explosions can be associated with a'a flows.

Fuel-coolant theory and experimental work by Wohletz (1983) and Sheridan & Wohletz (1983) indicate that the important factor in generating explosive lava-water interaction is the rate of heat transfer from liquid lava to water. To generate explosions water must be superheated to 250-300°C in milliseconds (e.g. Morrissey 1991). This superheated water can flash into steam and expand explosively, fragmenting the lava. The fragmentation increases the area of liquid lava-water interfacial surface which in turn generates more superheated water, and so on. Once started, fuel-coolant reactions are self-perpetuating as long as sufficient supplies of water and fluid lava are maintained. Whether or not strong littoral explosions are going to occur in a'a or pahoehoe flows will depend on the ability of somewhat restricted circumstances to initiate fuel-coolant reactions.

The vigor of fuel-coolant reactions, once initiated, is related to the ratio of water and lava (Wohletz 1983; Morrissey 1991). The maximum explosivity

is generated at a water:lava mass ratio of around 0.3. Increasing or decreasing the amount of water lowers the explosivity.

The minor steam explosions associated with the flow of pahoehoe into the ocean may be able to disrupt a few nearby pillows, but because the pillows are so small and discontinuous the availability of liquid lava is quickly exhausted. As noted above it is difficult for water to reach the interior of an a'a flow through a thick clinker layer to initiate explosive boiling. Although exposing a large area of incandescent lava to the ocean, the smooth-surfaced channelized lava of the 1950 Mauna Loa eruption generated very much steam but only small explosions. It was proposed by Macdonald (1972) that a layer of steam at the smooth ocean-lava interface prevented large-scale boiling, and the lava-water interaction was similar to that of pillow lava, although at a larger scale (Macdonald & Finch 1950). A crust on the lava would also have developed, and because the lava was entering the ocean without breaking up, explosive interaction did not occur.

An a'a flow with a thin clinker surface or flowing over a cliff into the ocean exposes a large area of its fluid interior to water, enhancing the possibility of fuel-coolant reactions. The 1840 a'a flow tumbled over a 15 m sea cliff (Brigham 1909), and the resulting explosions formed the Sand Hills. During the 1950 Mauna Loa eruption, the entry of the initial a'a front into the ocean produced steam explosions of a similar nature (Finch & Macdonald 1950). However, the channel rapidly developed to the coast and the explosions ceased; only small littoral cones were formed (see above). These are the two best historical examples of the "standard" formation of a littoral cone (Figure 3.1). In both cases pairs of half cones

were formed because littoral pyroclasts that landed on either the seaward side of the ocean entry or the active flow itself, were carried away. Only the material that fell on or beyond the stagnant margins was preserved.

The structure of a lava delta formed as a tube-fed flow enters the ocean provides a possible mechanism for the generation of strong littoral explosions. The main tube extends seaward and thus overlies the hyaloclastite base. Any strong disturbance (e.g. bench collapse) could cause the tube to collapse downward into the wet unconsolidated hyaloclastite. There would then be vigorous mixing of a large volume of fluid lava with water inland of the ocean entry. Continuous supply of lava through the tube and continuous influx of water through the hyaloclastites keep the fuel-coolant reaction going. Because the point of explosions is within the solid carapace of the tube-fed flow, littoral pyroclasts can build up in all directions, and complete circular cones develop. A similar mechanism has been proposed for the formation of rootless cones in Iceland (Thordarson & Self 1993). In that case the lava flowed into shallow lakes with unconsolidated bottom sediments. Collapse of lava tubes into these sediments generated secondary explosions to form the rootless cones.

A surface or channel-fed pahoehoe flow could also collapse into underlying hyaloclastites and produce strong explosions. Even though the explosions may be inland as at Puu Hou (Fisher 1968), half cones form instead of complete cones because pyroclasts landing on the moving surface get carried away.

SCENARIO FOR FORMATION OF CIRCULAR LITTORAL CONES

With the above considerations in mind it is possible to constrain the sequence of formation for the Pohue Bay and Auau cones. Any scenario for formation of these features must explain their large size, (even though they are associated with pahoehoe flows), their circular form, and the fact that they consist of both a lapilli/spatter outer rim with dense spatter and ponded lava within. I present a model that is consistent with my observations.

Initially, a tube-fed pahoehoe flow approached the coastline (Figure 3.28A). Pahoehoe lava deltas with flow foot hyaloclastite and pillows formed when lava reached the ocean and small littoral explosions might have occurred (Figure 3.28B). Because this delta was a very unstable structure parts of it collapsed on many occasions (Figure 3.28C). At a point inland from the coast the tube collapsed into the underlying water-saturated hyaloclastites leading to vigorous littoral explosions (Figure 3.28D). Explosions could also have taken place in large water-filled voids within the flow (or underlying flows). Pahoehoe lava flows are full of gas blisters, full or drained tubes and tumuli, and other voids. Furthermore, undercutting of the hyaloclastite layer can produce extensive sea caves. All of these void spaces are potential sites of strong explosions.

The strength of the explosions changed as the relative volumes of interacting lava and water varied. The bulk of the pyroclasts ranged from spatter to scoria lapilli. At times spatter accumulation was rapid enough so that spatter coalesced and flowed away to produce spatter-fed flows. The main cone built up on the solid flow surface and possibly partially in the

water offshore, and lava could continue to be fed to the point of explosions through the main tube. The final stage of main-cone building was the most explosive, and produced the angular fragment-rich upper layer (unit D of Figure 3.6) that is widely dispersed in the Puu Ki area.

Soon, however, the building up of littoral pyroclastic material began to block off the access of water to the tube (Figure 3.28E), and the vigor of the explosions decreased rather dramatically. Spatter and lava began to fill the newly-created rim. Activity within the main flow field continued, overlapping the outer base of the cones.

Eventually, supply of lava to this area ceased, and activity migrated along the coast to repeat the process. Wave action at both Pu`u Ki and the three-rim cone eroded the seaward parts of the outer rims to expose the ponded/spatter-fed lava (Figure 3.28F). At `Au`au cone, however, it appears that collapse of the seaward part took place while there was still molten lava in the ponded zone. This lava flowed into the ocean (Figure 3.28G), generating littoral explosions which threw out blobs of spatter. Those that traveled in a landward direction mantled the arcuate scarp and the S half of the cone. After activity finally ended, wave action eroded the northern straight part of the `Au`au cone scarp to its present form. Still later an a`a flow re-occupied the tube, forcibly extruding into the cone interior and resurfacing both it and the small peninsula (Figure 3.28H). The very last event was the eruption of an additional a`a flow that wrapped around `Au`au cone (Figure 3.28 I).

An additional complication at Pu`u Ki and the three-rim cone is provided by the large depression just inland from the cones (Jurado *et al.* 1991;

Figures 3.3 & 3.12). This depression appears to once have been a large lava rise (Walker 1991), and as such could have stored an appreciable volume of lava. If this large volume of stored lava drained out suddenly, it could have augmented the volumetric flow rate into the ocean that built the Pu`u Ki and three-rim cone. Associated with the SE-most cones of the Pohue Bay group is another large depression, and a channel that drains it leads to the vicinity of these cones. However, because the Pohue Bay flow had a high volumetric flow rate to begin with, draining of the depression was not required.

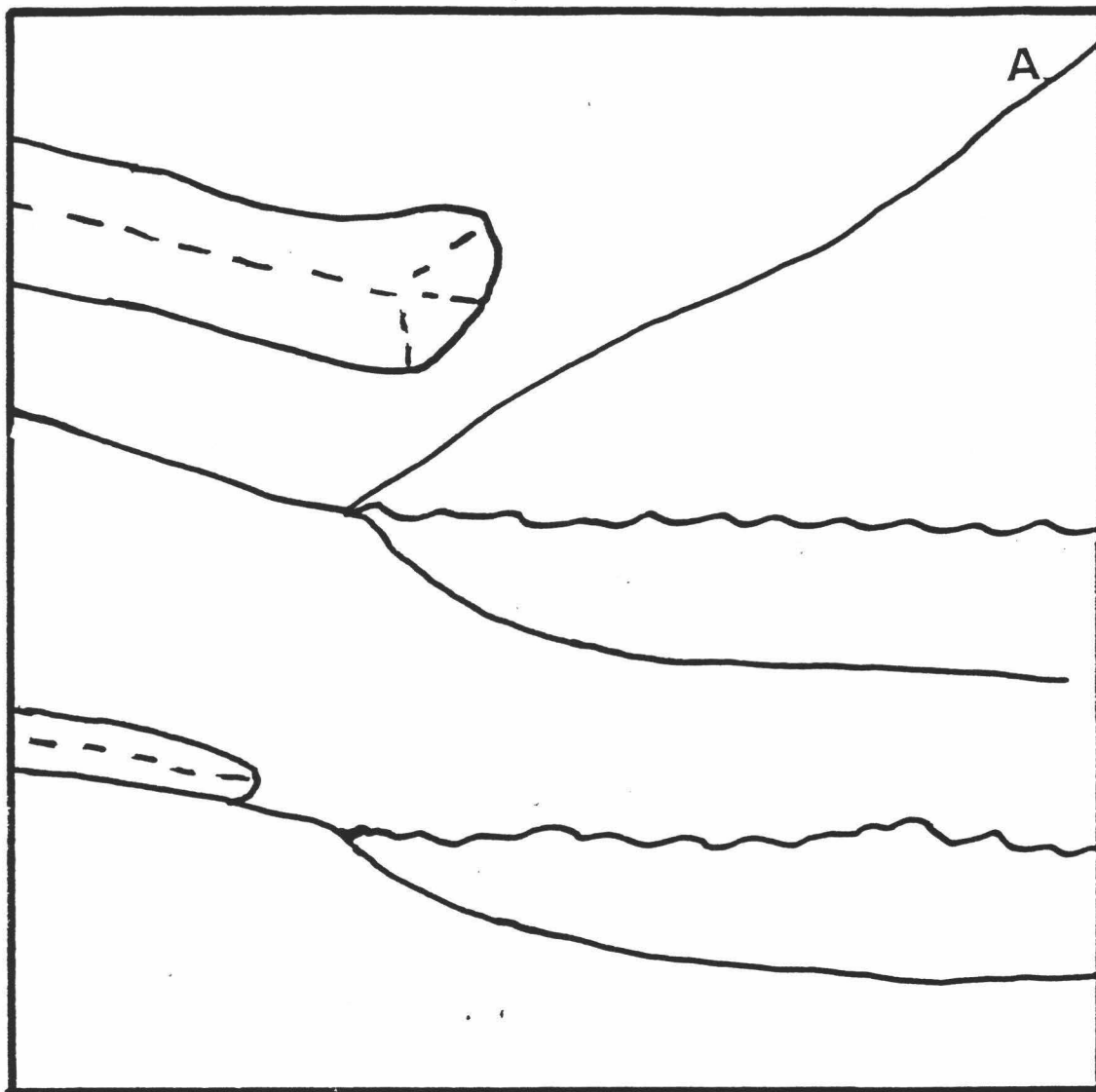


Figure 3.28. Sequential diagrams and cross-sections of circular littoral cone formation: a) lava approaches coastline.

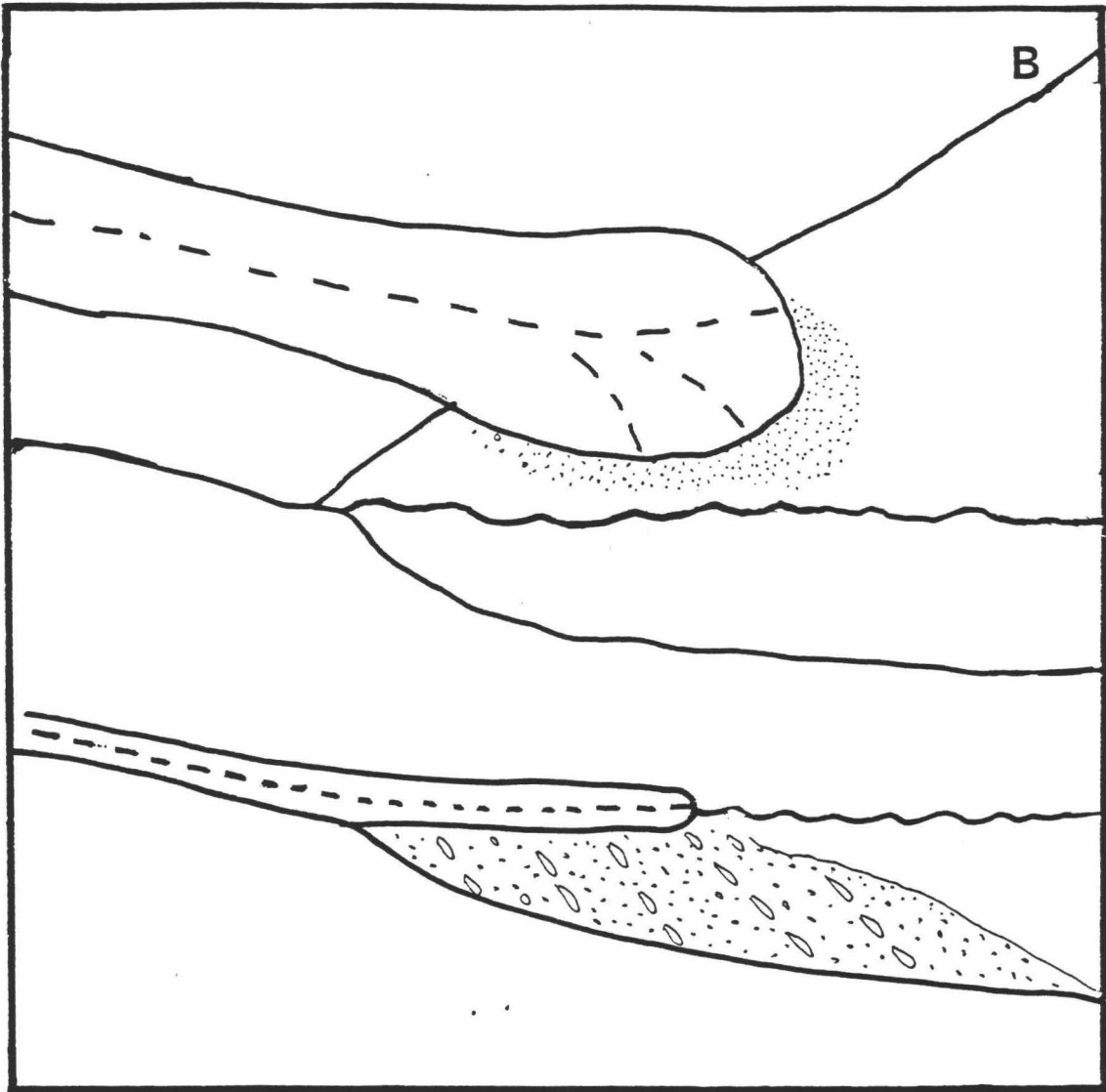


Figure 3.28 (continued) b) small littoral interaction forms hyaloclastites over which the lava extends, forming a bench.

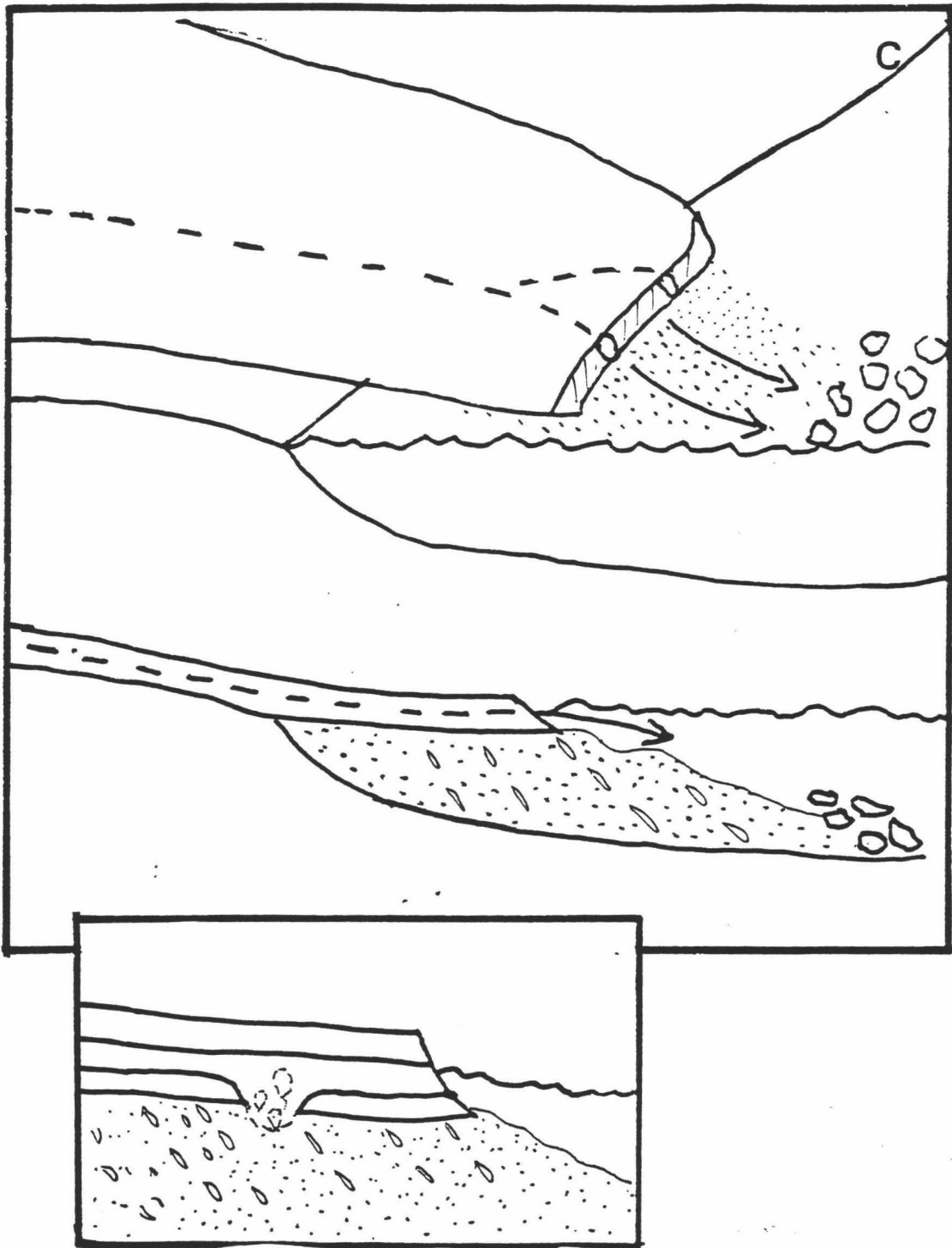


Figure 3.28 (continued) c) bench collapses. Disturbance in the hyaloclastite allows the tube to collapse downward. Molten lava mixes explosively with underlying wet hyaloclastites.

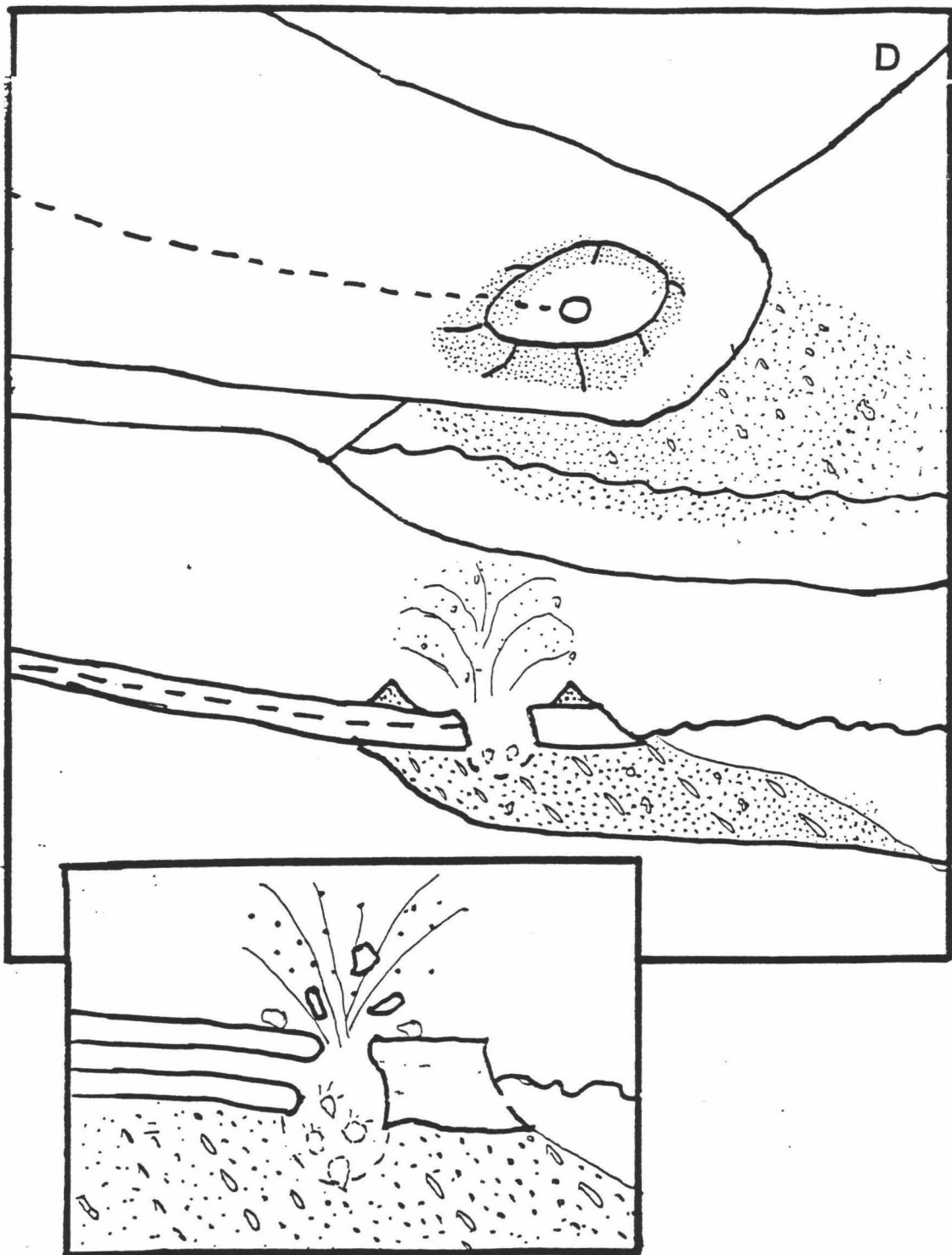


Figure 3.28 (continued) d) Explosions become stronger and break through the tube roof to start building the main littoral cone.

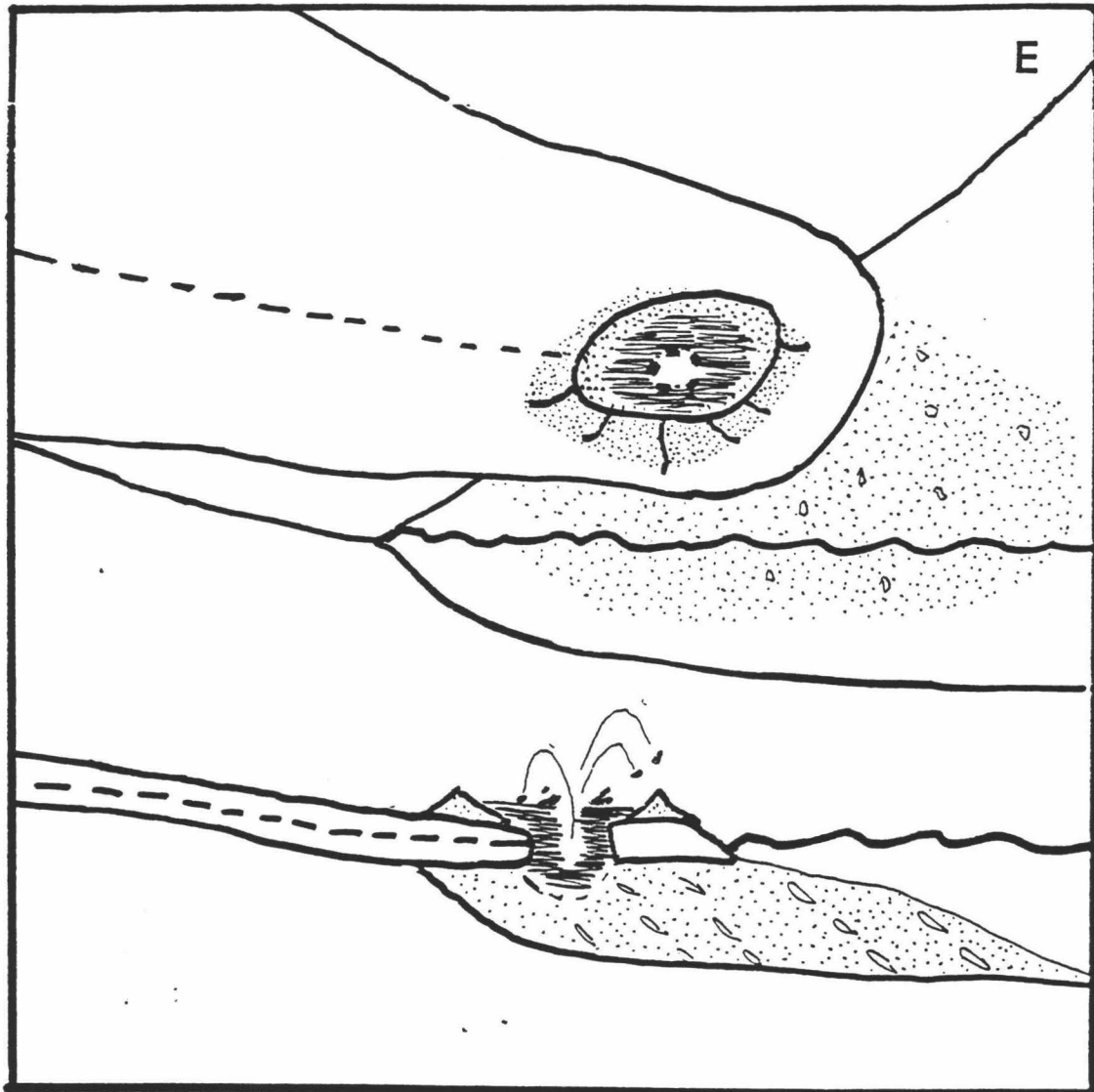


Figure 3.28 (continued) e) water supply diminishes and explosions weaken to spattering and produce the inner rims, lava ponds within the main rim.

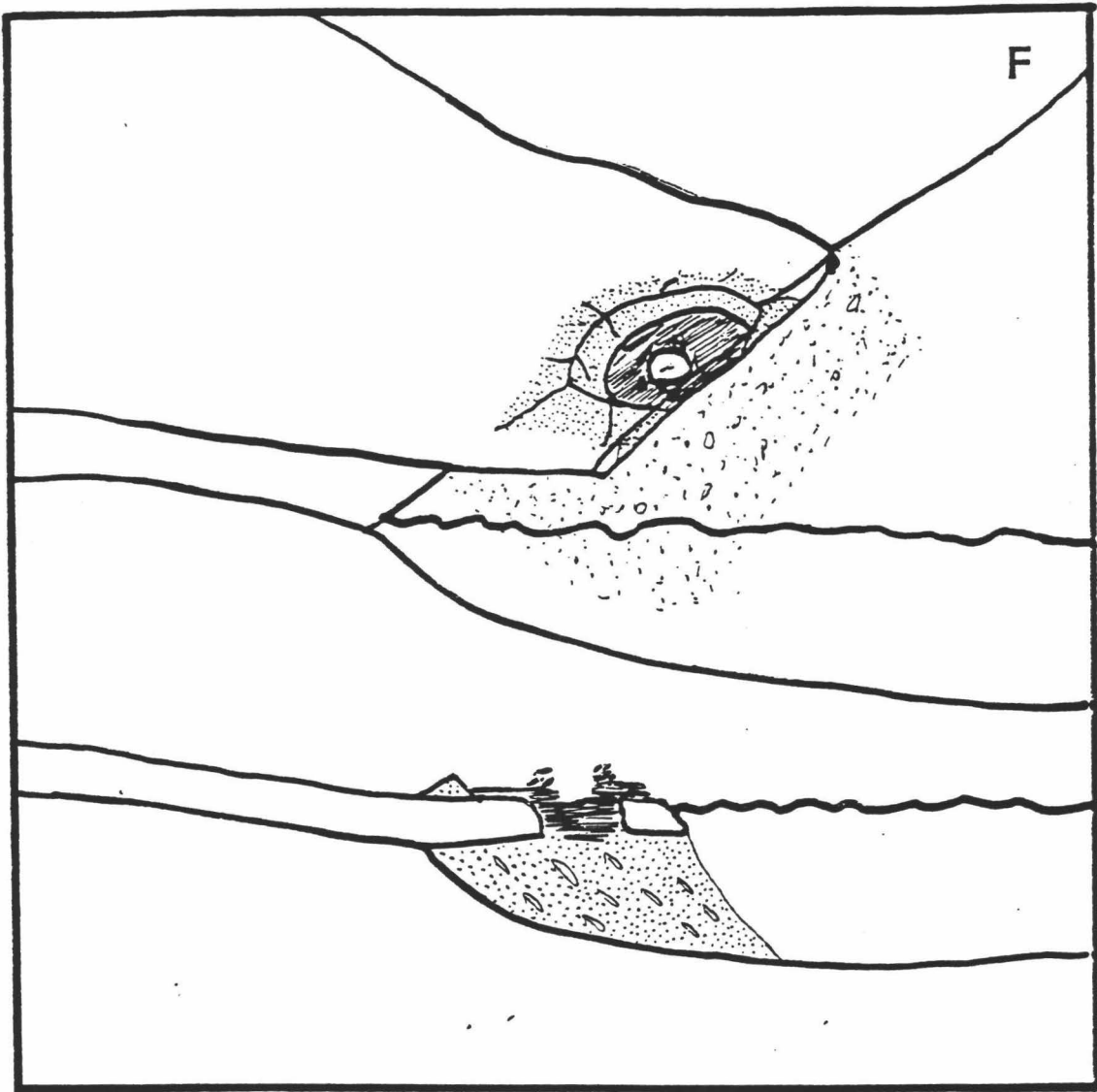


Figure 3.28 (continued) f) erosion/collapse due to marine action (Pu'u Ki and three-rim cone are at this stage).

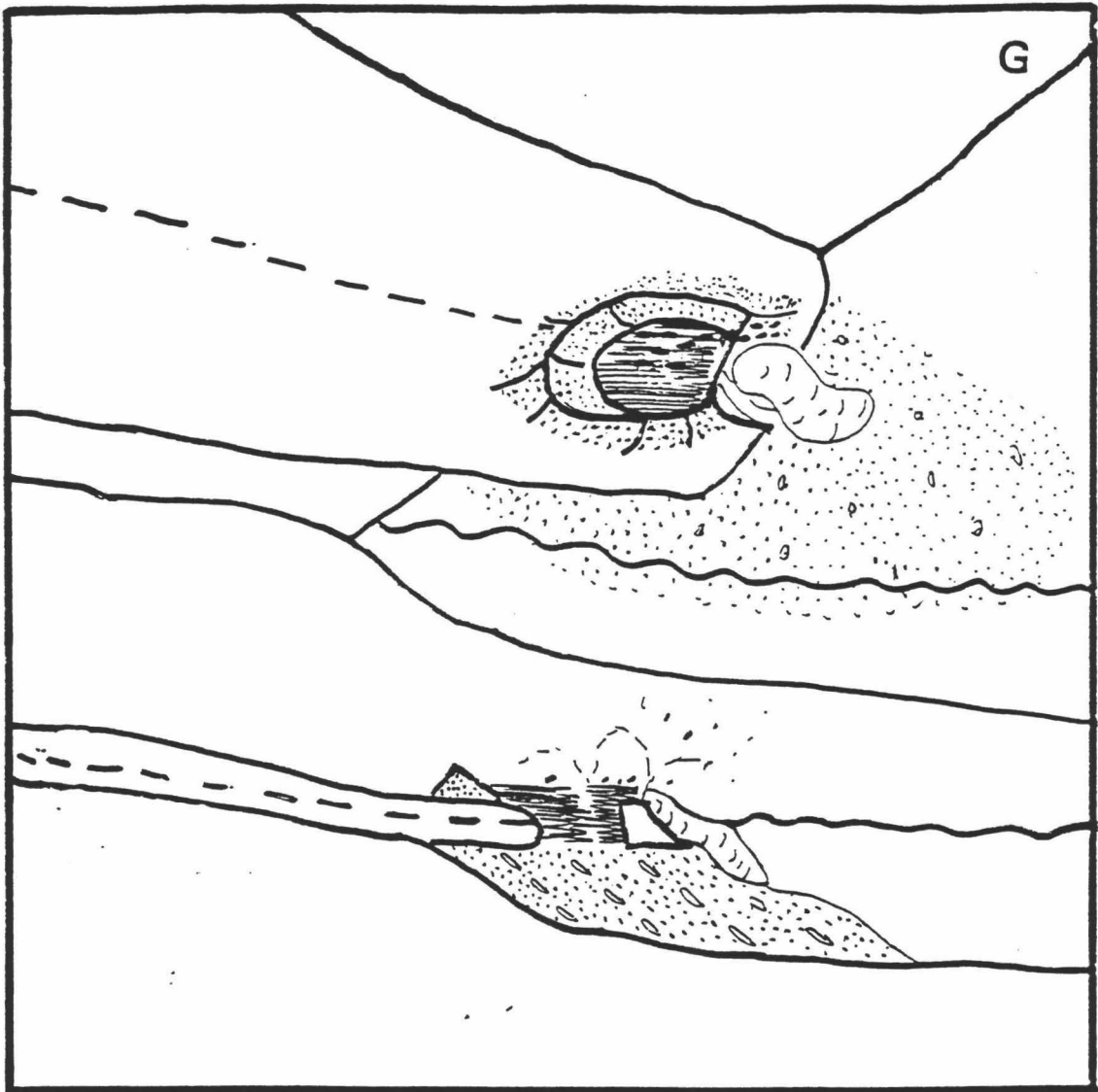


Figure 3.28 (continued) g) at 'Au'au cone--collapse takes place while molten lava remains in the ponded area and a small lava flow forms and spattering occurs.

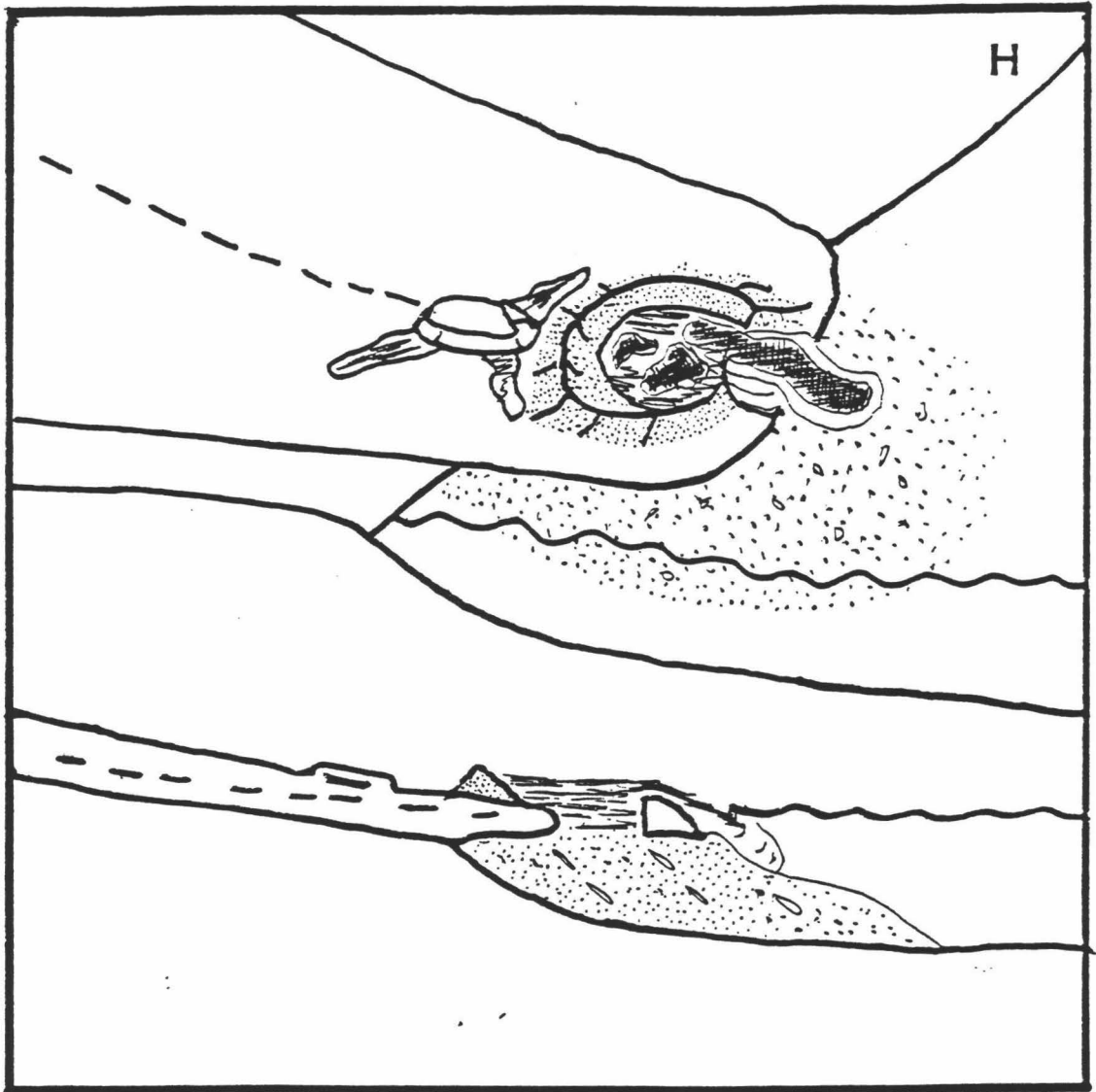


Figure 3.28 (continued) h) late-stage a'a (black) occupies the tube, forms a lava rise inland, and erupts through the ponded flows.

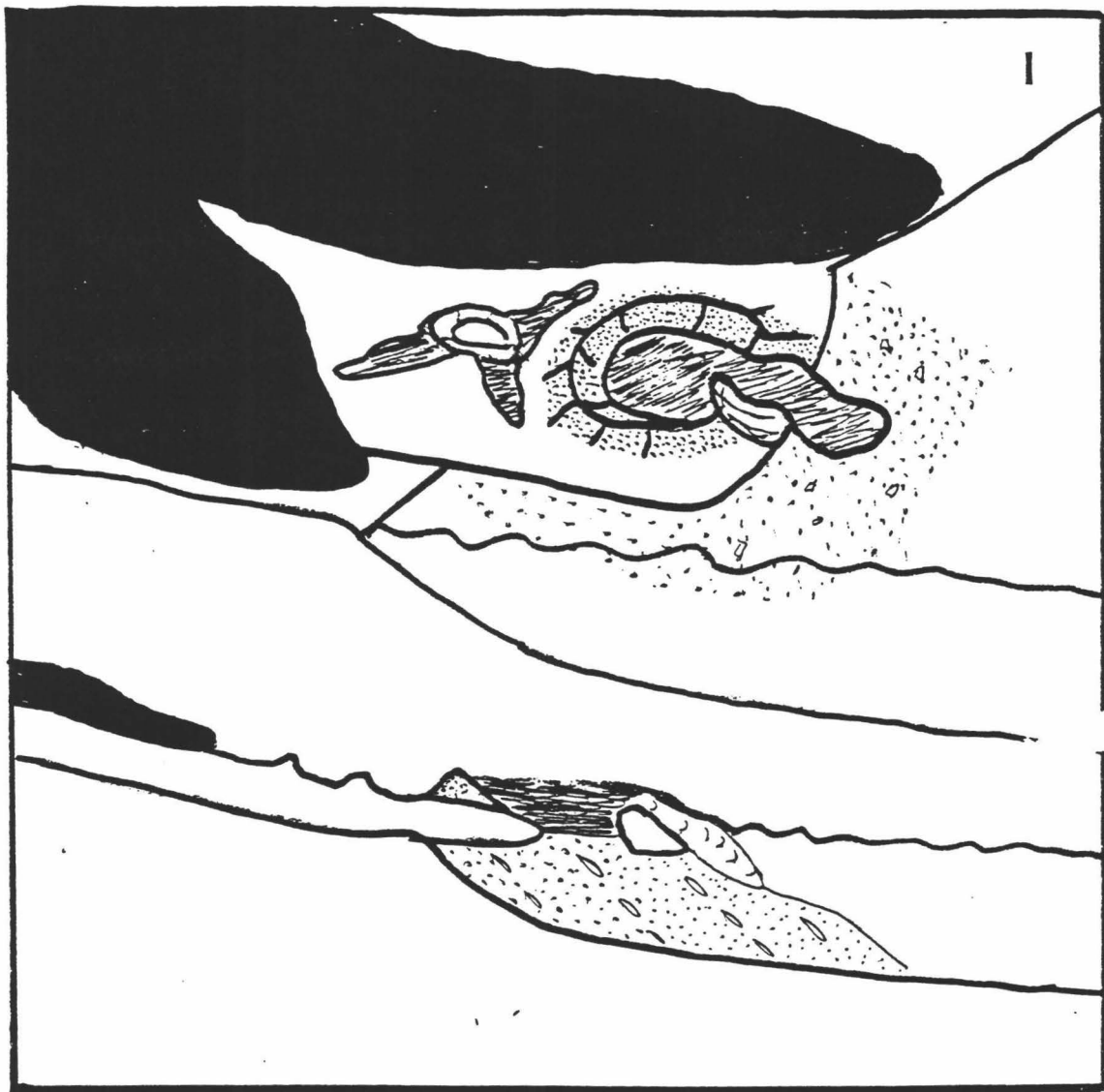


Figure 3.28 (continued) i) later a'a (possibly different eruption) surrounds the cone.

DISCUSSION AND CONCLUSIONS

I have described a group of cones having a similar structure consisting of an outer rim 100 to 400 m in diameter comprised mostly of spatter and lapilli that surrounds one or more inner cones comprised of dense spatter. These cones are closely associated with high volumetric flow-rate pahoehoe flows, and using a variety of evidence I conclude that they are littoral in origin. The essential requirements for forming circular littoral cones are: 1) a high volumetric flow-rate tube-fed pahoehoe flow; 2) efficient mixing of the lava and water at an inland location.

The lava flow involved in the formation of circular littoral cones must be tube-fed; in Hawaii that implies also that it must be pahoehoe. Any flow with an open channel or moving top surface (such as a`a) will carry away the littoral pyroclasts that land on it, either onshore or offshore, and the result will be the more traditional pair of cones formed on either side of the lava. A tube-fed pahoehoe flow, on the other hand, forms a static carapace during continued flow through tubes, and this allows littoral pyroclasts the opportunity to build up during the eruption without being carried off. Additional evidence for the close association with pahoehoe is the nature of the later spatter deposits. In order to form spatter, the lava must have a low viscosity, and this rules out the possibility that it is a`a.

I therefore conclude that the cones of the Pohue Bay and Kolo flows have a littoral origin. These cones closely resemble primary vents in many aspects and would have important consequences with respect to expected eruption locations on Mauna Loa if that were the case; (e.g. Macdonald

1972). It is important, therefore to examine them closely to determine their true nature. These structures also indicate that the entry of high volumetric flow-rate pahoehoe into the ocean can be dangerously explosive.

CHAPTER IV CONCLUSIONS

The Pohue Bay Flow had volumetric flow rates larger than any eruption that has been witnessed on Mauna Loa volcano. This unusual flow presents several interesting features. These include a large tube/channel system; overflows that made the transition to a'a and later generation of pahoehoe as their molten interiors welled out and circular littoral cones. I have studied each of these in detail and determined how they formed. The basic ingredient is a high volumetric flow rate pahoehoe lava, which is unusual in historic eruptions. In the case of the overflows this allows the interior of the lava to flow rapidly and remain relatively fluid while its surface undergoes several transformations: An a'a like surface does not mean an a'a flow interior. The definitions of pahoehoe and a'a should be restated to take this into account. In the case of the cones, a high volumetric flow rate provides the material for the formation of large cones but these will not necessarily have a circular shape. A tube-fed pahoehoe flow and explosions taking place inland are the necessary conditions to form circular littoral cones. These conditions provide the pyroclasts a stable surface to land on so that they are not carried away by the flow or the ocean. The danger of pahoehoe flows has been underestimated because historical flows have generally advanced slowly (Rowland & Walker 1990). However, as has been shown in this thesis pahoehoe can have high volumetric flow rates and equally high flow-front velocities. Large channels and tubes with fast moving overflows can develop, and when the lava reaches the ocean littoral explosions are strong enough to produce rings and cones up to 500 meters in diameter.

REFERENCES

- Anderson SW & Fink JH (1992). Crease structures: indicators of emplacement rates and surface stress regimes of lava flows. *Geol Surv Am Bull* 104: pp 615-625.
- Brigham WT (1909). The volcanoes of Kilauea and Mauna Loa on the island of Hawaii. *Mem Bernice Pauahi Bishop Museum* II no. 4: 608 pp.
- Bohnel H, Urrutia-Fucugauchi J, & Herrero-Bervera, H (1990). Paleomagnetic data from central Mexico and their use for paleosecular variation studies. *Physics of the Earth and Planetary Interiors* 64:224-236.
- Doell RR & Cox A (1971). Pacific geomagnetic secular variation. *Science* 71:248.
- Doell RR & Cox A (1972). The pacific geomagnetic secular variation anomaly and the question of lateral uniformity in the lower mantle. In: Nature of the solid Earth, edited by E.C Robertson. McGraw-Hill, New York. 245pp.
- Finch RY & Macdonald GA (1950). The June 1950 eruption of Mauna Loa. *Volcano Letter* 508:12 pp.
- Fink JH & Fletcher RC (1978). Ropy pahoehoe: surface folding of a viscous fluid. *J Volcanol Geotherm Res* 4:151-170.
- Fisher RA (1953). Dispersion on a sphere. *Proc. Roy. Soc., London, Ser. A*, 217:295-305.
- Fisher RV (1968). Pu`u Hou littoral cones, Hawaii. *Geol. Rundschau* 57:837-864.
- Fisher RV & Schmincke H-U (1984). Pyroclastic Rocks. Springer-Verlag, Berlin, 472 pp.
- Harris DM & Anderson AT Jr (1983). Concentrations, sources, and losses of H₂O, CO₂, and S in Kilauea basalt. *Geochem Cosmochem Acta* 47:1139-1150.

- Heliker CC & Wright TL (1991). The Pu`u `O`o -Kupaianaha eruption of Kilauea. *EOS* 72:521-530.
- Holcomb RT, Champion DE, & McWilliams MO (1986). Dating recent Hawaiian lava flows using paleomagnetic secular variation. *Geol. Soc. Am. Bull.*, 97:829-839.
- Holcomb RT (1987). Eruptive history and long-term behavior of Kilauea Volcano. *U.S. Geol. Surv. Prof. Pap.* 1350:261-350.
- Johnson AM (1970). Physical Processes in Geology. Freeman, Cooper & Co., 577 pp.
- Jurado Z, Rowland SK, & Walker GPL (1991). Littoral cones of the Pu`u Ki area, Hawaii: high-intensity explosions from major pahoehoe lava tubes. *EOS* 72 (no. 44):566.
- Jurado-Chichay Z & Rowland SK (1993). High volumetric flow-rate overflows and pahoehoe to a'a to pahoehoe transitions. *Bull Volcanol* (submitted).
- Kilburn CRJ (1981). Pahoehoe and a'a lavas: a discussion and continuation of the model of Peterson and Tilling. *J Volcanol Geotherm Res* 11:373-382.
- Lipman PW (1980a). The southwest rift zone of Mauna Loa--implications for structural evolution of Hawaiian volcanoes. *Am. J. Sci.* 280-A:752-776.
- Lipman PW (1980b). Rates of volcanic activity along the southwest rift zone of Mauna Loa Volcano, Hawaii. *Bull. Volcanol.* 43:703-725.
- Lipman PW, Banks NG (1987). A'a flow dynamics, Mauna Loa 1984. *US Geol Surv Prof Pap* 1350:1527-1568.
- Lipman PW & Swenson A (1984). Generalized geologic map of the southwest rift zone of Mauna Loa Volcano, Hawaii. *U.S. Geol. Surv. Misc. Investig. Ser. Map I-1323*.
- Lockwood JP & Lipman PW (1987). Holocene eruptive history of Mauna Loa volcano. *U.S. Geol. Surv. Prof. Pap.* 1350:509-535.

- Macdonald GA (1953). Pahoehoe a'a, and block lava. *Am J Sci.* **251**:169-191.
- Macdonald GA (1972). Volcanoes. Prentice-Hall, Englewood Cliffs, NJ 510 pp.
- Macdonald GA & Abbot AT (1970). Volcanoes in the Sea The Geology of Hawaii. University of Hawaii Press, Honolulu, 441 pp.
- Macdonald GA & Finch RY (1950). The June 1950 eruption of Mauna Loa. *The Volc. Lett.* **509**:8 pp.
- Macdonald GA, Abbott AT, & Peterson FL (1983). Volcanoes in the Sea the Geology of Hawaii second ed. University of Hawaii Press, Honolulu, 517 pp.
- Macfadden PL (1980). Determination on the angle in a Fisher distribution which will be exceeded with a given probability. *Geophys. J. R. Astron. Soc.*, **60**:391-396.
- Macfadden PL (1982). Two-tier analysis in Paleomagnetism. *Geophys. J. R. Astron. Soc.*, **71**:519-543.
- Macfadden PL & Lowes FJ (1981). The discrimination of mean directions drawn from Fisher distributions: Royal Astronomical Society. *Geophysical Journal*, **67**:19-63.
- Mattox TN, Heliker C, Mangan M, & Kauahikaua J (1992). A year of transition for Kilauea's decade-long eruption. *EOS* **73** (supplement):629.
- McWilliams MO, Holcomb RT, & Champion DE (1982). Geomagnetic secular variation from ¹⁴C dated lava flows on Hawaii and the question of the pacific non-dipole low. *Philos. Trans. R. Soc. London, Ser A*, **306**:211-222.
- Mills AA (1984). Pillow lavas and the Leidenfrost effect. *J Geol Soc* **141**:183-186.
- Moore JG (1975). Mechanism of formation of pillow lava. *American Scientist* **63**: pp 269-277.

- Moore JG & Ault WU (1965). Historic littoral cones in Hawaii. *Pacific Science* **19**:3-11.
- Moore JG & Fabbi BP (1971). An estimate of the juvenile sulfur content of basalt. *Contrib Mineral Petr* **33**:118-127.
- Moore JG, Phillips RL, Grigg RW, Peterson DW, & Swanson DA (1973). Flow of lava into the sea, 1969-71, Kilauea Volcano, Hawaii. *Bull Geol Soc Am* **84**: pp 537-546.
- Moore JG, Fornari DJ, & Clague DA (1985). Basalts from the 1877 submarine eruption of Mauna Loa, Hawaii: new data on the variation of palagonitization rate with temperature. *U.S. Geol. Surv. Bull.* **1663**:11 pp.
- Morrissey MM (1990). Application of results from Fe-Al melt-water explosion experiments to hydrovolcanic eruptions. Unpub. MS Thesis, Univ. of Texas, Arlington, 137 pp.
- Morrissey MM & Thordarson T (1991). Origin and occurrence of pseudocrater Fields in southern Iceland. *EOS* **72** (no. 44):566.
- Moulds TN, Heliker C, Hon K, Kauahikaua J, Wright, & Bussard W (1990). Kilauea eruption update. *EOS* **71**:1694.
- Peterson DW (1976). Processes of volcanic island growth, Kilauea Volcano, Hawaii, 1969-1973. in Gonzales-Ferran, ed. *Proc. Symp. Andean and Antarctic Volcanology Problems* (Santiago, Chile, Sept. 1974). IAVCEI special series:172-189.
- Peterson DW, Tilling RI (1980). Transition of basaltic lava from pahoehoe to a'a, Kilauea volcano, Hawaii: field observations and key factors. *J Volcanol Geotherm Res* **7**:271-293.
- Rowland SK & Walker GPL (1990). Pahoehoe and a`a in Hawaii: volumetric flow rate controls the lava structure. *Bull Volc* **52**:615-628.
- Rowland SK, Walker GPL (1987). Toothpaste lava: characteristics and origin of a lava structural type transitional between pahoehoe and a'a. *Bull Volcanol* **49**:631-641.

- Rowland SK & Walker GPL (1988). Mafic-crystal distributions, viscosities, and lava structures of some Hawaiian lava flows. *J Volcanol Geotherm Res* **35**:55-66.
- Sakai H, Casadevall TJ & Moore JG (1982). Chemistry and isotope ratios of sulfur in basalts and volcanic gases at Kilauea volcano, Hawaii. *Geochem Cosmochem Acta* **46**:729-738.
- Sansone FJ & Resig JA (1991a). Lava-seawater interactions and the resultant steam plume at Wahaula, Hawaii. *EOS* **72** (no. 44): 566.
- Sansone FJ & Resig JA (1991b). Nearshore lava-seawater interactions at Wahaula, Hawaii, 1990-1991: the effects of intensified lava input to the ocean. *EOS* **72** (no. 44):558.
- Sheridan MF & Wohletz KH (1983). Hydrovolcanism: basic considerations and review. *J Volcanol Geotherm Res* **17**:1-29.
- Soehren LJ (1966). Hawaii excavations, 1965. Prelim Rept, Bishop Museum Dept of Anthropology (Honolulu).
- Swanson DA & Fabbi BP (1973). Loss of volatiles during fountaining and flowage of basaltic lava at Kilauea volcano, Hawaii. *US Geol Surv J Res* **1**:649-658.
- Swanson DA, Duffield WA, Jackson DB, & Peterson DW (1979). Chronological narrative of the 1969-71 Mauna Ulu eruption of Kilauea volcano, Hawaii. *U.S. Geol. Surv. Prof. Pap.* **1056**:55 pp.
- Thordarson T & Self S (1991). Lava-sea Water interaction at the Kupaianaha flow front, Kilauea Volcano, Hawaii. *EOS* **72** (no.44):566.
- Thordarson T & Self S (1993). The Laki (Skaftar fires) and Grimsvotn eruptions in 1783-85. *Bull Volcanol* **55**: (in press).
- Thorarinsson S. (1953). The crater groups in Iceland. *Bull. Volcanol.* **14**:2-14.
- Tilling RI, Christiansen RL, Duffield WA, Endo ET, Holcomb RT, Koyanagi RY, Peterson DW & Unger JD (1987). The 1972-1974 Mauna Ulu eruption, Kilauea volcano: an example of quasi-steady-state magma transfer. *U.S. Geol. Surv. Prof. Pap.* **1350**:405-469.

- Walker GPL (1989). Spongy pahoehoe in Hawaii: a study of vesicle-distribution patterns in basalt and their significance. *Bull Volcanol* 51:199-209.
- Walker GPL (1991). Structure and origin by injection of lava under surface crust of tumuli, "lava rises", "lava-rise pits", and "lava inflation clefts" in Hawaii. *Bull. Volcanol.* 53:546-558.
- Walker GPL (1992). Pu`u Mahana near South Point in Hawaii is a primary Surtseyan ash ring, not a littoral cone. *Pacific Science* 46:1-10.
- Walker GPL & Croasdale R (1972). Characteristics of some basaltic pyroclasts. *Bull. Volcanol.* 35:303-317.
- Watson GS & Irving E (1957). Statistical methods in rock magnetism. *Mon. Not. R. Astron. Soc. Geophys. suppl.*, 7:65-97.
- Wentworth CK, Macdonald GA (1953). Structures and forms of basaltic rocks in Hawaii. *US Geol Surv Bull* 994: 98 pp.
- Wohletz KH (1983). Mechanisms of hydrovolcanic pyroclast formation: Grain size, scanning electron microscopy and experimental studies. *Journal of volcanology and Geothermal Research.* 17:31-63.
- Wood CA (1979). Monogenetic volcanoes of the terrestrial planets. *Proc 10th Lunar Planet Sci Conf*:2815:2840.